(Accepted version, post peer review and revisions)

Chapter 11 contents

Chapter 11

Noble gases and halogens in fluid inclusions: a journey through the Earth's crust

Mark A. Kendrick[1] and Pete Burnard[2]

1 – School of Earth Sciences, University of Melbourne, Victoria, Australia.
(mark.kendrick@unimelb.edu.au)
2 – CRPG- CNRS, Nancy-Université, 54501 Vandoeuvre-lès-Nancy Cedex, France
(peteb@crpg.cnrs-nancy.fr)

11.1 Introduction

The study of noble gases and halogens dissolved in crustal fluids has found wide application in a range of hydrogeological disciplines (e.g. Kipfer et al., 2002; Ballentine et al., 2002); these applications can be considerably extended into deeper crustal environments, or the geological past, by the analysis of fluid inclusions. This chapter aims to illustrate: i) how the noble gas composition of fluid inclusions can help constrain the origin of the major volatile phases, such as H_2O and CO_2, in fluid inclusions (e.g. Kelley et al., 1986; Simmons et al., 1987; Turner et al., 1993); and, ii) how additional insights on fluid origins and acquisition of salinity are provided by simultaneous analysis of halogens (Cl, Br, I) with noble gases (e.g. Böhlke and Irwin, 1992a; Kendrick et al., 2001a).

Fluid inclusions were initially investigated to search for ancient atmospheric noble gas components (Cadogan, 1977; Butterfield and Turner, 1985; Turner, 1988), and then to study ore deposits (e.g. Kelley et al., 1986; Simmons et al., 1987). The discovery of Simmons et al. (1987) that hydrothermal minerals can preserve mantle-derived ^3He proved to be of particular interest for investigating ore genesis, because the mantle is frequently invoked as an important source of heat or exotic metals (e.g. Pirajno, 2000). Hydrothermal ore deposits form in a variety of geologic environments from near surface basinal to mid-crustal greenschist or amphibolite facies magmato-metamorphic settings. Fluid inclusions enable metamorphic and magmatic fluids to be sampled from these environments, and in some cases trapping occurs before atmospheric noble gases are introduced via mixing with surface-derived groundwater. The range of fluid inclusions investigated for noble gases has recently been further expanded to include fluid inclusions formed during extensional deformation (Pili et al., 2011), and eclogite facies metamorphism relevant to subduction-recycling processes (Sumino et al., 2010; Kendrick et al., 2011a). As a result, fluid inclusions from ore deposits and metamorphic rocks have greatly expanded the range of crustal fluid types investigated for noble gases.

Basic information concerning the composition of the fluid inclusions major phases (H_2O, CO_2, CH_4, N_2 etc), salts, and the trapping pressure and temperature conditions can be obtained from petrographic observations of the fluid inclusions and microthermometric heating and cooling experiments (Fig 11.1; e.g. Roedder, 1984; Bodnar, 2003). Furthermore, textural evidence or mineralogical associations can provide information on the relative timing of fluid entrapment (Roedder, 1984).

In this chapter we provide an overview of the methods used to analyse noble gases in fluid inclusions and discuss two complementary approaches: i) noble gas analyses focused on

using He-Ar isotope systematics to quantify the presence of mantle and atmospheric components in crustal fluids (e.g. Stuart and Turner, 1992; Turner et al., 1993; Stuart et al., 1995; Burnard et al., 1999; Hu et al., 2004; Graupner et al., 2006); and ii) combined noble gas and halogen analysis, which is applied to irradiated samples (e.g. Böhlke and Irwin, 1992b; Turner and Bannon, 1992; Kendrick et al., 2001a). The combined noble gas and halogen approach represents an extension of ^{40}Ar-^{39}Ar methodology (Table 11.1; Kendrick, 2012), and it enables noble gases to be more closely linked with other fluid tracers than has previously been possible.

Fluid inclusions are providing important new insights on the behaviour of noble gases in the crust (Kendrick et al., 2011ab). This is illustrated primarily through noble gas and halogen data that illuminate the diverse fluid processes responsible for ore deposition in a range of sedimentary, magmatic and metamorphic environments.

11.2 Sample selection

The most important consideration for selecting fluid inclusion bearing samples is that the sample material contains fluid inclusions related to the geological process being investigated. However, the susceptibility of different minerals to post-entrapment modification must also be considered. The two possible modifications of greatest concern for noble gas analysis are: i) post-entrapment leakage of the light helium isotopes, which are known to diffuse through some of the minerals most commonly used for fluid inclusion studies (e.g. quartz) at relatively low temperatures; and ii) modification of the fluid inclusions noble gas isotope signature by post-entrapment decay of U, Th or K which produce a range of radiogenic noble gas isotopes (e.g. ^{4}He, $^{21}Ne^*$, $^{40}Ar^*$, $^{136}Xe^*$; Ballentine and Burnard, 2002).

Note that an asterix is commonly used to denote the radiogenic component of a noble gas isotope. For example, ^{40}Ar has atmospheric and radiogenic sources, whereas $^{40}Ar^*$ has been corrected for atmospheric contributions (e.g. $^{40}Ar^* = {}^{40}Ar$ – atmospheric ^{40}Ar). In most fluid inclusion studies, $^{40}Ar^*$ is broadly equivalent to excess ^{40}Ar ($^{40}Ar_E$), where excess ^{40}Ar has been corrected for both atmospheric ^{40}Ar and radiogenic ^{40}Ar produced by *in situ* decay of ^{40}K (Kendrick et al., 2006b). An asterix is not used for the ^{4}He isotope because the atmospheric contribution to ^{4}He is negligible and ^{4}He is usually assumed to have a purely radiogenic origin in the crust.

11.2.1 Fluid inclusion characterisation

Fluid inclusions can have complex parageneses, primary fluid inclusions trapped during mineral growth are typically identified because they occur in isolated clusters or define mineral growth planes (Roedder, 1984). Secondary fluid inclusions are trapped along annealed fractures, and post-date mineral growth (Roedder, 1984). Secondary fluid inclusions have ambiguous timing and are often introduced after the geological event of interest; however, secondary fluid inclusions can provide useful information in some situations. For example, secondary inclusions can record the passage of multiple fluid pulses in evolving hydrothermal systems, and might preserve fluids more closely related to gold deposition than primary fluid inclusions in some orogenic gold deposits, where gold is hosted on late fractures within quartz veins (Polito et al, 2001; Fairmaid et al., 2011).

Fluid inclusion bearing samples are usually analysed by either *in vacuo* crushing or stepped heating of bulk samples. As a result, it is advantageous if sample materials are dominated by a single fluid inclusion type, or a single assemblage of co-genetic inclusions.

Sequential analyses (e.g. repeat crushing analyses or stepped heating) can be undertaken to help characterise more complex samples. However, limitations imposed by imperfect sample material need to be considered during data interpretation. It is therefore essential that fluid inclusion samples used for noble gas analysis are studied petrographically in sufficient detail that the nature of the fluid inclusion assemblage can be documented.

11.2.2 Post-entrapment He loss

Fluid inclusions can be subject to post-entrapment modifications such as 'necking down' or physical rupture/leakage, which can be identified from fluid inclusions with irregular shapes and variable liquid/vapour volume ratios (e.g. Roedder, 1984). In addition, water can leak out of metamorphic fluid inclusions by diffusion of disassociated H^+ ions, which can significantly alter the fluid inclusions oxidation state or degree of fill (e.g. Mavrogenes and Bodnar, 1994; Scambelluri et al., 2001). Fortunately, the heavy noble gases (Ne, Ar, Kr, Xe) have lower diffusivities than H^+, and appear to be less prone to diffusional leakage than water (e.g. Kendrick et al., 2011a). However, it is not uncommon for fluid inclusions in quartz to have anomalously low He/Ar ratios, or very low helium abundances, that suggest the light helium isotopes are prone to leakage from fluid inclusions in many geological environments (Stuart and Turner, 1992; Graupner et al., 2006; Kendrick et al., 2011b).

Previous work indicates dense sulphide minerals, including pyrite and arsenopyrite, reliably trap helium over geological time periods (10^7 – 10^9 years; Turner and Stuart, 1992; Simmons et al., 1987; Burnard and Polya, 2004; Kendrick et al., 2011c). Native gold, chalcopyrite, sphalerite, scheelite, fluorite and magnetite also appear suitable helium traps (Stuart and Turner, 1992; Eugster et al., 1995; Pettke et al., 1997; Kendrick et al., 2002ab; 2011c). However, many of these minerals are opaque meaning it is difficult to characterise the nature of their fluid inclusions.

The preservation of helium in minerals like quartz, calcite and feldspar, that are suitable for petrographic study of fluid inclusions is variable (e.g. Stuart and Turner, 1992; Graupner et al., 2006; Kendrick et al., 2011b). Helium retention probably depends on the nature of lattice dislocations intersecting individual fluid inclusions, and no petrographic criteria have yet been identified for selecting reliable samples.

The best way to test for possible helium leakage is to analyse the full suite of noble gases (He, Ne, Ar, Kr, Xe). If fluid inclusions preserve $^4He/^{40}Ar^*$ ratios close to the crustal production ratio, or the He/Ar, Ne/Ar, Kr/Ar and Xe/Ar ratios show systematic behaviour consistent with uniform fractionation in a fluid phase, arguments can be made that significant helium loss has not occurred (e.g. Kendrick et al., 2011c). A real concern is that if helium leakage has occurred, the measured $^3He/^4He$ ratio of the trapped fluid could have been compromised by exchange with external fluids.

11.2.3 Post-entrapment production of radiogenic isotopes

Fluid inclusions trap sufficiently high abundances of noble gas in solution that *in situ* production of radiogenic noble gas isotopes (e.g. $^{40}Ar^*$, ^4He) from decay of dissolved K, U and Th is only a concern under exceptional circumstances (e.g. Precambrian U deposits). However, it is not unusual for a mineral to contain significant K, U or Th either within its lattice or within minor mineral impurities, and great care must be taken during analysis, to avoid mixing noble gases trapped in fluid inclusions with radiogenic noble gases produced in the mineral host.

Reliable fluid inclusion analyses are most easily obtained from minerals like quartz, calcite, olivine or sulphide that contain abundant fluid inclusions and very little K, U or Th. However, fluid inclusion and matrix noble gas components can be separated by in vacuum crushing analyses. Optimal seaparation of the fluid inclusion component is achieved by crushing fluid inclusion rich samples for short durations, because prolonged crushing eventually releases significant noble gas from the mineral matrix (cf. Stuart et al., 1995; Yokochi et al., 2005; Kendrick and Phillips, 2009). *In situ* radiogenic noble gas components can be quantified and corrected for if the samples K, Th and U concentrations are measured. The extended ^{40}Ar-^{39}Ar method enables simultaneous measurement of Ar isotopes with K and U (Table 11.1). Stepped heating enables determination of K and U in mineral as well as fluid inclusions, and wide application of this technique has shown that *in situ* production of radiogenic ^{40}Ar is negligible for the majority of Paleoproterozoic to recent quartz samples (e.g. Kendrick et al., 2006bc; 2007, 2008ab; 2011c).

Finally, in addition to ^{4}He ingrowth, there is a potential to produce ^{3}He by neutron capture on Li {^{6}Li(n,α)^{3}He} inside fluid inclusions within some neutron-rich geological environments. This can be significant because ^{3}He can have a very low abundance in hydrothermal fluids and ^{6}Li has a relatively large n-capture cross section (941.1 barns; Chang, 2011). High ^{3}He/^{4}He production ratios are most likely in Li-rich fluid inclusions surrounded by U-rich host rocks (Fig 11.2; Hu et al., 2009), because U can supply highly penetrative neutrons (without ^{4}He) from distances of ~1 m in silicate rocks (Andrews et al., 1982; Andrews and Kay, 1982). However, production *rates* are low, e.g. <10 ^{3}He atoms g^{-1} a^{-1} is estimated for fluid inclusions containing 50 ppm Li surrounded by a host-rock with 10 ppm U, meaning *in situ* ^{3}He production is only significant for fluid inclusions with low helium concentrations (see Hu et al., 2009). A second noble gas isotope that could feasibly be generated by this mechanism is ^{36}Ar, which is produced by neutron capture on ^{35}Cl (Fontes et al., 1991; Irwin and Reynolds, 1995).

11.2.4 Post-entrapment modification by cosmogenic production

Cosmogenic production represents the final *in situ* source of noble gas isotopes, but is only significant for ^{3}He and ^{21}Ne in terrestrial samples (Ozima and Podosek, 2002). Cosmic rays are rapidly attenuated in the Earth's atmosphere and significant cosmogenic isotopes are only generated in samples that are within ~1 m of the Earth's surface (Ozima and Podosek, 2002). As a result, this complexity can be avoided by selecting shielded samples from rapidly eroding environments, drill core or underground workings.

For He and Ne isotope analysis, it is best to avoid samples that have previously been exposed at the surface, or close to the surface, for periods of more than a few thousand years. The low abundances of ^{3}He and ^{21}Ne in mineral samples, means that relatively minor cosmogenic production could bias results. For example, ^{3}He contents in sulphide minerals are typically on the order of 0.5 - 50 $\times 10^{6}$ atoms g^{-1}. An equivalent concentration could be generated by only ~5 – 500 kyr exposure at sea level at high latitude (see Niedermann, 2002).

11.3 Analysis

11.3.1 Sample Preparation

Noble gases in fluid inclusions can be analysed in bulk mineral separates by either *in vacuo* crushing or furnace heating. High purity mineral separates are obtained by hand picking under a binocular microscope. Grains larger than a few mm are avoided because they might

contain hidden impurities and can be difficult to load into crushing devices. Crushing samples too finely will open many of the largest fluid inclusions and increase the time required for hand picking. However, Scheidegger et al. (2010) demonstrated crushing speleotherm material to <300 μm reduced the presence of undesirable modern air contaminants (section 3.6) by removing inter-crystal air cavities and that adsorption of atmospheric noble gases onto fine material was not a significant problem. Mineral separates are usually cleaned in acetone and distilled water with or without ultrasonic agitation; acid cleaning is not possible for soluble sulphide or carbonate minerals.

The irradiation procedure used for combined noble gas and halogen analysis is analogous to ^{40}Ar-^{39}Ar dating (McDougall and Harrison, 1999), except Cd-shielding is avoided in order to maximise production of halogen-derived noble gas isotopes from low energy thermal neutrons (Böhlke and Irwin, 1992b; Johnson et al., 2000; Kendrick, 2012). The noble gas proxy isotopes used to measure Cl, Br, I, K, Ca and U in irradiated samples are summarised in Table 11.1, and the method is described in detail by Kendrick (2012). Irradiated samples analysed for halogens and the more abundant heavy noble gases can be as small as 10-30 mg. In contrast, noble gas analysis of unirradiated samples for scarce He and Ne isotopes typically require 0.3-1.0 g of sample material. Once loaded into the ultra high vacuum for analysis, the samples are baked at temperatures of <120 °C for 12-48 hours, to remove surface contaminants and achieve ultra high vacuum. Higher temperatures are avoided to prevent fluid inclusion decrepitation.

11.3.2 Noble gas extraction methods

Noble gases can be extracted from samples by *in vacuo* crushing, stepped heating or laser ablation, and combinations of these techniques can be employed to provide information about the distribution of noble gases and halogens in the sample (e.g. fluid versus mineral inclusions or different fluid inclusion populations; e.g. Kendrick et al., 2001b; 2006a Kendrick, 2012).

Several crushing apparatus have been designed for fluid inclusion analysis (see Burnard et al. this volume). The different devices vary in efficiency (Kendrick and Phillips, 2009), but a significant proportion of the smallest fluid inclusions (often <<10 μm) remain in the coarser fractions of crushed samples in all devices (Fig 11.3a). Samples are typically analysed sequentially by multiple crushes to characterise variation in the fluid inclusion population.

Stepped heating can be used to analyse quartz hosted fluid inclusions by thermal decrepitation because quartz it is stable to high temperature and contains negligible K, U or noble gas in its lattice (Fig 11.3b; Kendrick et al., 2006a). In contrast, stepped heating of sulphides, sulphates or carbonate can produce potentially damaging pressures of gas (H_2S or CO_2) and is therefore not recommended. Stepped heating can help resolve different fluid inclusion types that have different decrepitation temperatures. For example, liquid carbon dioxide fluid inclusions typically decrepitate at lower temperatures than similarly sized water fluid inclusions. However, fluid inclusion decrepitation temperature is also size dependent (Bodnar et al., 1989). Aqueous fluid inclusions of >5 μm in diameter typically decrepitate between ~200 and ≤700 °C (Stuart et al., 1995; Kendrick et al., 2006a), but very small fluid inclusions of <1-2 μm in diameter are often undecrepitated during microthermometry at temperatures of ~600 °C, and it appears gases are only released from these small inclusions, at temperatures of >1200 °C (Fig 11.3b; Kendrick et al., 2006a). A similar 'bimodal' decrepitation profile has been reported for fluid inclusions in olivine (Tolstikhin et al., 2010); however, there is considerable variability in the degassing profiles of quartz (Fig 11.3b;

Kendrick et al., 2006a; Fisher and Kendrick, 2008; Fairmaid et al., 2011), and bimodal degassing is not a general feature of anhydrous minerals (Stuart et al., 1995). Note that most mineral inclusions, and the mineral lattice, are degassed between ~700 and 1600 °C depending on their size and composition (see Kendrick et al., 2006b).

Laser ablation was applied in the pioneering studies of Böhlke and Irwin (1992abc) to measure argon isotopes and halogens in ore deposit fluid inclusion wafers. However, based on the quantity of gas released and the performance of 266 nm lasers at that time, it is likely that this was achieved on groups of syngenetic, rather than individual fluid inclusions in the majority of cases (Böhlke and Irwin, 1992abc; Irwin and Reynolds, 1995; Irwin and Roedder, 1995; Kendrick et al., 2001b). More recently, 193 nm and 213 nm lasers which enable very controlled ablation of quartz have been used to investigate the presence of excess ^{40}Ar in ultra-high pressure minerals such as quartz and kyanite (e.g. Sherlock and Kelley, 2002). However, routine analysis of individual fluid inclusions remains a distant goal, because in comparison to magmatic glasses which can contain CO_2 vesicles with diameters ranging from >100 μm to mm-size (Burnard et al., 1994; 1997; Raquin et al., 2008), fluid inclusions in crustal environments are often smaller than 10-20 μm making analysis of the scarcest noble gas isotopes (e.g. ^{3}He and ^{22}Ne) unfeasible in individual fluid inclusions.

11.3.3 Purification

Noble gases released from fluid inclusions are purified using Zr-Al getter pumps that remove the major volatiles (e.g. H_2O, CO_2). A typical purification protocol would be to expose the extracted sample gas to a hot (250 °C) SAES getter for 20 minutes; then cool the getter over 15 minutes, prior to final clean up on a second Zr-Al getter pump at 250 °C for 5 minutes (Stuart et al., 1995). Relatively long gettering times are required due to the slow diffusion of water through the extraction line.

Stepped heating calcite or sulphide releases very large volumes of CO_2 or H_2S, even when the maximum extraction temperature is kept below the mineral breakdown temperature. There are no standard procedures for cleaning up these gases but hot (450 °C) Ag wool is efficient for removing H_2S, and 'flow-through' traps are significantly more effective than 'finger-type' traps (Phillips and Miller, 2006; Pujol et al., 2009).

The purified noble gases are usually cryogenically separated into at least light (He + Ne) and heavy (Ar, Kr, Xe) fractions for analysis (e.g. Burnard et al., 1999; Kendrick et al., 2011b; Kendrick, 2012). Neon isotope analyses are best if separated from helium using a cryogenic trap; if separation is not possible, the standard must have He/Ne ratios similar to the samples otherwise uncalibrated mass fractionation effects can occur (Hiyagon, 1989).

11.3.4 Precision relative to natural variation

Fluid inclusion noble gas isotope ratios of helium and argon vary over at least two orders of magnitude (Ballentine et al., 2002; Ozima and Podosek, 2002). As a result analytical precision, which varies from best values of <1 %, to much higher values, depending on the amount of gas available for analysis, rarely limits data interpretation. However, caution is required for neon isotope analysis because of possible interferences from CO_2 or $^{40}Ar^{++}$ (e.g. Osawa, 2004).

Detection limits for halogen measurement by the noble gas method are superior to most conventional techniques and enable Br/Cl and I/Cl ratio measurements with a precision

of ~1% in 10 mg sized samples (Böhlke and Irwin, 1992a; Jonhson et al., 2000; Kendrick, 2012; Kendrick et al., 2012). Detection limits for K or U are more variable and depend on the ability to resolve the irradiation produced $^{39}Ar_K$ or $^{134}Xe_U$ proxy isotopes from interfering isotopes such as $^{39}Ar_{Ca}$ and atmospheric xenon (Kendrick, 2012).

Machine blanks associated with noble gas measurement are variable depending on recent instrument useage and the noble gas extraction method. Blanks are often very small or negligible for laser ablation and crushing undertaken in modified Nupro® valves (Kendrick et al., 2011d; Kendrick, 2012). However, blank corrections sometimes control the uncertainty associated with He and Ne isotope measurements (Kendrick et al., 2011bc) and are usually important in high temperature heating steps (>1400 °C).

Robust blank corrections should be 'active' and mimic the sample analysis as closely as possible, by actuating the crusher, firing the laser, moving the parts required to place a sample in the furnace and using an empty foil packet if samples are wrapped in foil. In practice, reported corrections often represent 'passive' blanks in which for example, the crusher was not actuated. Stuart et al. (1995) demonstrated crushing inclusion free quartz using modified Nupro® valves did not contribute to the procedural blank of this crushing device. However, the use of passive blanks is less than satisfactory for some crushing procedures in which friction between moving parts could generate significant blank. Inadequate blank corrections represent a possible source of air-like contaminants present in some noble gas analyses (section 3.5).

11.3.5 Modern air contamination

Noble gas analyses of fluid inclusion bearing samples sometimes give variable compositions that can be partly explained by the presence of a modern air contaminant (e.g. Kelley et al., 1986; Turner and Bannon, 1992). Air contamination is usually only a concern for samples with very low noble gas abundances (Ballentine and Barfod, 2000). However, modern air contaminants could be significant in fluid inclusion samples if the sample contains 'empty' fluid inclusions filled by air. In cases where modern air contaminants are significant, the noble gases define mixing lines that intersect the composition of modern air (e.g. Turner et al., 1993; Irwin and Roedder, 1995).

Analysis of multiple noble gas isotopes (± Cl) enables the presence of modern air contaminants to be rigorously tested. Scheidegger et al. (2010) demonstrated crushing speleotherm material to <300 μm enabled determination of reliable noble gas concentrations for fluid inclusions, because air was efficiently removed from inter-grain boundaries. If present, modern air contaminants are usually removed by the first crushing or heating steps of coarser grained materials analysed by crushing or stepped heating in vacuum (e.g. Kendrick et al., 2001a; 2002a). Examples where the presence of modern air contaminants has been conclusively excluded using multi-isotope correlations are highlighted below (e.g. Kendrick et al., 2011ab). These studies suggest that while caution is required, modern air contamination can be overcome by careful sample preparation, and is significantly less pervasive in fluid inclusion samples than originally envisioned.

11.3.6 Noble gas concentrations

The majority of noble gas analyses reported for fluid inclusion bearing samples report the concentration of noble gas per gram of sample. As this parameter is strongly influenced by

the number of fluid inclusions in the sample, and the efficiency of *in vacuo* crushing (Fig 11.3a), it has very little geological significance.

Noble gas concentrations in fluid inclusions can be determined if H_2O is measured manometrically (e.g. Stuart et al., 1995). However, adsorption of water throughout the extraction line represents a significant challenge for these measurements and has only recently been overcome (see Kluge et al., 2008; Scheidegger et al., 2010).

A major advantage of measuring halogens simultaneously with noble gases is that the ^{36}Ar concentration of aqueous fluid inclusions can be calculated based on the measured $Cl/^{36}Ar$ ratio and fluid inclusion salinity (Kelley et al., 1986; Böhlke and Irwin, 1992a; Turner and Bannon, 1992; Kendrick et al., 2001a; 2002ab; 2007). The precision of the concentration measurement obtained by this technique depends on the homogeneity of the fluid inclusion assemblage and the possible presence of modern air contaminants. The influence of air contaminants is minimised by using the highest $Cl/^{36}Ar$ ratio measured during sequential analysis of a samples. Accuracy of 10-50 % is suggested for some samples, and as fluid inclusion ^{36}Ar concentrations vary by orders of magnitude, this can provide useful constraints on fluid processes (section 5).

11.4 Data terminology and definitions

11.4.1 Noble gas components

The noble gases have extremely variable isotopic signatures with characteristic values in the mantle, crust and atmosphere (Ozima and Podosek, 2002). Combined helium and argon isotope analysis, or neon isotope analysis, can be used to deconvolve contributions from all three reservoirs (Table 11.2). Crustal fluid inclusions commonly contain mixtures of noble gases from two or more of these reservoirs meaning mixing diagrams are widely used in interpretation of noble gas data. Mixing lines always appear straight in three isotope diagrams that have a common denominator (e.g. $^3He/^4He$ versus $^{40}Ar/^4He$), but mixing trends have curved trajectories in four isotope diagrams (e.g. $^3He/^4He$ versus $^{40}Ar/^{36}Ar$; Langmuir et al., 1978).

Radiogenic noble gas isotopes have predictable abundance ratios (e.g. $^4He/^{40}Ar^*$, $^{21}Ne^*/^{40}Ar^*$ and $^{136}Xe^*/^{40}Ar^*$) controlled by the (U+Th)/K ratio of the host rock (asterix denote radiogenic noble gas isotopes corrected for atmospheric contributions). In contrast, the non-radiogenic noble gases have characteristic abundance ratios (e.g. $^{20}Ne/^{36}Ar$, $^{84}Kr/^{36}Ar$, $^{130}Xe/^{36}Ar$) in air and air saturated water (Ozima and Podosek, 2002), but variable compositions in rocks (Table 11.3). Noble gas abundance ratios can provide useful constraints on fluid sources and physical processes that fractionate noble gases, including H_2O-CO_2 immiscibility (e.g. Kendrick et al., 2001; 2011b).

i. Air-saturated water (ASW)

Meteoric water and seawater are characterised by atmospheric noble gas isotope signatures (Table 11.2) and slightly different abundance ratios ($^{20}Ne/^{36}Ar$, $^{84}Kr/^{36}Ar$, $^{130}Xe/^{36}Ar$), because noble gas solubility is influenced by salinity (Smith and Kennedy, 1983). However, because both meteoric water and seawater are characterised by enrichment in heavy/light noble gases relative to air, and noble gas solubility is also temperature dependent (Smith and Kennedy, 1983), it is difficult to confidently resolve meteoric water from seawater based on noble gas abundance ratios alone. These fluids are therefore commonly referred to with the single moniker of Air Saturated Water (ASW).

ii. Modified ASW (MASW)

Modified Air Saturated Water (MASW) refers to fluids that preserve some of the features of ASW but have been modified during crustal residence (e.g. Burnard and Polya, 2004). The helium isotope system is more easily modified, than heavier noble gases, because the scarce helium isotopes have a very low abundance in ASW (Ozima and Podosek, 2002). In addition, α-particles recoil a mean distance of ~20 μm from their parent U nucleus in silicate minerals (Ziegler, 1980), and helium has a higher diffusivity than the heavy noble gases (Ozima and Podosek, 2002). These processes combine to mean the relative helium abundance in groundwater is altered much more quickly than the relative abundances of the heavy noble gases, and groundwaters rarely preserve either the $^{4}He/^{36}Ar$, or atmospheric $^{3}He/^{4}He$ ratio of ASW. Modifications to noble gas abundance ratios (e.g. $^{20}Ne/^{36}Ar$), with initially air saturation values, can occur by diffusion (Torgersen et al., 2004), adsorption/desorption processes (Pitre and Pinti, 2010), or interaction with hydrocarbons (Bosch and Mazor, 1988).

iii. Crustal components

A range of noble gas isotopes are produced in the crust by radioactive decay of U, Th and K (^{4}He and $^{40}Ar^{*}$), U fisson ($^{136}Xe^{*}$, $^{134}Xe^{*}$, $^{132}Xe^{*}$, $^{131}Xe^{*}$ and $^{86}Kr^{*}$) and α– or n-reactions (including $^{21}Ne^{*}$ and $^{22}Ne^{*}$). For simplicity, noble gas isotopes produced by all these pathways are sometimes collectively referred to simply as radiogenic noble gas isotopes (see Ballentine and Burnard, 2002 for review).

Radiogenic noble gas isotopes (e.g. ^{4}He, $^{21}Ne^{*}$, $^{40}Ar^{*}$ and $^{136}Xe^{*}$) are released to groundwaters by several process: α-particles (e.g. ^{4}He nuclei) recoil ~20 μm from their parent nuclide (e.g. U or Th) in silicate rocks (Ziegler, 1980); noble gases are also released by diffusion, mineral breakdown/dissolution reactions and as a result of fracturing (Honda et al., 1982; Torgersen and O'Donnell, 1991). The crust has a mean $^{4}He/^{40}Ar^{*}$ production ratio of ~5, but low temperature fluids ($T \leq 200$ °C) are typically enriched in $^{4}He/^{40}Ar^{*}$ as a result of preferential ^{4}He release by recoil ejection and diffusion (Ballentine and Burnard, 2002).

The radiogenic noble gas isotopes are often referred to as the crustal noble gas component. However, crustal rocks, especially sediments and rocks altered by ASW (e.g. altered volcanic rocks), also contain substantial quantities of the non-radiogenic atmospheric noble gas isotopes (e.g. ^{20}Ne, ^{36}Ar, ^{84}Kr, ^{130}Xe; Podosek et al., 1980; 1981; Staudacher and Allègre, 1988; Kendrick et al., 2011a). The relative importance of these crustally sourced 'atmospheric' noble gas isotopes is negligible in most shallow groundwaters (e.g. Pinti et al., 1997; Kipfer et al., 2002), but can be significant in some sedimentary environments (Kennedy et al., 2002), and is of overwhelming importance in metamorphic fluids (section 5.5; Kendrick et al., 2011a). The ranges of ^{36}Ar abundance in selected fluid and rock reservoirs are summarised in Table 11.3.

iv. Mantle components

Large mantle components are easily recognised in crustal fluids from $^{3}He/^{4}He$ and $^{20}Ne/^{22}Ne$ ratios of more than the atmospheric values (Table 11.2). Smaller components of mantle-derived noble gas can still be identified from $^{3}He/^{4}He$ ratios of more than ~0.1 Ra (that is typical of the crust) and elevated $^{3}He/^{36}Ar$ ratios. This is because helium has such a low concentration (and low $^{3}He/^{36}Ar$) in ASW, that $^{3}He/^{4}He$ ratios are usually controlled by mixing only mantle and crustal noble gas components.

It has been common practice in the fluid inclusion noble gas literature to use 'mantle' and 'magmatic' almost inter-changeably. However, caution is required in this practice because mantle-derived ^{3}He is common in rift-related sedimentary basins (Oxburgh et al., 1986; O'Nions and Oxburgh, 1988), and is decoupled from aqueous basinal fluids in these

settings. In addition, crustal melts formed as a result of crustal thickening, without input of mantle heat, will not be associated with ^{3}He anomalies (Stuart et al., 1995), implying some magmatic fluids have crustal ^{3}He/^{4}He ratios (Kendrick et al., 2011c).

Despite these caveats, fluid inclusion ^{3}He/^{4}He ratios have provided a litmus test for evaluating the involvement of magmatic fluids in many ore deposits (e.g. Stuart et al., 1995; Burnard et al., 1999; Burnard and Polya, 2004), and there is no other technique that is more sensitive than the ^{3}He/^{4}He ratio for detecting mantle-derived material in the crust.

11.4.1.1 Fluid types

In comparison to the terminology traditionally used in noble gas geochemistry which identifies the ultimate origin of noble gases as being atmospheric (non-radiogenic isotopes), crustal (radiogenic isotopes) or mantle (^{3}He), there are multiple ways of designating fluids in the geological literature.

Fluids of interest for understanding ore genesis or metamorphic processes include: meteoric water and seawater (ASW), sedimentary formation waters (which are also known as oil field brines or basinal brines), metamorphic fluids (H_2O or CO_2) produced by breakdown of hydrous or carbonate minerals; and magmatic fluids which can have highly variable salinity and CO_2 content (Cline and Bodnar, 1991; Baker, 2002). The distinction of these different fluids on the basis of noble gas signatures is illustrated through a series of case studies in section 5.

11.4.2 Halogens and the origin of salinity

Like the noble gases, the halogens (Cl, Br, I) are incompatible elements that have characteristic ratios that vary by orders of magnitude between different geological reservoirs (Table 11.4). Simultaneous measurement of halogens with noble gases has proven advantageous because while noble gases help constrain fluid source (section 4.1), halogens help constrain wall-rock interactions and the fluids aquisition of salinity (e.g. Böhlke and Irwin, 1992c; Yardley et al., 1993; Graupner et al., 2006; Fairmaid et al., 2011; Kendrick et al., 2011c; Fu et al., 2012). The origin of salinity is of special interest in ore deposits because the Cl-ligand is essential for efficient transport of base metals (e.g. Yardley, 2005).

The principal processes controlling the salinity and Br/Cl-I/Cl composition of surface-derived groundwaters are sub-aerial evaporation and subsequent fluid interaction with evaporite minerals and organic matter (Hanor, 1994; Kendrick et al., 2011d). Evaporitic brines preserve seawater Br/Cl and I/Cl ratios up until the point of halite saturation (~30 wt % salts; Zherebtsova and Volkova, 1966; McCaffrey et al., 1986). The low compatibility of Br and I in halite means that continued evaporation produces 'residual' halite-saturated brines (bittern brines) that evolve progressively higher Br/Cl and I/Cl ratios up to maximums of $\sim 11\times10^{-3}$ and 7×10^{-6}, respectively (Table 11.3; Zherebtsova and Volkova, 1966; Nissenbaum, 1977; McCaffrey et al., 1986). In contrast, evaporite deposits have generally low Br/Cl and I/Cl ratios, with the Br/Cl and I/Cl composition depending on the mineralogy of the deposit (e.g. sylvite accomodates more Br than halite; Holser, 1979), the presence of Br- and I-rich fluid inclusions (Bein et al., 1991), and the extent of post-depositional evaporite recrystalisation which preferentially mobilises remaining Br and I relative to Cl (Table 11.4; e.g. Fontes and Matray, 1993). Organic-rich sedimentary rocks represent the Earth's dominant iodine reservoir and organic matter contains high ppm-levels of both I and Br (Collins et al., 1971; Fuge and Johnson, 1986; Martin et al., 1993; Muramatsu et al., 2007). Fluid interaction with organic matter does not influence salinity but represents the dominant

control of fluid I/Cl, and can exert a significant influence on the Br/Cl ratio (Kendrick et al., 2011d).

Metamorphic fluids can have varied halogen composition and salinity. Fluids produced by devolatilisation of hydrous crustal minerals usually have low salinities (e.g. <5-10 wt % salts; Kendrick et al., 2006c), but higher salinities can be achieved in halogen rich lithologies like serpentinites (Scambelluri et al., 1997) and meta-evaporites (Oliver, 1995), or if retrograde hydration reactions lead to fluid desication (Markl and Bucher, 1998; Svensen et al., 2001). Some metamorphic fluids have higher salinities and higher Br/Cl ratios than can be achieved by sub-aerial evaporation, as a result of preferential incorportation of H_2O>Cl>Br into mica or amphibole (Svensen et al., 2001; Kendrick et al., 2006c). The involvement of organic matter remains the dominant control on I/Cl in metamorphic fluids and organic halogen components can sometimes be inferred from characteristic Br/I ratios of between about 1 and 10 (Fairmaid et al., 2011).

The halogen signature of magmatic fluids have been investigated by several workers (e.g. Irwin and Roedder, 1995; Banks et al., 2000; Kendrick et al., 2001a; Nahnybida et al., 2009). It seems magmatic fluids have consistently low I/Cl ratios that are close to mantle values (Kendrick et al., 2012), but more variable Br/Cl ratios, that encompass mantle-like and lower values (Table 11.4; section 5.4). The variation in Br/Cl depends in part on the composition of the host rocks through which the magma intrudes (Banks et al., 2000). Phase separation, degassing and crystallisation of Cl-bearing minerals could also contribute to variation in the halogen composition of magmatic fluids; however, systematic variations in halogen ratios that can be explained by these processes have not yet been documented.

11.5 Fluids in the Earth's crust: top to bottom

The purposes of this section are to provide a historical perspective for noble gas fluid inclusion studies, illustrate how noble gases and halogens distinguish different fluid types and show that fluid inclusions are providing new insights into the behavior of noble gases in a wide variety of crustal environments. The environments investigated are loosely ordered according to their depths in the Earth's crust and the section concludes with a brief comparison of unusual fluid compositions sampled by both fluid inclusions and bore holes.

11.5.1 Ground water

Surface-derived fluids in sedimentary aquifers, aged from a few hundred to many thousands of years, commonly preserve non-radiogenic noble gas isotope (^{20}Ne, ^{36}Ar, ^{84}Kr, ^{130}Xe) concentrations close to air saturation levels (e.g. Kipfer et al., 2002). As noble gas solubility is dependent on salinity as well as temperature, many studies have focused on low salinity groundwaters and used noble gas concentrations to re-construct the palaeo-temperature of surface recharge (e.g. Andrews and Lee, 1979; Aeschbach-Hertig et al., 2000). This information can be combined with groundwater dating techniques (Phillips and Castro, 2003), to reconstruct changes in palaeo-climate, and is now being extended even further back into the geological record through the concentration of noble gases in speleothem fluid inclusions (Kluge et al., 2008; Scheidegger et al., 2010; 2011; Brennwald et al., this volume).

Noble gases have higher solubility in gaseous and liquid hydrocarbons than in aqueous fluids (Smith and Kennedy, 1983; Kharaka and Specht, 1988; Ozima and Podosek, 2002). As the relative solubility of noble gases is systematically related to atomic mass, noble gas concentrations and fractionation of noble gas relative abundance ratios (e.g.

$^{20}Ne/^{36}Ar$, $^{84}Kr/^{36}Ar$ and $^{130}Xe/^{36}Ar$), can provide important constraints on groundwater-hydrocarbon interactions (Bosch and Mazor, 1988; Ballentine et al., 2002).

Model ages can be calculated for groundwater in sedimentary aquifers based on the fluids ^{4}He concentration (Andrews and Lee, 1979; Castro et al., 2007). Models used to calculate ages have varying levels of sophistication. The simplest case assumes the fluid originated as air saturated water with negligible ^{4}He at time zero, and that ^{4}He is acquired from the aquifer rocks at a predictable rate approximating its production within the aquifer. In such a case, the concentration of ^{4}He in the fluid depends only on the residence time of the fluid in the aquifer, the aquifer porosity and aquifer U and Th content (Andrews and Lee, 1979). Similar groundwater model ages can also be calculated from the concentrations of the $^{21}Ne^*$ or $^{40}Ar^*$ isotopes. However, important uncertainties in model ages relate to the partial retention of noble gas in aquifer rocks, which is more significant for $^{40}Ar^* > {}^{21}Ne^* > {}^{4}He$; and the possible flux of these isotopes from outside the aquifer (Phillips and Castro, 2003; Torgersen, 2010).

11.5.1.1 Applicability to hydrothermal fluids?

The well documented behaviour of noble gases in ground water, summarized above and in detail by Kipfer et al. (2002) and Ballentine et al. (2002), cannot be easily applied to higher temperature crustal fluids or hydrothermal ore deposits. Reasons for caution include: 1) most hydrothermal systems have much higher temperatures than <100 °C ground waters; 2) many of the ground waters examined for noble gases preserve O and H isotope signatures similar to meteoric water (e.g. Pinti et al., 1997; Zuber et al., 1997), indicating limited chemical interaction with aquifer rocks, which contrasts starkly with ore fluids (e.g. Taylor, 1997); 3) few studies have examined the noble gas systematics of saline ground waters with >10 wt. % salts (Zaikowski et al., 1987; Pinti et al., 2011); 4) some 'saline formation waters' involved in ore genesis are much older than typical groundwater (e.g. millions of years old), having possibly had connate origins at the time of sediment deposition (Hanor, 1994; Kharaka and Hanor, 2003); 5) the hydrothermal fluids in some magmato-metamorphic ore deposits are not expected to have had surface origins, meaning initially ASW $^{20}Ne/^{36}Ar$, $^{84}Kr/^{36}Ar$, $^{130}Xe/^{36}Ar$ abundance ratios should not be assumed; 6) the relative solubilities of noble gases in aqueous and carbonic fluids at the pressures and temperatures relevant to magmato-metamorphic environments are poorly known; and 7) the prevalence of fracture generated permeability in most ore deposits and deeper crustal environments means noble gases accumulate within fluids in a fundamentally different way compared to sedimentary aquifers. Ground water model ages are not valid for fracture-hosted fluid regimes because ^{4}He and other radiogenic noble gas isotopes collect in rocks and minerals isolated from fluid flow (Andrews et al., 1989); and stored ^{4}He is rapidly released from locations proximal to newly propagating fractures (Torgersen and O'Donnell, 1991). As a result, radiogenic noble gas isotopes (^{4}He, $^{21}Ne^*$, $^{40}Ar^*$, ^{136}Xe) can collect in fracture-hosted fluids much more quickly than they are produced.

11.5.2 Sediment-hosted ore deposits

Mississippi Valley-type (MVT) ore deposits include a broad family of sediment-hosted epigenetic Pb-Zn-fluorite-barite deposits that form at depths of less than ~1-2 km (Heyl et al., 1974; Sverjensky, 1986; Leach et al., 2001). The majority of these deposits are carbonate-hosted but minor mineralisation is found within the Lamotte sandstone beneath the Viburnum

trend MVTs of the USA (Viets and Leach, 1990), and similar sandstone-hosted Pb-Zn mineralisation is found at Laisvall, and in similar deposits, in Scandinavia (Kendrick et al., 2005).

Mississippi Valley-type ore deposits are associated with $CaCl_2$-rich fluid inclusions with typical salinities of 10-30 wt % salts and homogenisation temperatures of ~60 °C to ~200 °C (Roedder, 1971a; Heyl et al., 1974; Leach and Rowan, 1986; Kendrick et al., 2011d). Liquid hydrocarbons are present in the fluid inclusions of some deposits (Gize and Barnes, 1987; Etminan and Hoffmann, 1989). The ore fluids have δD and $\delta^{18}O$ indistinguishable from sedimentary formation waters (Taylor, 1997), which can attain Pb and Zn concentrations of ~100 ppm (Carpenter et al., 1974; Ferguson et al., 1993; Hitchon, 2006), but even higher concentrations (e.g. 1000's of ppm) are reported for ore fluids (Wilkinson et al., 2009).

Mississippi Valley-Type mineralisation occurs in several tectonic settings. In some cases, continent-scale brine migration over 100's of km, occurs through foreland basins as a result of topography driven fluid flow triggered by distal orogenesis (Leach and Rowan, 1986; Garven and Raffensperger, 1997; Leach et al., 2001). However, the Lennard Shelf deposits in Australia are associated with extension (Wallace et al., 2002), and fluorite-rich MVT ore deposits, typified by the Illinois-Kentucky (USA) and Pennine (UK) districts have been attributed to active rifting with possible involvement of mantle volatiles (Russell and Smith, 1979; Plumlee et al., 1995).

The majority of MVT deposits investigated, including fluorite-rich MVT from the Pennines (UK) and Asturias in Spain, are associated with fluid inclusions that have typical crustal $^3He/^4He$ ratios of 0.01-0.1 (Fig 11.4; Stuart and Turner, 1992; Kendrick et al., 2002b; 2005; Sanchez et al., 2010). However, the Illinois-Kentucky fluorspar deposit is associated with fluid inclusions that have slightly elevated $^3He/^4He$ ratios of 0.17-0.35 Ra (Kendrick et al., 2002a), indicating a mantle helium component of up to ~6% in this deposit (Kendrick et al., 2002a). The fluid inclusions from all of the investigated MVT deposits have $^4He/^{40}Ar^*$ ratios of much greater than the crustal production ratio of ~5 (Fig 11.4), which is consistent with the expectation that ^4He collects in low temperature fluids preferentially compared to $^{40}Ar^*$ (Stuart and Turner, 1992; Kendrick et al., 2002ab; 2005).

Fluid inclusions in carbonate-hosted MVT have typical $^{40}Ar/^{36}Ar$ of 300-2000, with the majority <1000 (Fig 11.5b; Böhlke and Irwin, 1992a; Stuart and Turner, 1992; Turner and Bannon, 1992b; Kendrick et al., 2002ab; 2011c). This range of values is similar to that documented in carbonate sediments (Matsuda and Nagao, 1986; Zhou and Ye, 2002), and in saline fluids or gases from a large number of sedimentary basins (e.g. Zaikowski et al., 1987; Bosch and Mazor, 1988; Ballentine et al., 1991; Zuber et al., 1997 Pinti et al., 2011). In contrast, fluid inclusions in the sandstone-hosted Scandinavian deposits have maximum $^{40}Ar/^{36}Ar$ of 16,000 (Kendrick et al., 2005). Despite the obvious difference in host lithology, the concentration of $^{40}Ar^*$ in fluid inclusions from the Scandinavian deposits was estimated to exceed what could be reasonably derived from the K-poor sandstone host-rocks or interbedded shale (Kendrick et al., 2005). The high $^{40}Ar/^{36}Ar$ ratios were therefore attributed to fluid interaction with old, K-rich basement rocks, underlying the deposit (Kendrick et al., 2005). This may be significant because the Scandinavian deposits formed close to the Caledonian orogen and in contrast to most MVT deposits, tectonic pumping of fluids through the basement was more likely to have been a driver of fluid flow (Kendrick et al., 2005).

The ore fluids from the Hansonburg MVT were suggested to have maintained air-saturation ^{36}Ar and ^{84}Kr concentrations (Böhlke and Irwin, 1992a), but the fluids are significantly enriched in $^{130}Xe/^{36}Ar$ (Fig 11.5ab). In contrast, ore fluids in all the other MVT investigated have estimated ^{36}Ar concentrations of greater than air saturation levels (Turner and Bannon, 1992; Kendrick et al., 2002ab; 2005; 2011). The elevated ^{36}Ar concentrations

were attributed to the presence of modern air contaminants in several of the early studies (e.g. section 3.6; Stuart and Turner, 1992; Kendrick et al., 2002ab). However, the extensive database now available indicates $^{40}Ar/^{36}Ar$ is not simply correlated with $^{130}Xe/^{36}Ar$ (Fig 11.5b), suggesting air contamination is not a major control on measured noble gas compositions. Instead, higher than ASW ^{36}Ar concentrations appear to be a real characteristic of the MVT ore fluids investigated (Kendrick et al., 2011d).

The ore fluids greater than ASW ^{36}Ar concentrations, and variable $^{84}Kr/^{36}Ar$ and $^{130}Xe/^{36}Ar$ ratios, could result from dissolution of hydrocarbons which can have high noble gas concentrations and are present in some MVT fluid inclusions (cf. Figs 5a and 5c). However, Kendrick et al. (2011d) argued that the most important source of excess ^{36}Ar was recrystallisation of the carbonate aquifer rocks. This was suggested because fractionation of noble gases between an exclusive ASW source and hydrocarbons does not account for the presence of excess $^{40}Ar^*$ in the ore fluids. In contrast, acquisition of noble gases from carbonate rocks, with $^{40}Ar/^{36}Ar$ slightly above the atmospheric values (Matsuda and Nagao, 1986; Zhou and Ye, 2002), could potentially account for the presence of excess $^{40}Ar^*$ and the range of fluid inclusion $^{84}Kr/^{36}Ar$ and $^{130}Xe/^{36}Ar$ ratios (Fig 11.5d; Kendrick et al., 2011d). Noble gases could be released from the carbonates by diffusion, or during the extensive dolomitisation and recrystallization that is usually associated with MVT mineralisation.

A large number of studies have shown MVT ore fluids commonly have greater than seawater Br/Cl ratios (e.g. Crocetti and Holland, 1989; Kesler et al., 1995; Viets et al., 1996; Kesler, 2007). This has usually been interpreted to indicate acquisition of salinity by sub-aerial evaporation of seawater beyond the point of halite saturation (~30 wt. % salts; cf. Chi and Savard, 1997). Variable dilution of the brines is then required to produce the observed range of fluid inclusion salinities (10-30 wt % salts). This is significant for interpretation of the noble gas data because air saturated bittern brines, have even lower ^{36}Ar concentrations than seawater (Table 11.3).

The combined noble gas and halogen method enables precise measurement of iodine, together with Br and Cl which is advantageous for assessing the possible influence of organic matter on fluid Br/Cl ratios (Kendrick et al., 2011d). Sedimentary marine pore fluids associated with CH_4 transport in oceanic sediments (e.g. Muramatsu et al., 2001; 2007; Fehn et al., 2003; Tomaru et al., 2007ab; 2009) define a linear array in Br/Cl versus I/Cl space that has a seawater intercept and a molar Br*/I slope of 0.5-1.5 (seawater-corrected $Br^* = Br - Cl \times 0.0015$; Fig 11.6; see Kendrick et al., 2011d). Organic matter in sediments usually has higher Br*/I ratios than pore fluids, with the difference explained by preferential mobilization of I relative to Br, under some diagenetic conditions (e.g. Martin et al., 1993; Muramatsu et al., 2001; Biester et al., 2004). The majority of MVT ore fluids plot between the seawater evaporation trajectory and the sedimentary pore fluid trend (which defines the minimum Br*/I of organic matter; Fig 11.6). As the addition of organic halogens does not influence salinity, this confirms sub-aerial evaporation as an important source of fluid salinity (Fig 11.6; Kendrick et al., 2011d). However, some previous interpretations of fluid Br/Cl that did not allow for organic Br, could have over-estimated the degree of evaporation required to generate a given Br/Cl ratio (cf. Fig 11.6), or underestimated the possible importance of evaporite dissolution (Kendrick et al., 2011d).

In the majority of cases, the combined noble gas and halogen data for MVT ore fluids show systematic variation between minerals deposited in different stages of the paragenetic sequence. This has been interpreted to favour fluid migration through independent aquifers providing the potential for fluid mixing at the site of ore deposition (Crocetti and Holland, 1989; Kendrick et al., 2002a; 2011d). Kendrick et al. (2011d) demonstrated that among samples from Lennard Shelf MVT deposits, the fluid inclusions with the highest I/Cl ratio had the lowest ^{36}Ar concentrations. This was suggested to reflect interaction of aqueous

fluids and hydrocarbons, with noble gases partitioning into hydrocarbons and organic halogens partitioning into the aqueous fluids that were trapped as fluid inclusions (Kendrick et al., 2011d).

11.5.3 Mid-ocean ridge VMS deposits

Volcanogenic massive sulphide (VMS) deposits formed by hydrothermal systems at mid-ocean ridge spreading centres and in back-arc rifts, represent important sites for monitoring global volatile fluxes (Turner and Stuart, 1992; Jean-Baptiste and Fouquet, 1996), and are major sources of base metals (Robb, 2005). Noble gas data are available for vent fluids from a variety of modern systems (e.g. Kennedy, 1988; Lupton et al., 1989; Baker and Lupton, 1990); in addition, liquid-vapour fluid inclusions trapped at temperatures of between 200 and 360 °C in pyrite, anhydrite, sphalerite and chalcopyrite have been analysed from the East Pacific Rise, Mid-Atlantic Ridge and various back-arc basins (Turner and Stuart, 1992; Stuart et al., 1994; Jean-Baptiste and Fouquet, 1996; Stuart and Turner, 1998; Zeng et al., 2001; Lueders and Niedermann, 2010; Webber et al., 2011).

In most cases, the helium and argon isotope systematics of sulphide-hosted fluid inclusions are indistinguishable from vent fluids. The majority of workers have therefore concluded that sulphide-hosted fluid inclusions faithfully retain noble gases (including helium) over millions of years, at ambient seafloor conditions (Turner and Stuart, 1992; Jean-Baptiste and Fouquet, 1996; Lueders and Niedermann, 2010). This is consistent with the diffusion data available for helium in sulphides (Boschmann et al., 1984).

Sulphide fluid inclusions have atmospheric or near-atmospheric $^{40}Ar/^{36}Ar$ ratios of 296-310 that reflect the vent fluids dominant origin from seawater (Turner and Stuart, 1992; Zeng et al., 2001; Lueders and Niedermann, 2010; Webber et al., 2011). The $^{3}He/^{4}He$ ratio of vent fluids vary from typical mantle values (e.g. ~8 Ra; Turner and Stuart, 1992; Jean-Baptiste and Fouquet, 1996), to significantly lower values (e.g. ~2-4 Ra; Stuart et al., 1994; Zeng et al., 2001; Webber et al., 2011). Jean-Baptiste and Fouquet (1996) found that high temperature minerals preferentially trap the vent fluid and best preserve mantle $^{3}He/^{4}He$ ratios, whereas lower temperature minerals are more likely to contain an ambient seawater component with lower $^{3}He/^{4}He$. Stuart et al. (1994) reported $^{3}He/^{4}He$ data for sulphides from bare-rock and sediment-covered hydrothermal vent systems. This study interpreted variation in fluid inclusion $^{3}He/^{4}He$ to reflect mixing of mantle ^{3}He derived from local basalts and radiogenic ^{4}He associated with sediments overlying some of the spreading centres (Stuart et al., 1994). In a later study, Stuart and Turner (1998) observed vent fluids with small excesses of $^{40}Ar^{*}$ and two distinct groupings of $^{4}He/^{40}Ar^{*}$ that were suggested to reflect magmatic components acquired during different stages of magma degassing (Stuart and Turner, 1998).

Vent fluid inclusions typically have heavy noble gas abundance ratios intermediate of seawater and air and are strongly enriched in helium, but some systems also have elevated $^{20}Ne/^{36}Ar$ ratios (Fig 11.7; Turner and Stuart, 1992; Zeng et al., 2001; Lueders and Niedermann, 2010). Luedders and Niedermann (2010) suggested noble gas abundance ratios intermediate of seawater and air could reflect gas loss and re-equilibration at elevated temperature; however, these values are also consistent with the presence of a modern air contaminant (section 3.5; Turner and Stuart, 1992). Modern vent fluids are uniformly depleted in all noble gases relative to seawater (Kennedy, 1988; Winckler et al., 2000). Therefore, the lack of strongly fractionated noble gas abundance ratios could indicate the noble gases all have similarly low solubilities in saline fluids at vent temperatures.

The salinity of vent fluid inclusions ranges from at least 1.5 to 15 wt % NaCl eq. (Lueders and Niedermann, 2010). Vent fluids can acquire lower than seawater noble gas concentrations, and high salinities, in the residual brines as a result of phase separation

(Kennedy, 1988; Winckler et al., 2000). In contrast, high noble gas concentrations should be expected in the vapour phase, and high noble gas concentrations together with high salinities might also result from preferential incorporation of H_2O>Cl>^{36}Ar into hydrous minerals during extensive hydration of seafloor lithologies (e.g. Bach and Frueh-Green, 2010). The combined noble gas and halogen method has not been applied to fluid inclusions in mid-ocean ridge sulphides, but Luedders and Niedermann (2010) report variable Br/Cl ratios fractionated around the seawater value.

In summary, the range of noble gas compositions recorded by fluid inclusions in seafloor sulphides reflect mixing hot seawater-derived vent fluids and ambient seawater with a magmatic volatile component present in some cases. Seawater-derived fluids are suggested to acquire significant ^{3}He by fluid interaction with young basalts, or underlying gabbros and lithospheric mantle. The presence of a magmatic volatile component may be related to the age of the hydrothermal system (below).

11.5.3.1 Helium and heat

Studies of modern vent fluids indicate that the concentration of ^{3}He is systematically related to the vent fluids temperature, over a large range of temperatures, which is explained because both ^{3}He and heat are ultimately derived from the mantle in mid-ocean ridge settings (e.g. Lupton et al., 1989; Baker and Lupton, 1990; Lupton et al., 1999; Baker et al., 2011). Vent fluids above magmatically quiescent mature mid-ocean ridges have low ^{3}He/heat ratios of 0.4-1×10^{-17} mol/J; whereas vent fluids associated with newly erupted lavas have higher ^{3}He/heat ratios of 2-7×10^{-17} mol/J, that decrease back toward the lower 'steady state' value over the space of a few years as the magma cools (Baker and Lupton, 1990; Lupton et al., 1999).

The ^{3}He/heat ratio carries information about how heat is transferred from the mantle through the crust (Baker and Lupton, 1990). High ^{3}He/heat values favour advective transport of heat with magmatic volatiles, whereas low ^{3}He/heat values favour conductive transfer of heat into circulating seawater (Baker and Lupton, 1990; Turner and Stuart, 1992). Fluid inclusions provide the potential for extending the study of ^{3}He/heat back into the geological record (Turner and Stuart, 1992; Jean-Baptiste and Fouquet, 1996). This could be advantageous for further unravelling the causes of ^{3}He/heat variations or determining the periodicity of 'event plumes' (cf. Lupton et al., 1999; Baker et al., 2011).

11.5.4 Magmatic fluids and hydrothermal ore deposits

11.5.4.1 'Gold-only' ore deposits

Gold-only ore deposits, in which gold is either the only or by far the dominant economic commodity, include: i) 'orogenic-gold deposits' (also known as 'lode', 'mesothermal' or 'greenstone' gold; Goldfarb et al., 2001; Groves et al., 2003), and ii) 'intrusion-related gold deposits' (Lang and Baker, 2001). These deposits form at crustal depths ranging from <3 to 15 km and because both deposit types can be characterised by very similar low salinity H_2O-CO_2 fluid inclusions, their genesis and distinction is contentious (section 5.5.2; Baker, 2002; Mernagh et al., 2007). Magmatic fluids are implicated in intrusion-related gold deposits that are spatially associated with moderately reduced (ilmenite series) I-type felsic magmatism (Lang and Baker, 2001; Baker, 2002). In contrast, orogenic-gold deposits are variably attributed to the involvement of either distally sourced magmatic fluids or metamorphic fluids

(section 5.5.2; Groves et al., 2003; Phillips and Powell, 1993; Groves et al., 2003; Elmer et al., 2006).

The noble gas systematics of the ~50 Ma greenstone-hosted Ailaoshan gold deposits in SW China provide an example of how noble gases can be used to conclusively demonstrate the involvement of a magmatic fluid in a hydrothermal ore deposit (Burnard et al., 1999; Sun et al., 2009). Fluid inclusions trapped in pyrite and scheelite from Ailaoshan gold deposits have $^{3}He/^{4}He$ ranging from crustal values of 0.05 Ra up to values of 1.3 Ra that indicate a substantial mantle component (Burnard et al., 1999; Sun et al., 2009). The fluid inclusion $^{40}Ar/^{36}Ar$ values vary from 300 up to 9000, and define a parabolic mixing trend in $^{40}Ar/^{36}Ar$ versus $^{3}He/^{4}He$ space (Fig 11.8a; Burnard et al., 1999; Sun et al., 2009). The shape of the mixing trend is governed by the relative concentrations of the denominator isotopes (e.g. ^{4}He and ^{36}Ar) in the two end-members. This is a general relationship applicable to binary mixing in any four component diagram and the curvature is described by the *r*-value (Langmuir et al., 1978), which in this case is written as (equation 11.1):

$$r = \frac{\left(^{4}He/^{36}Ar\right)_{magmatic}}{\left(^{4}He/^{36}Ar\right)_{fluid-2}} \qquad \text{Equation 11.1}$$

Where $(^{4}He/^{36}Ar)_{magmatic}$ and $(^{4}He/^{36}Ar)_{fluid\text{-}2}$ represent two fluid end-members. The concentrations of ^{3}He and ^{36}Ar in crustal fluids are such that He-Ar mixing curves are often strongly parabolic (e.g. Fig 11.8a). As a result, helium can 'appear' to be decoupled from argon, and the $^{40}Ar/^{36}Ar$ value of the magmatic end-member is only poorly defined as being greater than the highest measured value (Fig 11.8a). In contrast, the magmatic fluid end-member at Ailaoshan has a well constrained mixed crust-mantle $^{3}He/^{4}He$ signature of ~1.3 Ra (Fig 11.8a).

Caution is always required in the interpretation of mixing diagrams, a mixing model should define the same end-members in diagrams including any combination of the chosen components. In this instance, the trend in Fig 11.8a represents a pseudo-binary trend, and a third end-member is revealed by plotting the data in a $^{4}He/^{40}Ar$ versus $^{3}He/^{40}Ar$ diagram (Fig 11.8b; Burnard et al., 1999). The three end-members were interpreted as: 1) a magmatic fluid with $^{3}He/^{4}He$ of ~1.3 Ra and $^{40}Ar/^{36}Ar$ of >9000; 2) a crustal fluid with $^{3}He/^{4}He$ of <0.05 Ra and $^{40}Ar/^{36}Ar$ of ~300; and 3) a second crustal fluid that has low $^{4}He/^{40}Ar$ and a poorly defined $^{3}He/^{4}He$ intermediate of 0.05 Ra and ASW (Fig 11.8b; Burnard et al., 1999). The mixed crust-mantle signature of noble gases trapped in sulphide and scheelite fluid incluisions is in excellent agreement with scheelite Sr and Nd isotope data, that also indicate a source from a transitional crust-mantle zone (Sun et al., 2009).

Several other Chinese gold-only ore deposits have fluid inclusions with mixed crust-mantle noble gas signatures similar to the Ailaoshan deposits. These include porphyry-related gold deposits along the Red River–Jinshajiang fault belt, south of the Ailaoshan deposits (Fig 11.8c; Hu et al., 2004); the Bangbu orogenic-gold deposit in Tibet (Wei et al., 2010), and the Dongping orogenic-gold deposit of northern China where fluid inclusions have a maximum $^{3}He/^{4}He$ of 5.2 Ra (Mao et al., 2003). The mixed crust-mantle noble gas signatures reported for all of these deposits are consistent with the involvement of magmatic fluids in a variety of gold-only ore deposits.

In contrast, several orogenic-gold deposits from other parts of the world give maximum fluid inclusion $^{3}He/^{4}He$ ratios of less than ~0.4 Ra (Pettke et al., 1997; Graupner et al., 2006; 2010; Li et al., 2010; Kendrick et al., 2011c). The lack of high $^{3}He/^{4}He$ ratios in samples from Phanerozoic deposits is unlikely to be explained by post-entrapment modification (Pettke et al., 1997; Graupner et al., 2006; 2010), conclusively demonstrating

that some orogenic-gold deposits are formed from crustal fluids, with a range of $^{3}He/^{4}He$ similar to MVT ore fluids (section 5.2). These low $^{3}He/^{4}He$ ratios do not preclude the possible involvement of a magmatic fluid sourced from a largely crustal magma (e.g. Kendrick et al., 2011c), or diluted by modified ASW (Graupner et al., 2006; 2010). However, these dominantly crustal noble gas signatures are also consistent with metamorphic fluids (sections 5.5 and 5.6).

11.5.4.2 Porphyry-style ore deposits

Porphyry-style deposits represent the world's most important source of copper and molybdenum and significant sources of gold (Robb, 2005; Sillitoe, 2010). Porphyry copper, and porphyry copper-gold or molybdenum, ore deposits are zoned around relatively oxidized (magnetite series) felsic porphyry stocks or dykes, formed from 'I-type' calc-alkaline arc magmas (see Sillitoe, 2010 for review). Hydrothermal mineralisation is associated with extensive veining and brecciation at typical emplacement depths of 2-4 km; however, the stocks and dykes act to focus magmatic volatiles, copper and gold, from much larger batholithic intrusions at depth (Sillitoe, 2010). The fluid inclusions in porphyry style quartz veins are dominantly aqueous, although significant CO_2 is present in some systems (Roedder, 1971; Rusk et al., 2004). The classic fluid inclusion assemblage associated with high temperature potassic alteration comprises high salinity aqueous fluid inclusions (40-50 wt % NaCl eq.) with coexisting vapour fluid inclusions, that cool from maximum temperatures of >600 °C to temperatures of ~350 °C (e.g. Roedder, 1971; Heinrich, 2003). The fluid inclusions provide evidence for cooling of magmatic fluids that have separated into low-salinity vapour and high-salinity liquid phases during 'hydrothermal boiling' (Roedder, 1971; Heinrich, 2003).

Noble gas and halogen data are available from several classic porphyry copper deposits of North America including Bingham Canyon, Butte and several Arizonan deposits including Ray, Pinto Valley, Globe-Miami, Silverbell and Mission (Figs 4 and 8c; Irwin and Roedder, 1995; Kendrick et al., 2001ab). Noble gas data are also available for copper and gold deposits associated with porphyry intrusions along the Red River–Jinshajiang fault belt in SW China (Fig 11.8c; Hu et al., 1998; 2004).

The porphyry deposits investigated all have sulphide and quartz hosted fluid inclusions with $^{3}He/^{4}He$ ratios of 0.3 to 2.5 Ra and $^{40}Ar/^{36}Ar$ of 300 to 3000 (Hu et al., 1998; 2004; Irwin and Roedder, 1995; Kendrick et al., 2001a). The data can be modeled to reflect mixing between a magmatic fluid and modified ASW (e.g. Fig 11.8c; Hu et al., 1998; 2004). However, it is interesting that of the deposits in SW China, it is the gold deposits that best define the noble gas mixing trend (Fig 11.8c). In general, the noble gases in the porphyry copper deposit fluid inclusions, especially the Arizonan deposits, appear to be 'well mixed' and do not define an obvious trend (Fig 11.8c). The generally low $^{40}Ar/^{36}Ar$ ratios of ore fluids in the Bingham and Arizonan deposits (Fig 11.4 and 8c) were originally interpreted to reflect mixing of magmatic fluids with elevated $^{40}Ar/^{36}Ar$ and meteoric water with $^{40}Ar/^{36}Ar$ of ~300 (Kendrick et al., 2001a). However, given atmospheric noble gases are recycled through magmatic arcs to some extent (cf. Kendrick et al., 2011a; Staudacher and Allègre, 1988), further work is required to test if the mixed noble gas signatures with high abundances of atmospheric noble gas could be characteristic of magmatic fluids exsolved from porphyry arc magmas. If this proves to be the case, the noble gas signature of porphyry ore fluids could be explained with minimal involvement of meteoric water (cf. Fig 11.8c).

Application of the ^{40}Ar-^{39}Ar method to porphyry copper quartz samples has shown the fluid inclusions have variable ^{36}Ar concentrations ranging from air saturation values (0.3-0.7×10^{-10} mol g^{-1}) to much lower concentrations of 0.04-0.1×10^{-10} mol g^{-1} (Fig 11.9; Irwin

and Roedder, 1995; Kendrick et al., 2001a). The low ^{36}Ar concentrations could be a characteristic of magmatic fluids (Irwin and Roedder, 1995), or the result of hydrothermal boiling (Kendrick et al., 2001a). Additional evidence for hydrothermal boiling is provided by variation in $^{40}Ar^*/Cl$ ratios and extreme enrichments in $^{130}Xe/^{36}Ar$ and $^{84}Kr/^{36}Ar$ values (Fig 11.10). Hydrothermal boiling reduces the $^{40}Ar^*/Cl$ ratio and increases the Xe/Ar and Kr/Ar ratios of the residual liquid phase, because noble gases are partitioned into the vapour phase on the order Ar>Kr>Xe but Cl is preferentially retained by the liquid phase (Fig 11.10; Kendrick et al., 2001a).

Fluid inclusions associated with the majority of porphyry copper ore deposits have a very limited range of Br/Cl and I/Cl (Irwin and Roedder, 1995; Kendrick et al., 2001a; Nahnybida et al., 2009), with the Br/Cl values tending to be lower than the MORB mantle value (Fig 11.11a; Kendrick et al., 2012). Fluid inclusions in the Silverbell porphyry deposit of Arizona, record higher I/Cl ratios than the majority of porphyry ore fluids (Fig 11.11a), and the variation in I/Cl was interpreted to reflect mixing of the dominant magmatic fluid with sedimentary formation waters in this deposit (Kendrick et al., 2001a).

11.5.4.3 Tungsten-bearing ore deposits

Tin-tungsten ore deposits are commonly zoned around reduced (ilmenite series) granites of 'S-type' affinity emplaced at depths of <10 km (Robb, 2005). Noble gas data are available for a variety of tin-tungsten deposits including Carrock Fell in the north of England, several occurrences in Cornwall (UK) (Kelley et al., 1986; Turner and Bannon, 1992; Böhlke and Irwin, 1992c; Irwin and Roedder, 1995) and the Panasqueria deposit of Portugal (Burnard and Polya, 2004; Polya et al., 2000).

The initial studies applied ^{40}Ar-^{39}Ar methodology to quartz veins and documented fluid inclusion $^{40}Ar/^{36}Ar$ values of between 300 and 2200, and fluid inclusion ^{36}Ar concentrations of equal to or above air saturation levels (Fig 11.9; Kelley et al., 1986; Turner and Bannon, 1992). Three dimensional ^{40}Ar-^{36}Ar-K-Ca-Cl correlation diagrams were employed by Kelley et al (1986) and Turner and Bannon (1992) to resolve multiple ^{40}Ar components. In addition to Cl-correlated excess $^{40}Ar^*$ trapped in fluid inclusions, these studies resolved a K-correlated radiogenic ^{40}Ar component, associated with mica impurities in some of the fluid inclusions. The ages of the accidentally trapped mica, in quartz vein fluid inclusions, vary from 250 ± 15 Ma to 270 ± 20 Ma, compared to the probable granite intrusion and mineralisation age of 280-295 Ma (Kelley et al., 1986; Turner and Bannon, 1992). The small discrepancy in ages partly reflects the low retentivity of ^{40}Ar in micron-sized mica crystals (Kendrick et al., 2006b), but nonetheless these cooling ages suggest a maximum time period of ~20 Myr between intrusion of the granites and cessation of hydrothermal activity (Kelley et al., 1986; Turner and Bannon, 1992).

In comparison to porphyry copper ore fluids exsolved from I-type granites, mineralisation-related fluid inclusions at St Austell have slightly lower Br/Cl and higher I/Cl ratios (Fig 11.11a). Assuming the halogens dissolved within these fluids had a dominantly magmatic origin, the difference could reflect anatexis of crustal sedimentary rocks with variable Br/Cl and I/Cl, as opposed to melting dominantly igneous rocks to generate I-type porphyry intrusions (Fig 11.11a; Irwin and Roedder, 1995). Irwin and Roedder (1995) demonstrated that fluid inclusions within granite xenoliths from Ascension Island, that have not had the opportunity of assimilating large amounts of crustal material, preserve MORB-like Br/Cl and I/Cl values (Fig 11.11a; Irwin and Roedder, 1995).

The Panasqueria tin-tungsten deposit of Portugal is hosted by metasediments, overlain by coal bearing sediments, and associated with the ~290 Ma Panasqueria granite (Polya et al., 2000). The Panasqueria granite is of 'S-type' affinity with $^{87}Sr/^{86}Sr$ of 0.713 suggesting

≥50% of the Sr had a crustal source (see Polya et al., 2000; Burnard and Polya, 2004). Quartz-hosted fluid inclusions have salinities of 7-9 wt. % NaCl eq. and homogenisation temperatures of 250-260 °C (Polya et al., 2000). Considering the largely crustal origin of the Panasqueria granite, it was surprising that sulphide-hosted fluid inclusions record $^{3}He/^{4}He$ ratios of up to 6.7 Ra (Fig 11.8d), implying >75% of the helium in the ore fluids has a mantle origin (Burnard and Polya, 2004). The discrepancy between the $^{87}Sr/^{86}Sr$ and $^{3}He/^{4}He$ isotope systems was explained by suggesting that after partial crystallisation, a renewed pulse of mantle volatiles and heat passed through the magma chamber resulting in a final pulse of magmatic fluids with disproportionately high $^{3}He/^{4}He$ (Burnard and Polya, 2004). In a sense, mineralisation may have been related to a pulse of mantle-derived fluids that used the granite as a high permeability pathway (Burnard and Polya, 2004).

The Panasqueria ore fluids have δD values extending from typical magmatic values of around -40 ‰ to unusually low values of -130 ‰ (Polya et al., 2000). Considering the paleolatitude of the deposit, these low δD values can only be explained by either strong fractionation during magmatic degassing, or fluid interaction with organic-rich sediments and coal (Polya et al., 2000). The fluids have a strongly magmatic $^{3}He/^{4}He$ signature (Fig 11.8d), but elevated Br/Cl and I/Cl ratios and low $^{40}Ar/^{36}Ar$ values that are more akin to sedimentary formation waters than typical magmatic fluids (Fig 11.11; Polya et al., 2000). The combined noble gas, halogen and δD data could be explained by mixing magmatic fluids and sedimentary formation waters (e.g. Fig 11.8d; Burnard and Polya, 2004). However, if magmatic fluids acquired the low δD by interaction with organic-rich coals (cf. Polya et al., 2000), the implied fluid-rock ratio of 0.02-0.002 means a magmatic fluid could also have acquired significant Br, I and atmospheric noble gas during interaction with the organic-rich sediments and coal. The K-poor coal was young at the time of ore deposition, meaning it would not have contained significant excess ^{40}Ar (Polya et al., 2000); however, the typical concentrations of atmospheric noble gas in sediments, and the ppm-levels of Br and I in organic matter, would be extremely significant at water-rock ratios of <0.02 (Tables 3 and 4). The key points are therefore that combined noble gas and halogen analysis provides strong evidence for both the involvement of magmatic fluids and extensive fluid interaction with the crustal lithologies overlying the ore deposit (cf. Polya et al., 2000; Burnard and Polya, 2004). However, the way these signals were mixed together is to some extent a question of interpretation.

Finally, the Dae Hwa tungsten-molybdenum deposit of South Korea is associated with 'I-type' granite and is famous for its large zoned scheelite crystals. The scheelite zones contain primary fluid inclusions that record a progressive outward decrease in homogenisation temperature (400-200 °C), which on the basis of $\delta^{18}O$, δD and $\delta^{34}S$ was interpreted to reflect dilution of a magmatic fluid by meteoric water (So et al., 1983; Shelton et al., 1987). Noble gases analysed in a representative zoned scheelite crystal have a maximum $^{3}He/^{4}He$ of 2.7 Ra and show inter-zonal variation that is broadly correlated with $\delta^{18}O$ and fluid inclusion homogenisation temperature (Burgess et al., 1992; Stuart et al., 1995). The noble gas data further constrain the magmatic-meteoric mixing model with the magmatic fluid shown to have $^{3}He/^{4}He$ of >2.7 Ra, and the lower temperature fluid recording characteristically elevated $^{4}He/^{40}Ar^{*}$ ratios of up to 50, $^{3}He/^{4}He$ of <0.2 and $^{40}Ar/^{36}Ar$ of ~400 (Fig 11.4; Burgess et al., 1992; Stuart et al., 1995).

11.5.5 Metamorphic fluids and hydrothermal ore deposits

The range of noble gas compositions expected in metamorphic fluids produced by breakdown of hydrous or carbonate minerals in the Earth's crust is poorly constrained (Kendrick et al.,

2006a). Metamorphic fluids should have the noble gas isotope signature of either the minerals that breakdown, or perhaps more likely, they could have signatures representative of their source region, as a result of diffusion of noble gases into the fluid phase from the surrounding country rock.

11.5.5.1 Serpentine breakdown fluids

The composition and abundance of noble gases in antigorite-serpentinites was recently investigated to test if serpentine subduction could provide a pathway for transfer of atmospheric noble gases into the Earth's mantle (Kendrick et al., 2011a). The results of this study help illustrate some important features of metamorphic fluids.

Antigorite-serpentinites from Erro Tobbio (Italy) have near atmospheric $^{40}Ar/^{36}Ar$ ratios of between 300 and 360 and high abundances of ^{20}Ne, ^{36}Ar, ^{84}Kr and ^{130}Xe (Table 11.3), that were introduced from seawater-derived fluids during seafloor serpentinisation (Kendrick et al., 2011a). Fluid inclusions trapped in olivine bearing veins formed during prograde metamorphism and partial breakdown of antigorite have salinities of up to 40 wt % NaCl eq. (Fig 11.12d; Scambelluri et al., 1997), and record ranges of $^{20}Ne/^{36}Ar$, $^{84}Kr/^{36}Ar$, $^{130}Xe/^{36}Ar$ and $^{40}Ar/^{36}Ar$ that are fairly representative of the host rocks (Fig 11.12; Kendrick et al., 2011a).

Based on a salinity of 40 wt. % NaCl eq. and the measured $Cl/^{36}Ar$ ratio, the fluids are estimated to have a minimum ^{36}Ar concentration of $(9 \pm 1)\times10^{-10}$ mol g^{-1} (1σ), which is 30 times higher than the concentration of ^{36}Ar in 25 °C seawater (Kendrick et al., 2011a). Note that the range of fluid inclusion $^{40}Ar/^{36}Ar$ and $Cl/^{36}Ar$ values do not favour the presence of any kind of modern air contaminant, because the mixing line in Fig 11.12a does not intersect the composition of air (cf. section 3.5).

The elevated salinity and ^{36}Ar concentration of the metamorphic breakdown fluids could reflect any of the following: i) preferential extraction of $^{36}Ar>Cl>H_2O$ during partial breakdown of antigorite; ii) diffusive addition of ^{36}Ar and dissolution of water soluble Cl during fluid migration; or iii) retrograde hydration of relic mantle minerals removing H_2O from solution.

These data are relevant to the interpretation of noble gases in fluid inclusions and crustal fluids more generally, because they indicate: i) high concentrations of ^{36}Ar can be acquired by crustal fluids with a metamorphic origin, or by fluid-rock interaction; ii) crustal fluids can have a range of noble gas concentrations up to values of much greater than ASW (Fig 11.9); and iii) the presence of atmospheric noble gases (alone) does not provide reliable evidence that a fluid originated at the Earth's surface as ASW. The data indicate noble gas signatures can have complex histories and can survive metamorphic hydration and dehydration reactions in some cases.

11.5.5.2 Orogenic gold deposits

Orogenic gold deposits (e.g. lode-, mesothermal- or greenstone-gold deposits) have formed during periods of orogenesis throughout Earth history (Goldfarb et al., 2001; Groves et al., 2003). They occur in metamorphic terranes and are hosted by quartz and carbonate veins containing low salinity (<10 wt % NaCl eq.) aqueous and CO_2 fluid inclusions (e.g. Mernagh et al., 2007). Low salinity CO_2-bearing fluids could be mobilized by either metamorphic or magmatic processes during orogenesis and the origin of fluids in gold deposits is therefore contentious (Groves et al., 2003).

The metamorphic model explains the global association of gold-only ore deposits with seawater-altered volcanic rocks that occur proximally to, or host, mineralization (Phillips and Powell, 1993). Phase equilibrium modeling indicates transitional greenschist-amphibolite

facies metamorphism of altered-volcanic rock produces low salinity H_2O-CO_2 fluids similar to gold deposit fluid inclusions (Powell et al., 1991; Phillips and Powell, 1993; Elmer et al., 2006). However, the high fluid flux necessary for economic gold mineralization may be more easily explained if externally derived fluids are focused into the mineralization zone (e.g. Yardley et al., 1993; Groves et al., 2003), and many gold deposits are spatially or temporally associated with granites or lamprophyres (e.g. Rock and Groves, 1988; Neumayer et al., 2009). Furthermore, magmatic fluids are clearly involved in intrusion-related gold deposits that appear to form a continuum with orogenic gold deposits (section 5.4.1; Lang and Baker, 2001).

Noble gases can help provide new constraints on the origin of gold-related fluids. Seawater-altered volcanic rocks are characterized by atmospheric Ne, Ar, Kr and Xe signatures (e.g. Staudacher and Allègre, 1988; Burnard and Harrison, 2005), but because seawater contains very little helium (Ozima and Podosek, 2002), seawater altered volcanic rocks can retain mantle ^3He components for prolonged periods (altered-basalts of Jurassic age have near atmospheric $^{40}Ar/^{36}Ar$ signatures but $^3He/^4He$ ratios of up to 0.4 Ra; Staudacher and Allègre, 1988). These limited data suggest fluids generated by metamorphism of altered volcanic rocks are likely to be characterized by low $^{40}Ar/^{36}Ar$ and variable, but generally low, $^3He/^4He$ ratios. In contrast, magmatic fluids are often characterized by high $^{40}Ar/^{36}Ar$ and high $^3He/^4He$ ratios (e.g. Fig 11.8; section 5.4.1). Halogens can provide further information because they have a fairly limited range of signatures in magmatic fluids (Fig 11.11).

i. Tienshan province, Uzbekistan

The giant Muruntau, Charmitan and related gold deposits of the southern Tienshan gold province, are associated with quartz, scheelite and sulphide hosted fluid inclusions that have $^3He/^4He$ of 0.02-0.4 Ra and $^{40}Ar/^{36}Ar$ of 300-1200 (Graupner et al., 2006; 2010). The ore fluids from these deposits have high concentrations of atmospheric noble gas that are strongly enriched in $^{20}Ne/^{36}Ar$ and $^3He/^{36}Ar$ relative to ASW (Fig 11.13; Graupner et al., 2006; 2010). These data were interpreted to favour a dominant role for modified air-saturated water with the minor mantle component introduced by magmatic fluids sourced from lamprophyres close to the Muruntau and Charmitan deposits (Graupner et al., 2006; 2010), or associated with granitic magmatism (Morelli et al., 2007). While we agree the data are consistent with this interpretation, the discussion above suggests they are equally compatible with a dominant role for metamorphic fluids (Fig 11.13). Furthermore, the Muruntau ore fluids have Br/Cl ratios of $(0.6\text{-}2.3)\times10^{-3}$ (Graupner et al., 2006), that are similar to metamorphic fluids in gold deposits from Brussen ($1.6\text{-}2.3\times10^{-3}$; Yardley et al., 1993); Victoria, Australia ($0.6\text{-}3.6\times10^{-3}$; Fairmaid et al., 2011; Fu et al., 2012), Alleghany in the Sierra Nevada ($1.2\text{-}2.4\times10^{-3}$; Böhlke and Irwin, 1992c) and the Yilgarn craton of Western Australia ($0.6\text{-}3.3\times10^{-3}$; Kendrick et al., 2011c). Therefore further work is still required to establish a strong link between magmatism and gold mineralisation in the Tienshan province.

ii. Brusson, NW Italy

Native gold from the 32 Ma Brusson gold deposit of Italy traps fluid inclusions with $^3He/^4He$ of 0.2 ± 0.1 Ra (2σ) that are within error of crustal values (Table 11.2), $^{40}Ar/^{36}Ar$ of 330-5900 (Eugster et al., 1995; Pettke et al., 1997), and $^{136}Xe/^{132}Xe$ values that are slightly enriched in the fission component (Eugster et al., 1995). The fluid inclusions preserve elevated $^4He/^{40}Ar^*$ and $^3He/^{36}Ar$ ratios that together with the gas release spectra favour variable trapping of H_2O and a CO_2 vapour phase enriched in the light noble gases (Pettke et al., 1997). The elevated He/Ar ratios also confirm gold is retentive of helium (Eugster et al., 1995; Pettke et al., 1997).

The Brusson vein gold system was further constrained by Sr and Pb isotope data that suggest calc-schists and intercalated meta-ophiolites, underlying the 10 km thick Monte Rosa Nappe, provide the closest possible fluid source (Pettke and Diamond, 1997; Pettke and Frei, 1996). Two samples of meta-ophiolite gave modern day $^{40}Ar/^{36}Ar$ of 330-670, whereas two samples of metagranite in the Monte Rosa nappe gave modern day $^{40}Ar/^{36}Ar$ of 1700-4700 (Pettke et al., 1997). The $^{40}Ar/^{36}Ar$ composition of the fluids (330-5900) is therefore broadly consistent with the metamorphic model and suggests fluids with low $^{40}Ar/^{36}Ar$ may have acquired additional excess $^{40}Ar^*$ during migration through the Monte Rosa nappe. Pettke et al. (1997) suggested the fluids slightly elevated ^{3}He content could have been acquired from the metaophiolites or by fluid interaction with plutonic igneous rocks.

Ion chromatography indicates that the fluid inclusions in these deposits have Br/Cl of $(1.6\text{-}2.3)\times10^{-3}$ and I/Cl of $(2\text{-}73)\times10^{-6}$ (Yardley et al., 1993). The relatively low I/Cl values indicate very little interaction of the fluids with organic-rich sedimentary rocks (cf. Fig 11.14).

iii. Victoria, Australia

The ~440-360 Ma orogenic-gold deposits in Victoria are hosted by a sedimentary package comprising turbidites and shale, underlain by altered volcanic rocks of Cambrian age (Phillips et al., 2012). Helium data are not yet available for the Victorian gold deposits; however, the regional scale of halogen and Ar-Kr-Xe studies provide some important insights (Fairmaid et al., 2011; Fu et al., 2012).

Low salinity $H_2O\text{-}CO_2$ fluid inclusions have $^{40}Ar/^{36}Ar$ of 300-1500 in the majority of deposits, but higher values of up to ~5000 were observed in the regions largest deposits at Stawell and Ballerat (Fairmaid et al., 2011; Fu et al., 2012). The fluid inclusions have elevated ^{36}Ar concentrations of several times air-saturation levels (e.g. similar to serpentine breakdown fluids; Fig 11.9). The high noble gas concentrations and range of $^{84}Kr/^{36}Ar$ and $^{130}Xe/^{36}Ar$ values were interpreted to result from preferential desorption, or diffusive release, of Ar>Kr>Xe from rock units, and the range of fluid inclusion $^{40}Ar/^{36}Ar$ values was considered representative of altered-volcanic source rocks and the meta-sedimentary host rocks (Fairmaid et al., 2011; Fu et al., 2012).

The Br/Cl and I/Cl ratios of gold-related fluids in Victoria encompass a similar range as reported for the Muruntau, Brusson and Alleghany deposits (Böhlke and Irwin, 1992c; Yardley et al., 1993; Graupner et al., 2006; Fairmaid et al., 2011; Fu et al., 2012). However, they show systematic variation across Victoria with basalt-like Br/Cl of $(0.9\text{-}1.6)\times10^{-3}$ and I/Cl of $(11\text{-}91)\times10^{-6}$ in the western-most Stawell deposit, and much higher I/Cl values of up to $(5200)\times10^{-6}$ in the eastern-most deposits that are situated in the shale-rich Melbourne zone (Fig 11.14; Fu et al., 2012). Similar mixing between two halogen components can be observed at the deposit scale, where mixing trends define Br/I ratios of ~6 (Fig 11.14b), that are similar to Br/I ratios of organic matter (Fairmaid et al., 2011). As it is known iodine is lost to the fluid phase during metamorphism (Muramatsu and Wedepohl, 1998), these data were interpreted to reflect derivation of halogens from two lithologies: altered-basalts and shale (Fairmaid et al., 2011; Fu et al., 2012).

The interpretation of the halogen and noble gas data in Victoria is analogous to stable isotope data which shows the fluids were partially rock-buffered and preserve a range of $\delta^{13}C$ characteristic of both igneous and sedimentary C sources (Fu et al., 2012). While most models for orogenic gold favour deep metamorphic or magmatic sources for the fluids and gold, it has recently been suggested that diagenetic pyrite within sedimentary rocks in Victoria was the most important gold source (Large et al., 2011; Thomas et al., 2011). The halogen data provide strong supporting evidence for extensive fluid interaction with the

sediments; however, the largest gold deposits are not associated with the most I-rich fluids or the most shale-rich parts of the Victorian gold province (Fu et al., 2012).

iv. St Ives, Western Australia

The ~2.65 Ga St Ives gold deposits in theYilgarn craton of Western Australia formed at estimated depths of 5-7 km during late Archean greenschist facies metamorphism of ~2.7 Ga greenstones (Groves et al., 2003; Kendrick et al., 2011c). There was abundant magmatism throughout the terrane overlapping the period of mineralisation and metamorphism, including U-rich potassic granites that were derived from anatexis of ~100-600 Myr old basement rocks (Champion and Sheraton, 1997). Noble gas and halogen analyses were used to test if H_2O-CO_2 and CH_4 fluid inclusions associated with gold mineralisation at St Ives had similar origins. This is significant because independently sourced abiogenic CH_4 has been suggested as a trigger for gold mineralisation (Neumayr et al., 2008), but CH_4 could alternatively have been produced by localised wall-rock reactions (Polito et al., 2001).

In contrast to all the other gold deposits studied to date, fluid inclusions from the St Ives goldfield preserve a huge range in $^{40}Ar/^{36}Ar$, with the highest values in samples containing CH_4 fluid inclusions (Fig 11.15). The lowest $^{40}Ar/^{36}Ar$ ratios of <2000, indicate that some of the fluid inclusions have relatively high abundances of atmospheric noble gas. These values are similar to those observed in the majority of gold deposits and were suggested to represent metamorphic fluids derived from seawater-altered greenstones (Kendrick et al., 2011c). In contrast, the fluids with $^{40}Ar/^{36}Ar$ ratios of 20,000-50,000 were suggested to have had an external origin. It was argued that 100-600 Myr old basement rocks underlying the greenstones at 2.65 Ga represent the most likely source of the strongly radiogenic noble gas isotope signature, because the basement was significantly older than the greenstones and had not been altered by seawater (Kendrick et al., 2011c).

Noble gases could have been released from the basement by either crustal anatexis and exsolution of magmatic fluids from the potassic granites, or they could have been released by basement metamorphism (Kendrick et al., 2011c). It was suggested the fluids were then focused into the site of mineralisation, where atmospheric noble gases derived from the greenstone reduced the fluids $^{40}Ar/^{36}Ar$ ratio (Fig 11.15). This interpretation of the noble gas data is analogous to the interpretation of other radiogenic isotopes (Pb and Sr) that also indicate fluid solutes had multiple sources from both the basement and greenstones (Ho et al., 1992). The noble gas data were regarded as being consistent with interaction of independently sourced CH_4 and H_2O-CO_2 during mineralisation (Neumayr et al., 2008); however, the ultimate source of the abiogenic CH_4 remains open to speculation (Kendrick et al., 2011c).

Interpretation of noble gas signatures in Archean age samples needs to make allowance for high Archean production rates of radiogenic noble gas isotopes. The 1.25 Gyr half life of ^{40}K implies that for any given K content, the $^{40}Ar^*$ production rate was ~4 times higher at 2.65 Ga than it is today. Therefore, the most radiogenic $^{40}Ar/^{36}Ar$ signatures measured for the St Ives ore fluids are comparable to those obtained for magmatic fluids in the Ailaoshan gold deposits (Fig 11.8a). Highly radiogenic noble gas components in Archean and Proterozoic age ore fluids are discussed more fully below (section 5.6).

11.5.5.3 Fluids in eclogites

Eclogites have mafic composition and are defined as containing garnet and omphacite, but also contain accessory hydrous minerals such as phengite. Eclogites can form by hydration of granulites (e.g. Boundy et al., 1997; Svensen et al., 2001), or prograde metamorphism of blueschists (Ernst, 1971). Fluid inclusions are commonly trapped in

omphacite, garnet, kyanite and quartz (Svensen et al., 2001). However, hydrous minerals like phengite represent an important reservoir of excess ^{40}Ar (e.g. Arnaud and Kelley, 1995; Kelley, 2002; Sherlock and Kelley, 2002), and probably other (non-radiogenic) noble gases, reflecting the increased compatibility of noble gases in many hydrous minerals in high pressure environments (see Kelley (2002) for review).

The noble gas content of eclogite fluid inclusions has not yet been systematically investigated. However, based on previous $^{40}Ar/^{39}Ar$ studies, the trapped argon component within phengite, and eclogite facies fluid inclusions, typically has $^{40}Ar/^{36}Ar$ in the range of 300-5000 (Arnaud and Kelley, 1995; Reddy et al., 1997; Giorgis et al., 2000; Kendrick, 2007). Unsurprisingly noble gases enter the fluid phase when present, but are partitioned into phengite at low water-rock ratios as the fluid phase is consumed by hydration reactions. Eclogite facies minerals often show variable ^{40}Ar-^{39}Ar apparent ages that reflect a heterogenous distribution of extraneous ^{40}Ar*. This is usually interpreted to result from limited fluid mobility during prograde metamorphism, or redistribution of ^{40}Ar* between mineral phases during retrograde chemical exchange (e.g. Boundy et al., 1997; Giorgis et al., 2000; Warren et al., 2011).

The composition of Cl, Br and I was investigated in primary fluid inclusions trapped within omphacite and garnet from the Western Gneiss Region of Norway (Svensen et al., 2001). The high salinity of ~40-50 wt. % recorded by these primary fluid inclusions is typical of eclogite facies fluid inclusions (e.g. Fu et al., 2001; 2002). The high salinity of these brines is suggested to result from preferential incorporation of H_2O>Cl into hydrous minerals. Svenson et al. (2001) demonstrated the high salinity brine inclusions (which are much more saline than can be achieved by sub-aerial evaporation), have molar Br/Cl ratios of between 2.2×10^{-3} and 14.3×10^{-3}, and molar I/Cl of between 8×10^{-6} and 29×10^{-6}. The range of Br/Cl values is slightly greater than achieved on the seawater evaporation trajectory (Fig 11.16), demonstrating strong fractionation of the halogens can occur during metamorphism at sufficiently low water-rock ratio (Svensen et al., 2001).

11.5.6 Basement noble gas components

In this final section of case studies, we discuss the significance of the highly radiogenic crustal noble gas isotope signatures (e.g. $^{21}Ne/^{22}Ne > 0.2$, $^{40}Ar/^{36}Ar$>30,000, and $^{136}Xe/^{130}Xe > 3$) recently reported for fluid inclusions from several Proterozoic or Archean ore deposits in different parts of Australia and Canada (Kendrick et al., 2006c; 2007; 2008ab; 2011bc); and we compare the fluid inclusions with CO_2 well gases from Colorado (Gilfillan et al., 2008) and ancient ground waters from South Africa (Lippmann et al., 2003; Lippmann-Pipke et al., 2011).

These highly radiogenic noble gas signatures get special attention because: i) extra care must be taken to test Proterozoic and Archean age samples for the effects of post-entrapment radiogenic ingrowth; ii) such highly radiogenic noble gas signatures had not been observed in shallow ground waters previously; and ii) the interpretation of strongly radiogenic noble gas isotope signatures requires significant geological background, which is illustrated through a case study of the Mt Isa Inlier.

11.5.6.1 Excluding radiogenic ingrowth in ancient samples

Several arguments can be made to suggest the noble gas compositions reported for Archean and Proterozoic samples are fairly representative of the fluid inclusions initial composition. Most importantly, stepped heating irradiated quartz from the Mt Isa Inlier and Yilgarn craton yield apparent ^{40}Ar-^{39}Ar ages of up to 11 Ga, that demonstrate the samples do not contain

enough K either within their fluid inclusions, or within mineral impurities, to generate the observed $^{40}Ar/^{36}Ar$ ratios (Fig 11.17). The low K content of these samples unequivocally demonstrates that the measured $^{40}Ar/^{36}Ar$ ratios of up to 50,000 are representative of the fluid inclusions initial composition (Kendrick, 2006c; 2007; 2008ab; 2011bc).

Secondly, stepped heating irradiated quartz samples gives $^{134}Xe_U$ concentrations indicating <100 ppb U in the quartz matrix of all Mt Isa samples analysed, and the samples with the highest $^{21}Ne/^{22}Ne$ ratios have concentrations of only 2-20 ppb U (Kendrick et al., 2007; 2008a; 2011b). Crushing released 0.5-4.0×10^{-15} mol $^{21}Ne^*$ per gram of these samples (Kendrick et al., 2011b) which is <<100% of the $^{21}Ne^*$ in the samples (Fig 11.3a). Nonetheless, *in situ* production of the measured $^{21}Ne^*$ over a period of 1.55 Ga, would require a U concentration of 1000-8000 ppb (calculated using the equations in Ballentine and Burnard (2002)). As this is up to 1000 times greater than the measured U concentrations, it conclusively demonstrates that $^{21}Ne^*$ released by crushing, like $^{40}Ar^*$, represents a trapped component. Similar arguments indicate $^{21}Ne^*$ is also a trapped component in ~2 Ga fluid inclusions from the Kapvaal craton (Lipmann-Pipke et al., 2011), and 2.65 Ga fluid inclusion samples from the Yilgarn (Kendrick et al., 2011c).

The majority of fluid inclusion samples from both the Yilgarn and Mt Isa Inlier have fluid inclusion $^{21}Ne^*/^{40}Ar^*$ and $^{136}Xe^*/^{40}Ar^*$ ratios close to the crustal production ratios that would be expected in high temperature fluids (Kendrick et al., 2011bc). However, samples dominated by CO_2 fluid inclusions from the Mt Isa Inlier, are systematically enriched in $^{21}Ne^*/^{136}Xe^*$ relative to possible production ratios (Fig 11.18a). As both $^{21}Ne^*$ and $^{136}Xe^*$ are produced from U, this is impossible to explain by *in situ* production, but is consistent with fractionation of noble gases between H_2O and CO_2 prior to trapping (Fig 11.18a; Kendrick et al., 2011b).

Helium isotope ratios are more sensitive to overprinting than Ne, Ar or Xe isotope ratios. Measured $^{4}He/^{40}Ar^*$ ratios indicate helium leaked out of Mt Isa quartz samples (Kendrick et al., 2011b); but the $^{4}He/^{40}Ar^*$ ratios measured for gold-related fluid inclusions from St Ives are in the range of expected Archean production ratios (Fig 11.18b; Kendrick et al., 2011c). Minor He leakage or *in situ* production of ^{4}He in these samples is likely; however, the data are most easily explained if the measured $^{3}He/^{4}He$ ratios of ~0.01 Ra remains close to their initial values; and dominantly crustal $^{3}He/^{4}He$ ratios are expected in fluids with extremely radiogenic $^{40}Ar/^{36}Ar$, $^{21}Ne/^{22}Ne$ and $^{136}Xe/^{130}Xe$ ratios (Kendrick et al., 2011c). Preservation of near original $^{3}He/^{4}He$ ratios requires the samples low salinity water and CH_4- or CO_2-only fluid inclusions have very high (noble gas)/(U + Th) ratios and negligible U and Th.

The range of $^{136}Xe/^{132}Xe$ reported for Proterozoic and Archean age fluid inclusions (Kendrick et al., 2011bc) is similar to that reported for fluid inclusions in Phanerozoic gold deposits (Sun et al., 2009), modern well gases (Gilfillan et al., 2008) and fracture-hosted waters from the Witwatersrand basin (Lippmann et al., 2003) (see Table 11.5). Calculated $^{21}Ne^*/^{22}Ne^*$ ratios for Proterozoic and Archean fluid inclusions range from unusually low values of 0.1, whereas high values would be expected to result from *in situ* production of $^{21}Ne^*$, up to maximum values that are similar to fracture hosted ground waters in the Witwatersrand basin (3.3 ± 0.2; Lippmann-Pipke et al., 2011). These observations are all consistent with noble gases in the fluid inclusions being largely representative of their initial compositions.

11.5.6.2 The Mt Isa Inlier, Australia

The Proterozoic Mt Isa Inlier of northeastern Australia is famous for its high heat producing granites (McLaren et al., 1999; Sandiford et al., 2002) and rich endowment with ore deposits that formed in hydrothermal systems spanning at least 170 Myr of crustal evolution (Oliver, 1995; Oliver et al., 2008). Noble gas and halogen data are available for a large number of ore deposits from two contrasting settings within the inlier (Heinrich et al., 1993; Kendrick et al., 2006abc; 2007; 2008a; 2011a; Fisher and Kendrick, 2008).

Iron-oxide-copper-gold (± U ± REE) deposits and related regional-scale Na-Ca alteration (albitisation) are found throughout the Eastern Fold Belt (Oliver et al., 2004; Mark et al., 2006; Kendrick et al., 2006ab; 2007; 2008a; 2011b; Fisher and Kendrick, 2008). The Eastern Fold Belt comprises greenschist-amphibolite facies meta-sediments (including meta-evaporitic calc-schists) intruded by regionally extensive 1550 to 1490 Ma Williams-Naraku Batholiths (Page and Sun, 1998; Foster and Rubenach, 2006). The iron-oxide-copper-gold deposits are spatially associated with regional faults (Mark et al., 2006). Ernest Henry (166 Mt of 1.1 % Cu and 0.5 ppm Au) and several other deposits overlap intrusion of the 1550 to 1490 Ma Williams-Naraku Batholiths, whereas the Osborne and Starra deposits are suggested to have formed at ~1595-1570 Ma (Oliver, 1995; Page and Sun, 1998; Oliver et al., 2004; 2008; Mark et al., 2006; Duncan et al., 2011). Mineralisation and alteration related fluid inclusions include high salinity brines (e.g. 60 wt% NaCl eq.) and liquid CO_2 trapped at estimated depths of 8-10 km (e.g. Kendrick et al., 2011b). Carbonate veins in regional Na-Ca alteration have $\delta^{13}C$ ranging from magmatic values of -6 ‰ to country rock values of -1 ‰ (Oliver, 1995; Oliver et al., 1993). Sulphur, O and H isotopes are consistent with, but do not prove, the involvement of magmatic fluids in ore deposition (Mark et al., 2004; 2006). Two major uncertainties in the genesis of these deposits are therefore the extent of magmatic fluid involvement and the role of evaporites in generating high salinity brines (e.g. Barton and Johnson, 1996; Pollard, 2000; 2001).

The Mt Isa copper deposit (250 Mt of 3.3 wt % Cu) of the Western Fold Belt differs to iron-oxide-copper-gold deposits in several important aspects. Copper mineralization is superimposed on earlier Pb-Zn mineralization; it is hosted by greenschist facies shales (Perkins, 1984; Swager, 1985), and minor pegmatites represent the only known igneous activity within the Western Fold Belt during the Isan orogeny (Connors and Page, 1995). The deposit is associated with mine-scale silica-dolomite rather than regional Na-Ca alteration; copper (with minor cobalt) is the only economic commodity, and iron forms sulphides not oxides (Swager, 1985; Heinrich et al., 1989). Fluid inclusions hosted by silica and dolomite alteration are dominantly two phase liquid-vapour with salinities of 5-25 wt. % salts (Heinrich et al., 1989). In contrast to the iron-oxide-copper gold systems, high salinity brine inclusions are lacking and CO_2 is rare (Heinrich et al., 1989; Kendrick et al., 2006c). The S, O and H isotope data indicate the presence of locally derived sedimentary S and are consistent with introduction of additional S as seawater sulphate in evolved basinal brines or derived during metamorphism under oxidizing conditions (Andrew et al., 1989; Heinrich et al., 1989; Painter et al., 1999).

i. Noble gases and halogens

Despite the substantially different geological settings of the iron-oxide-copper-gold mineralization and Mt Isa style copper mineralization (above), the fluid inclusions from both styles of ore deposit have maximum $^{40}Ar/^{36}Ar$ ratios of ≥30,000 and combined Ne-Ar-Xe systematics that suggest mixing of noble gases from three very similar reservoirs: i) ancient basement rocks with highly radiogenic noble gas signatures; ii) air-saturated water; and iii) a third component representative of the meta-sedimentary country rocks (Fig 11.19a). The mixing model in Fig 11.19 is undoubtedly an over simplification of a complex system (see Kendrick et al., 2011b); however, the model is consistent with both Fold Belts comprising a

relatively thin layer of meta-sediments underlain by much older and broadly similar pre-Barramundi basement lithologies (MacCready et al., 1998). The model therefore provides a useful starting point for interpretion of the fluid inclusion noble gas signatures (Kendrick et al., 2011b).

A highly radiogenic basement noble gas signature is expected in magmatic fluids derived from the Williams-Naraku Batholiths in the Eastern Fold Belt, because these intrusions have Nd isotope signatures that indicate a basement source with an average age of ~650-700 Myr at 1550 Ma (Page and Sun, 1998; Mark, 2001). Sequential analysis of iron-oxide-copper-gold or Na-Ca alteration related samples, demonstrates the fluid inclusions within each sample have compositions that vary between characteristic limits (see Fig 11.19). The noble gas mixing trends defined for the CO_2 fluid inclusions and Ernest Henry ore fluids are comparable to stable isotope data that show mixing of magmatic and meta-sedimentary C components (cf. Fig 11.19a; Oliver et al., 1993). The distinct curvature of mixing trends obtained for samples dominated by CO_2 fluid inclusions, probably results from fractionation of noble gas elemental abundance ratios during CO_2-H_2O interaction (e.g. Fig 11.18a; see *r*-values definition in section 5.4.1). The involvement of magmatic fluids in the Ernest Henry deposit is further constrained because the fluids with the most radiogenic noble gas signatures have the most 'magmatic' halogen signatures, whereas fluids with less radiogenic noble gas signatures are associated with 'halite dissolution' halogen signatures (Fig 11.20). Taken together, the data (Figs 19 and 20) provide strong evidence for magmatic fluids in the Ernest Henry iron-oxide-copper-gold deposit and regional Na-Ca alteration in the northern part of the Eastern Fold Belt (Kendrick et al., 2006a; 2007; 2008a). However, basin derived metamorphic fluids that interacted with scapolite (or halite) were also present and dominated much of the Na-Ca alteration system (Kendrick et al., 2008a), as well as the southernmost Osborne deposit, which predated intrusion of the Williams-Naraku batholiths (Fisher and Kendrick, 2008).

The strongly radiogenic noble gas isotope signature of low salinity fluid inclusions associated with the Mt Isa copper mineralization in the Western Fold Belt is unlikely to reflect the involvement of magmatic fluids but could be explained if: i) surface-derived basinal fluids were advected into the >10-15 km deep basement (which was the source of the Williams-Naraku batholiths in the Eastern Fold Belt); or ii) basement metamorphism produced a metamorphic fluid that ascended to the site of mineralization (Kendrick et al., 2006, 2011b). Mt Isa copper related fluid inclusions have much higher Br/Cl than the iron-oxide-copper-gold deposits (Fig 11.21a; Heinrich et al., 1993; Kendrick et al., 2006c). If the Mt Isa ore fluids had a surface origin, the Br/Cl data indicate sub-aerial evaporation as the dominant source of salinity (Fig 11.21a; Kendrick et al., 2006c). However, Kendrick et al. (2006c) argued that because fairly few lithologies have $^{40}Ar/^{36}Ar$ of >>30,000, a surface-derived fluid could not easily acquire a $^{40}Ar/^{36}Ar$ ratio of ≥30,000 without significantly increasing its ^{36}Ar concentration above air saturation levels (ground waters with air saturated ^{36}Ar concentrations usually have meteoric O-H isotope signatures and $^{40}Ar/^{36}Ar$ of <500; section 5.1; Phillips and Castro, 2003). Furthermore, it was estimated the ^{36}Ar concentration of the silica fluid inclusions with the highest $^{40}Ar/^{36}Ar$ ratios are in the range that would be expected in basement-derived metamorphic fluids (based on typical OH and ^{36}Ar concentrations; Fig 11.21b; Kendrick et al., 2006c).

The total variation in fluid inclusion Br/Cl, I/Cl, ^{36}Ar concentration and $^{40}Ar/^{36}Ar$ in silica and dolomite fluid inclusions (Fig 11.21), was interpreted to result from mixing basement-derived metamorphic fluids and basinal fluids (best preserved in the dolomite fluid inclusions which have the highest salinity), with an additional contribution of noble gases (including ^{36}Ar) derived from the meta-sedimentary country rocks (Fig 11.21; Kendrick et al., 2006c). The viability of this model depends on the relative timing of copper mineralization

and fluid producing mineral breakdown reactions in the basement. The model is broadly consistent with mineralization during the latter part of the Isan orogeny (Perkins et al. 1999), but is not consistent with the younger post-orogenic Re-Os age of ~1370 Ma (Gregory et al., 2008). However, this age is not defined by a statistical isochron (cf. Gregory et al., 2008), and is difficult to reconcile with constraints on the relative timing of copper mineralization (Perkins, 1984; Swager, 1985). An Isan age is preferred here, suggesting the <1500 Ma South Nicholson Group sediments can be excluded as a source of basinal fluids during mineralization (cf. Wilde, 2011).

11.5.6.3 Comparison of fluid inclusions and unusual geo-fluids

The CO_2 fluid inclusions associated with Na-Ca alteration in the Eastern Fold Belt of the Mt Isa Inlier (Fig 11.19) have Ne, Ar and Xe isotope signatures similar to CO_2 well gases in the Doe Canyon and McElmo Dome gas fields of the Colorado plateau, USA (Table 11.5; Gilfillan et al., 2008). The CO_2 well gases therefore provide a useful analogue for the CO_2 fluid inclusions and *vice versa*.

Helium leaked out of the CO_2 fluid inclusions; however, the McElmo Dome well gases have a $^3He/^4He$ ratio of ~0.13-0.17 Ra (Gilfillan et al., 2008), that demonstrate a small mantle helium component could potentially have been present in the CO_2 fluid inclusions. The Williams-Naraku batholiths had an igneous basement source with a mean age of 650-700 Myr at the time of melting (Page and Sun, 1998; Mark, 2001). The strongly radiogenic Ne-Ar-Xe signature of the CO_2 fluid inclusions is consistent with a source from a basement derived magma (Kendrick et al., 2011b). However, input of a minor mantle component has been suggested as a heat source, to explain the presence of mafic lithologies, and abundant CO_2 fluid inclusions (Oliver et al., 2008). Comparison of the CO_2 fluid inclusions and well gases underlines that the noble gas data (Fig 11.19) do not preclude input of a minor mantle component in the Eastern Fold Belt mineral systems (Kendrick et al., 2011b).

The CO_2 gases in the Colorado Plateau have variable magmatic or metamorphic sources but have been trapped in sedimentary reservoirs for millions of years, meaning they are important natural analogues for testing long term CO_2 sequestration and storage (Gilfillan et al., 2009). The CO_2 well gases have undoubtedly interacted with modern ground waters to a much greater extent than CO_2 trapped in fluid inclusions at depths of 8-10 km (cf. Gilfillan et al., 2009; Kendrick et al., 2011b). However, fluid inclusion studies could provide new insights on the possible origins of atmospheric noble gases in deeply sourced CO_2 fluids (Kendrick et al., 2011b). This could have important implications for interpreting the extent of CO_2 well gas interaction with groundwater, and therefore quantifying the long term viability of CO_2 storage (Gilfillan et al., 2009).

Fracture-hosted waters in deep gold mines in South Africa with a dominantly surface origin have extremely radiogenic noble gas signatures similar to fluids inclusions from the Mt Isa Inlier and St Ives goldfield of Western Australia (Table 11.5; Lippmann et al., 2003; Lippmann-Pipke et al., 2011; Kendrick et al., 2011bc). These waters contain abiogenic CH_4, the origin of which is of great interest for determining the potential depth of the biosphere (e.g. Lippmann et al., 2003; Lippmann-Pipke et al., 2011). However, interpretation of strongly radiogenic noble gas isotope signatures in modern fracture-hosted ground waters and ancient fluid inclusions is not exactly analogous. The interpretation that strongly radiogenic noble gas isotope signatures in the Mt Isa Inlier and Yilgarn craton had basement origins is based on the premise that at the time of mineralization, both terranes comprised a layer of relatively young meta-sediment, or altered volcanic rocks (e.g. lithologies with significant atmospheric noble gas), underlain by much older igneous basement (with low abundances of

non-radiogenic noble gas; cf. Table 11.3). In contrast, the much greater age of the Kapvaal craton at the present day (>3 Ga), implies that highly radiogenic noble gas signatures could potentially be acquired by fluid interaction with a much greater range of lithologies, making it more difficult to infer a source.

11.5.6.4 Neon isotope systematics of basement lithologies

Neon isotope data are conventionally presented in a three isotope diagram (Fig 11.22) and the ratio of nucleogenic $^{21}Ne^*$ to $^{22}Ne^*$ is obtained by correcting the data for an atmospheric contribution based on the non-radiogenic ^{20}Ne isotope (implicitly assuming that there is no mantle Ne contribution). Neon data for a variety of natural gases from all over the world have a limited range of $^{21}Ne^*/^{22}Ne^*$, with a best fit value of ~0.52 (Kennedy et al., 1990; Ballentine and Burnard, 2002). The $^{21}Ne^*$ and $^{22}Ne^*$ isotopes are produced by alpha particles interacting with ^{18}O or ^{19}F, respectively. The empirically determined relationship between $^{21}Ne^*/^{22}Ne^*$ and O/F (Hünemohr, 1989), indicates the average $^{21}Ne^*/^{22}Ne^*$ of 0.52 determined for fluids in sedimentary basins corresponds an average U mineral O/F ratio of ~113 in sedimentary basins (Kennedy et al., 1990).

In contrast to natural gases in sedimentary basins, fluid inclusions in metamorphic environments have extremely variable $^{21}Ne^*/^{22}Ne^*$ (Fig 11.22). The minimum $^{21}Ne^*/^{22}Ne^*$ values of ~0.1, obtained for H_2O dominated fluid inclusions in samples from the Eastern Fold Belt of the Mt Isa Inlier (Fig 11.22), are equivalent to an O/F ratio of ~22, that may be representative of U minerals in halogen-rich metasediments (Kendrick et al., 2011b). In contrast, much higher $^{21}Ne^*/^{22}Ne^*$ values of up to ~3.3, in the Witwatersrand basin (Lippmann-Pipke, et al., 2011), are equivalent to a U mineral O/F ratio of ~720 that is close to the O/F ratio of average crust (e.g. Rudnick and Gao, 2003). Similarly high $^{21}Ne^*/^{22}Ne^*$ values are obtained for fluid inclusions suggested to contain basement-derived noble gases in the Mt Isa Inlier (Kendrick et al., 2011b) and Yilgarn craton (Fig 11.22; Kendrick et al., 2011c).

The variable $^{21}Ne^*/^{22}Ne^*$ reported for metamorphic environments indicate U and F are unevenly distributed through the crust and that fluids in low porosity metamorphic environments (<<0.1 % porosity) are much more poorly mixed than fluids in sedimentary basins (Kendrick et al., 2011b).

A second important consideration for interpretation of neon data is that, if the anomalous neon signature is representative of an igneous basement source (e.g. Fig 11.19), the atmosphere corrected $^{21}Ne^*/^{22}Ne^*$ ratio is unlikely to be representative of the $^{21}Ne/^{22}Ne$ production ratio (Kendrick et al., 2011bc). This is because comparison with basalt glasses suggests that igneous basement lithologies, that are not exposed to seawater, would probably have had a prominent mantle noble gas component at time zero (basalt glasses have mixed mantle and atmospheric noble gas signatures; e.g. Graham, 2002). If the igneous basement had an initially mantle signature, the $^{21}Ne/^{22}Ne$ production ratio would be obtained by a vector from the mantle composition, implying a $^{21}Ne/^{22}Ne$ production ratio of significantly less than the air corrected $^{21}Ne^*/^{22}Ne^*$ ratio (see Fig 11.22; Kendrick et al., 2011bc). It should be noted that the broad mixing trend between the 'anomalous crustal neon' with very high $^{21}Ne/^{22}Ne$ and air does not indicate the basement had an initially atmospheric composition. This trend probably reflects mixing of the distinct basement signature with atmospheric noble gases present in either ground water or meta-sediments (e.g. Fig 11.19; Kendrick et al., 2011bc). Noble gas mixing trends have complicated histories that are only unraveled by fully understanding the ultimate origin and evolution of noble gases in the Earth's deep crust (see Fig 11.19 and section 5.6.2; Kendrick et al., 2011bc).

11.6. Summary

Noble gases and halogens record a range of distinct compositions in the fluid inclusions of different types of ore deposit (section 5). The isotopes of helium provide a sensitive means for detecting the presence of mantle-derived components and the orders of magnitude variation in noble gas and halogen signatures means they can provide powerful constraints on fluid origins. Considerable advances have been made in improving the interpretation of these signatures over the last 5 – 10 years.

Investigation of modern pore fluids in marine sediments (Fehn et al., 2000; 2003; 2006; 2007; Muramatsu et al., 2001; 2007; Tomaru et al., 2007ab; 2009), and regional-scale studies focused on sediment-hosted ore deposits (Fairmaid et al., 2011; Fu et al., 2012), have conclusively demonstrated halogens (Br as well as I) are partly buffered by organic matter in both sedimentary and metamorphic environments (Fig 11.14). In addition, the Br/Cl versus I/Cl three element diagram has been demonstrated as a powerful tool for deconvolving organic Br contributions (Fairmaid et al., 2011; Kendrick et al., 2011d).

The investigation of eclogite facies fluid inclusions has provided evidence for halogen fractionation during metamorphism (Svensen et al., 2001; Kendrick et al., 2011a), and new work has started to document the halogen composition of the MORB mantle and hydrous mineral phases (Kendrick et al., 2011a; 2012; Kendrick, 2012).

Investigation of noble gases in metamorphic minerals and fluid inclusions has demonstrated atmospheric noble gases are introduced into crustal lithologies during seawater alteration (Kendrick et al., 2011a). Furthermore, fluid inclusions associated with a range of ore deposits in the Mt Isa Inlier have an identifiable contribution of atmospheric noble gas derived from wall-rock (Fig 11.19a). In most crustal environments the $^{3}He/^{4}He$ isotope signature of a magmatic fluid is more conservative than the heavy noble gases (e.g. Section 5.4.3; Fig 11.8). However, fluid interaction with basalt is recognized as an important source of ^{3}He in mid-ocean ridge vent fluids (e.g. Abrajano et al., 1988; 1990; Stuart et al., 1994); and igneous rocks intruded into the crust can preserve mantle $^{3}He/^{4}He$ signatures for 10's of Myr (Staudacher and Allegre, 1988; Moreira et al., 2003), suggesting mobilization of ^{3}He during metamorphism is possible.

These observations indicate simplistic interpretations of noble gases in crustal fluids based on equating atmospheric noble gases with the presence of ASW, or diminutive mantle ^{3}He components with a magmatic fluid, are not applicable to high temperature fluids trapped in fluid inclusions. Several examples have been highlighted in this chapter were constraints from noble gases have shown good agreement with other stable (O, H, C, S) or radiogenic (Sr, Nd, Pb) isotope systems, and it has been highlighted that the interpretation of fluid inclusion noble gas isotope signatures is often analogous to other isotope systems (Fig 11.19; Fairmaid et al., 2011; Kendrick et al., 2011bc; Fu et al., 2012). Noble gases can reveal features of hydrothermal systems that are overprinted in other isotopic systems because their signatures vary by such large amounts (e.g. orders of magnitude; Table 11.2 and 4), not because they behave 'conservatively': noble gas abundances in rocks are significant at the low water/rock ratios relevant to many crustal fluids (Table 11.3).

Finally the behavior of noble gases in the crust depends on the crustal setting (temperature and water-rock ratio) and timescale over which the behavior is observed. Over long time periods, there is a true exchange of noble gases between solid lithological and fluid reservoirs. Atmospheric noble gases initially adsorbed onto sedimentary materials are incorporated into mineral structures during diagenesis (Podosek et al., 1980; 1981); and atmospheric noble gases are trapped in hydrous lithologies formed during seawater alteration

(Kendrick et al., 2011a). Trapped atmospheric noble gases are then released to the fluid phase, along with radiogenic noble gas isotopes, during dehydration metamorphism. This results in most fluid inclusions (with strongly rock-buffered O and H isotope signatures), having greater than ASW ^{36}Ar concentrations (Fig 11.9). In contrast, preservation of uniform ASW ^{36}Ar concentrations in all crustal fluids would imply the crust acted as a permanent sink for introduced atmospheric noble gases.

11.6.1 Future directions

Noble gas and halogen analysis has been demonstrated as a powerful tool for constraining fluid origins in ore deposits and these techniques can be applied to geological processes in other settings. In particular, future work is required to better understand the long term exchange of noble gases between atmospheric and crustal reservoirs. Future studies may therefore combine investigation of fluid inclusion and mineral phases or whole rocks to a much greater extent than has previously been the case (e.g. Pettke et al., 1997).

The available data indicate most geological fluids have elevated noble gas concentrations (Fig 11.9), and changes in concentration have been suggested as a means to infer the way in which noble gas isotope signatures are altered during fluid-rock interaction (Fig 11.21b; Kendrick et al., 2006c). Provided steps are taken to minimise the adsorption of water, manometric determination of total gas (CO_2, CH_4, H_2O) pressures during fluid inclusion analysis would allow wider determination of noble gas concentrations, enabling these ideas to be more widely evaluated.

Further improvements in fluid inclusion analysis are possible. The work of Scheidegger et al. (2010) has demonstrated that simple variations in sample preparation procedure can help eliminate undesirable modern air contaminants. Laser ablation of individual fluid inclusions is unlikely to be widely applicable; however, 213 and 193 nm lasers could be used for controlled ablation of unusually large fluid inclusions or groups of related fluid inclusion. Opaque sulphide minerals have been demonstrated as robust containers of helium, suggesting routine application of near infra-red microscopy techniques to characterise the fluid inclusions trapped in these minerals is desirable.

Analysis of neon isotopes can be used to test for mantle components in quartz samples that do not always retain helium. Furthermore, rigorous investigation of quartz samples with variable helium retentivities, using transmission electron microscopy, may enable the properties that cause helium leakage to be identified. The potential for helium (and other noble gases) to diffuse into, or out of, fluid inclusions should be studied systematically. Experimental studies establishing a thermodynamic basis for noble gas retention in fluid inclusions hosted by different minerals over a range of temperatures and pressures is desirable.

The combined behaviour of halogens and noble gases during groundwater-hydrocarbon interaction is poorly constrained (Kendrick et al., 2011d). Significant advances could be made by combined investigation of ground waters and fully characterised fluid inclusions (Ballentine et al., 1994; Lippmann-Pipke et al., 2011). These areas provide exciting avenues for further research.

References

Abrajano TA, Sturchio NC, Bohlke JK, Lyon GL, Poreda RJ, Stevens CM (1988) Methane-hydrogen gas seeps, Zambales Ophiolite, Philippines: Deep or shallow origin? Chemical Geology 71(1-3):211-222

Abrajano TA, Sturchio NC, Kennedy BM, Lyon GL, Muehlenbachs K, Bohlke JK (1990) Geochemistry of reduced gas related to serpentinisation of the zambales Ophiolite, Phillippines. Applied Geochemistry 5(5-6):625-630

Aeschbach-Hertig W, Peeters F, Beyerle U, Kipfer R (2000) Palaeotemperature reconstruction from noble gases in ground water taking into account equilibration with entrapped air. Nature 405(6790):1040-1044

Ague JJ (2003) Fluid Flow in the Deep Crust. In: Treatise on Geochemistry, vol 3. Elsevier Ltd., pp 195-228

Amari S, Ozima M (1988) Extra-terrestrial noble gases in deep sea sediments. Geochimica et Cosmochimica Acta 52(5):1087-1095

Andrew AS, Heinrich CA, Wilkins RWT, Patterson DJ (1989) Sulfur Isotope Systematics of Copper Ore Formation at Mount Isa, Australia. Econ. Geol. 84:1614-1626

Andrews JN, Giles IS, Kay RLF, Lee DJ, Osmond JK, Cowart JB, Fritz P, Barker JF, Gale J (1982) Radioelements, Radiogenic Helium and Age Relationships for Groundwaters from the Granites at Stripa, Sweden. Geochimica et Cosmochimica Acta 46(9):1533-1543

Andrews JN, Hussain N, Youngman MJ (1989) Atmospheric and radiogenic gases in groundwaters from the Stripa granite. Geochimica et Cosmochimica Acta 53(8):1831-1841

Andrews JN, Kay RLF (1982) Natural Production of Tritium in Permeable Rocks. Nature 298(5872):361-363

Andrews JN, Lee DJ (1979) Inert gases in groundwater from the Bunter Sandstone of England as indicaters of age and paleoclimate trends. Journel of Hydrology 41:233

Arnaud NO, Kelley SP (1995) Evidence for excess argon during high pressure metamorphism in the Dora Maira Massif (western Alps, Italy), using an ultra-violet laser ablation microprobe 40Ar-39Ar technique. Contributions to Mineralogy and Petrology 121(1):1-11

Bach W, Frueh-Green GL (2010) Alteration of the Oceanic Lithosphere and Implications for Seafloor Processes. Elements 6(3):173-178

Baker ET, Lupton JE (1990) Changes in submarien Hydrothermal He-3/Heat Ratios as an Indicator of Magmatic Tectonic Activity. Nature 346(6284):556-558

Baker ET, Lupton JE, Resing JA, Baumberger T, Lilley MD, Walker SL, Rubin KH (2011) Unique event plumes from a 2008 eruption on the Northeast Lau Spreading Center. Geochem. Geophys. Geosyst. 12

Baker T (2002) Emplacement depth and carbon dioxide-rich fluid inclusions in intrusion-related gold deposits. Econ. Geol. Bull. Soc. Econ. Geol. 97(5):1111-1117

Ballentine CJ, Barfod DN (2000) The origin of air-like noble gases in MORB and OIB. Earth and Planetary Science Letters 180(1-2):39-48

Ballentine CJ, Burgess R, Marty B (2002) Tracing fluid origin, transport and interaction in the crust. In: Porcelli D, Ballentine CJ, Wieler R (eds) Noble Gases in Geochemistry and Cosmochemistry, vol 47. Geochemical Society/ Mineralogical Society of America, pp 539-614

Ballentine CJ, Burnard PG (2002) Production, release and transport of noble gases in the continental crust. In: Porcelli D, Ballentine CJ, Wieler R (eds) Noble gases in geochemistry and cosmochemistry, vol 47. Geochemical society/ Mineralogical Society of America, pp 481-538

Ballentine CJ, Mazurek M, and Gautschi A, (1994) Thermal constraints on crustal rare gas release and migration: Evidence from Alpine fluid inclusions. Geochimica et Cosmochimica Acta 58: 4333-4348.
Ballentine CJ, O'Nions RK, Oxburgh ER, Horvath F, Deak J (1991) Rare gas constraints on hydrocarbon accumulation, crustal degassing and groundwater flow in the Pannonian Basin. Earth and Planetary Science Letters 105(1-3):229-246
Banks DA, Green R, Cliff RA, Yardley BWD (2000) Chlorine isotopes in fluid inclusions: Determination of the origins of salinity in magmatic fluids. Geochim. et Cosmochim. Acta 64:1785-1789
Barton MD, Johnson DA (1996) Evaporitic-source model for igneous related Fe oxide (REE-Cu-Au-U) mineralization. Geology 24:259-262
Bein A, Hovorka SD, Fisher RS, Roedder E (1991) Fluid Inclusions in Bedded Permian Halite, Palo Duro Basin, Texas - Evidence for Modification of Seawater in Evaporite Brine-Pools and Subsequent Early Diagenesis. Journal of Sedimentary Petrology 61(1):1-14
Biester H, Keppler F, Putschew A, Martinez-Cortizas A, Petri M (2004) Halogen retention, organohalogens, and the role of organic matter decomposition on halogen enrichment in two Chilean peat bogs. Environ. Sci. Technol. 38(7):1984-1991
Bodnar RJ (2003) Interpretation of Data from Aqueous-Electrolyte Fluid Inclusions. In: Samson I, Anderson A, Marshall D (eds) Fluid Inclusions Analysis and Interpretation, vol 32. Mineralogical Association of Canada, Vancouver, British Columbia, pp 81-101
Bodnar RJ, Binns PR, Hall DL (1989) Synthetic fluid inclusions - VI. Quantitative evaluation of the decrepitation behaviour of fluid inclusions in quartz at one atmosphere confining pressure. Journal of metamorphic geology 7:229-242
Böhlke JK, Irwin JJ (1992a) Brine Histroy Indicated by Argon, Krypton, Chlorine, Bromine and Iodine Analyses of Fluid Inclusions from the Mississippi Valley Type Lead-Fluorite-Barite Deposits at Hansonburg, New-Mexico. Earth and Planetary Science Letters 110(1-4):51-66
Böhlke JK, Irwin JJ (1992b) Laser microprobe analyses of noble gas isotopes and halogens in fluid inclusions: Analyses of microstandards and synthetic inclusions in quartz. Geochim. Cosmochim. Acta 56:187-201
Böhlke JK, Irwin JJ (1992c) Laserprobe analyses of Cl, Br, I, and K in fluid inclusions: Implications for the sources of salinity in some ancient hydrothermal fluids. Geochimica et Cosmochimica Acta 56:203-225
Bosch A, Mazor E (1988) Natural-gas association with water and oil as depicted by atmospheric noble-gases - case studies from the southeastern Mediterranean coastal-plain. Earth and Planetary Science Letters 87(3):338-346
Boschmann W, Becker R, Lippolt HJ (1984) Eignungsprufung von Erzmineralien fur U + Th/He Datiering. Verlag-Chemie:361-373
Boundy TM, Hall CM, Li G, Essene EJ, Halliday AN (1997) Fine-scale isotopic heterogeneities and fluids in the deep crust: a40Ar/39Ar laser ablation and TEM study of muscovites from a granulite-eclogite transition zone. Earth and Planetary Science Letters 148(1-2):223-242
Burgess R, Taylor RP, Fallick AE, Kelley SP (1992) Ar-40-Ar-39 Laser Microprobe Study of Fluids in Different Color Zones of a Hydrothermal Scheelite Crystal from the Dae-Hwa W Mine, South Korea. Chemical Geology 102(1-4):259-267
Burnard P, Graham D, Turner G (1997) Vesicle-specific noble gas analyses of "popping rock"; implications for primordial noble gases in the Earth. Science 276:568-571

Burnard P, Harrison D (2005) Argon isotope constraints on modification of oxygen isotopes in Iceland Basalts by surficial processes. Chemical Geology 216(1-2):143-156
Burnard PG, Hu R, Turner G, Bi XW (1999) Mantle, crustal and atmospheric noble gases in Ailaoshan Gold deposits, Yunnan Province, China. Geochimica Et Cosmochimica Acta 63(10):1595-1604
Burnard PG, Polya DA (2004) Importance of mantle derived fluids during granite associated hydrothermal circulation: He and Ar isotopes of ore minerals from Panasqueira. Geochimica et Cosmochimica Acta 68(7):1607-1615
Burnard PG, Stuart F, Turner G (1994) C---He---Ar variations within a dunite nodule as a function of fluid inclusion morphology. Earth and Planetary Science Letters 128(3-4):243-258
Butterfield AW, Turner G (1985) Ancient argon in cherts. Terra Cognita 5:201-202
Cadogan PH (1977) Palaeoatmospheric argon in Rhynie chert. Nature 268:38
Carpenter AB, Trout ML, Pickett EE (1974) Preliminary report on the origin and chemical evolution of lead- and zinc-rich oil field brines in central Mississippi. Econ. Geol. 69:1191-1206
Castro MC, Hall CM, Patriarche D, Goblet P, Ellis BR (2007) A new noble gas paleoclimate record in Texas — Basic assumptions revisited. Earth and Planetary Science Letters 257(1–2):170-187
Champion DC, Sheraton JW (1997) Geochemistry and Nd isotope systematics of Archaean granites of the Eastern Goldfields, Yilgarn Craton, Australia: implications for crustal growth processes. Precambrian Research 83(1-3):109-132
Chang J (2011) Table of Nuclides, KAERI (Korea Atomic Energy Research Institute). Available at: http://atom.kaeri.re.kr/ton/. Retrieved Feb 2011.
Chi GX, Savard MM (1997) Sources of basinal and Mississippi Valley-type mineralizing brines: mixing of evaporated seawater and halite-dissolution brine. Chemical Geology 143(3-4):121-125
Cline JS, Bodnar RJ (1991) Can Economic Porphyry Copper Mineralization be Generated by a Typical Calc-Alkaline Melt? Journal of Geophysical Research-Solid Earth and Planets 96(B5):8113-8126
Collins AG, Bennett JH, Manuel OK (1971) Iodine and Algae in Sedimentary Rocks Associated with Iodine-Rich Brines Geol. Soc. Am. Bull. 82(9):2607-&
Connors KA, Page RW (1995) Relationships between magmatism, metamorphism and deformation in the western Mount Isa Inlier, Australia. Precambrian Research 71:131-153
Crocetti CA, Holland HD (1989) Sulfur-Lead Isotope Systematics and the Composition of Fluid Inclusions in Galena from the Viburnum Trend, Missouri. Econ. Geol. 84:2196-2216
Cumbest RJ, Johnson EL, Onstott TC (1994) Argon composition of metamorphic fluid inclusions - Implications for 40Ar-39Ar Geochronology. Geol. Soc. Am. Bull. 106(7):942-951
Drescher J, Kirsten T, Schäfer K (1998) The rare gas inventory of the continental crust, recovered by the KTB Continental Deep Drilling Project. Earth and Planetary Science Letters 154(1-4):247-263
Drever JI (1997) The Geochemistry of Natural Waters: Surface and Groundwater Environments, vol. Prentice-Hall Inc., Upper Saddle River, New Jersey
Duncan RJ, Stein HJ, Evans KA, Hitzman MW, Nelson EP, Kirwin DJ (2011) A New Geochronological Framework for Mineralization and Alteration in the Selwyn-Mount Dore Corridor, Eastern Fold Belt, Mount Isa Inlier, Australia: Genetic Implications for Iron Oxide Copper-Gold Deposits. Econ. Geol. 106(2):169-192

Elmer FL, White RW, Powell R (2006) Devolatilization of metabasic rocks during greenschist-amphibolite facies metamorphism. Journal of Metamorphic Geology 24(6):497-513
Ernst WG (1971) Metamorphic Zonations on Presumably Subducted Lithospheric Plates from Japan, California and Alps. Contributions to Mineralogy and Petrology 34(1):43-&
Etminan H, Hoffmann CF (1989) Biomarkers in fluid inclusions: A new tool in constraining source regimes and its implications for the genesis of Mississippi Valley-type deposits. Geology 17(1):19-22
Eugster O, Niedermann S, Thalmann C, Frei R, Kramers J, Krahenbuhl U, Liu YZ, Hofmann B, Boer RH, Reimold WU, Bruno L (1995) Noble gases, K, U, Th, and Pb in native gold. J. Geophys. Res.-Solid Earth 100(B12):24677-24689
Fairmaid AM, Kendrick MA, Phillips D, Fu B (2011) The Origin and Evolution of Mineralizing Fluids in a Sediment-Hosted Orogenic-Gold Deposit, Ballarat East, Southeastern Australia. Econ Geol 106(4):653-666
Fehn U, Lu Z, Tomaru H (2006) 129I/I ratios and halogen concentrations in pore water of Hydrate Ridge and their relevence for the origin of gas hydrates: a progress report. In: Trehu AM, Bohrmann G, Torres ME, Colwell FS (eds) Proceedings of the Ocean Drilling Program, Scientific Results, vol 204. pp 1-25
Fehn U, Moran JE, Snyder GT, Muramatsu Y (2007) The initial 129I/I ratio and the presence of [`]old' iodine in continental margins. Nuclear Instruments and Methods in Physics Research Section B: Beam Interactions with Materials and Atoms 259(1):496-502
Fehn U, Snyder G, Egeberg PK (2000) Dating of pore waters with I-129: Relevance for the origin of marine gas hydrates. Science 289(5488):2332-2335
Fehn U, Snyder GT, Matsumoto R, Muramatsu Y, Tomaru H (2003) Iodine dating of pore waters associated with gas hydrates in the Nankai area, Japan. Geology 31(6):521-524
Ferguson J, Etminan H, Ghassemi F (1993) Geochemistry of Deep Formation Waters in the Canning Basin, Western Australia and Their Relationship to Zn-Pb Mineralisation. Australian Journal of Earth Sciences 40(5):471-483
Fisher L, Kendrick MA (2008) Metamorphic fluid origins in the Osborne Fe oxide–Cu–Au deposit, Australia: evidence from noble gases and halogens. Mineralium Deposita 43:483-497
Fontes JC, Andrews JN, Walgenwitz F (1991) Evaluation de la production naturelle in situ d'argon-36 via le chlore-36; implications geochimiques et geochronologiques; Evaluation of natural in situ production of argon-36 via chlorine-36; geochemical and geochronological implications. Comptes Rendus de l'Academie des Sciences, Serie 2, Mecanique, Physique, Chimie, Sciences de l'Univers, Sciences de la Terre 313(6):649-654
Fontes JC, Matray JM (1993) Geochemistry and origin of formation brines from the Paris Basin, France 1. Brines associated with Triassic salts. Chemical Geology 109:149-175
Foster DRW, Rubenach MJ (2006) Isograd pattern and regional low pressure, high-temperature metamorphism of pelitic, mafic and calc-silicate rocks along an east-west section through the Mt Isa Inlier. Australian Journal of Earth Science 53:167-186.
Fu B, Kendrick MA, Fairmaid AM, Phillips D, Wilson CJL, Mernagh TP (2012) New Constraints on Fluid Sources in Orogenic Gold Deposits, Victoria, Australia. Contributions to Mineralogy and Petrology 163:427-447
Fu B, Touret JLR, Zheng YF (2001) Fluid inclusions in coesite-bearing eclogites and jadeite quartzite at Shuanghe, Dabie Shan (China). Journal of Metamorphic Geology 19(5):531-547

Fu B, Zheng Y-F, Touret JLR (2002) Petrological, isotopic and fluid inclusion studies of eclogites from Sujiahe, NW Dabie Shan (China). Chemical Geology 187(1-2):107-128
Fuge R, Johnson CC (1986) The geochemistry of iodine - a review. Environmental Geochemistry Health 8:31-54
Garven G, Raffensperger JP (1997) Hydrology and Geochemistry of Ore Genesis in Sedimentary Basins. In: Barnes HL (ed) The Geochemistry of Hydrothermal Ore Deposits, vol. John Wiley and Sons, Inc., New York, pp 125-190
Gilfillan SMV, Ballentine CJ, Holland G, Blagburn D, Lollar BS, Stevens S, Schoell M, Cassidy M (2008) The noble gas geochemistry of natural CO2 gas reservoirs from the Colorado Plateau and Rocky Mountain provinces, USA. Geochimica et Cosmochimica Acta 72(4):1174-1198
Gilfillan SMV, Lollar BS, Holland G, Blagburn D, Stevens S, Schoell M, Cassidy M, Ding Z, Zhou Z, Lacrampe-Couloume G, Ballentine CJ (2009) Solubility trapping in formation water as dominant CO2 sink in natural gas fields. Nature 458(7238):614-618
Giorgis D, Cosca M, Li S (2000) Distribution and significance of extraneous argon in UHP eclogite (Sulu terrain, China): insight from in situ 40Ar/39Ar UV-laser ablation analysis. Earth and Planetary Science Letters 181(4):605-615
Gize AP, Barnes HL (1987) The organic geochemistry of two mississippi valley-type lead-zinc deposits. Econ. Geol. 82(2):457-470
Goldfarb RJ, Groves DI, Gardoll S (2001) Orogenic gold and geologic time: a global synthesis. Ore Geology Reviews 18(1-2):1-75
Graham DW (2002) Noble Gas Isotope Geochemistry of Mid-Ocean Ridge and Ocean Island Basalts: Characterisation of Mantle Source Reservoirs. In: Porcelli D, Ballentine CJ, Wieler R (eds) Noble Gases in Geochemistry and Cosmochemistry, vol 47. pp 245-317
Graupner T, Niedermann S, Kempe U, Klemd R, Bechtel A (2006) Origin of ore fluids in the Muruntau gold system: Constraints from noble gas, carbon isotope and halogen data. Geochimica et Cosmochimica Acta 70(21):5356-5370
Graupner T, Niedermann S, Rhede D, Kempe U, Seltmann R, Williams CT, Klemd R (2010) Multiple sources for mineralizing fluids in the Charmitan gold(-tungsten) mineralization (Uzbekistan). Mineralium Deposita 45(7):667-682
Gregory M, Schaefer B, Keays R, Wilde A (2008) Rhenium–osmium systematics of the Mount Isa copper orebody and the Eastern Creek Volcanics, Queensland, Australia: implications for ore genesis. Mineralium Deposita 43(5):553-573
Groves DI, Condie KC, Goldfarb RJ, Hronsky JMA, Vielreicher RM (2005) 100th Anniversary Special Paper: Secular changes in global tectonic processes and their influence on the temporal distribution of gold-bearing mineral deposits. Econ. Geol. 100(2):203-224
Groves DI, Goldfarb RJ, Robert F, Hart CJR (2003) Gold deposits in metamorphic belts: Overview of current understanding, outstanding problems, future research, and exploration significance. Econ. Geol. Bull. Soc. Econ. Geol. 98(1):1-29
Hanes JA, York D, Hall CM (1985) An Ar-40/Ar-39 Geochronological and Electron-Microprobe Investigation of an Archean Pyroxenite and its Bearing on Ancient Atmospheric Compositions. Canadian Journal of Earth Sciences 22(7):947-958
Hanor JS (1994) Origin of saline fluids in sedimentary basins. In: Parnell J (ed) Geofluids: Origin, Migration and Evolution of fluids in Sedimentary Basins, vol 78. Geological Society Special Publication, pp 151-174

Heinrich CA, Andrew AS, Wilkins WT, Patterson DJ (1989) A Fluid Inclusion and Stable Isotope Study of Synmetamorphic Copper Ore Formation at Mount Isa, Australia. Econ. Geol. 84:529-550
Heinrich CA, Bain JHC, Fardy JJ, and Waring CL, (1993) Br/Cl geochemistry of hydrothermal brines associated with Proterozoic metasediment-hosted copper mineralisation at Mount Isa, northern Australia. Geochimica et Cosmochimica Acta 57: 2991-3000.
Heinrich CA (2003) Fluid-fluid interactions in magmatic-hydrothermal ore formation. In: Liebscher A, Heinrich CA (eds) Fluid-Fluid Interactions, vol 65. Mineralogical Society of America, Geochemical Society, pp 363-387
Hermann AG (1980) Bromide distribution between halite and NaCl-saturated seawater. Chemical Geology 28:171-177
Heyl AV, Landis GP, Zartman RE (1974) Isotopic Evidence for the Origin of Mississippi Valley-Type Mineral Deposits: A Review. Econ. Geol. 69(6):992-1006
Hitchon B (2006) Lead and zinc in formation waters, Alberta Basin, Canada: Their relation to the Pine Point ore fluid. Applied Geochemistry 21(1):109-133
Hiyagon H (1989) Neon Isotope Measurement in the Presence of Helium. Mass Spectrometry 37:325-330
Ho SE, Groves D, McNaughton NJ, Mikucki EJ (1992) The source of ore fluids and solutes in Archaean lode-gold deposits of Western Australia. Journal of Volcanology and Geothermal Research 50:173-196
Holland G, Ballentine CJ (2006) Seawater subduction controls the heavy noble gas composition of the mantle. Nature 441(7090):186-191
Holser WT (1979) Trace elements and isotopes in evaporites. In: Burns RG (ed) Marine minerals: Mineralogical Society of America Short Course Notes, vol 6. pp 295-346
Honda M, Kurita K, Hamano Y, Ozima M (1982) Experimental Studies of He and Ar Degassing During Rock Fracturing. Earth and Planetary Science Letters 59(2):429-436
Hough MA, Bierlein FP, Ailleres L, McKnight S (2010) Nature of gold mineralisation in the Walhalla Goldfield, southeast Australia. Australian Journal of Earth Sciences 57(7):969-992
Hu R-Z, Burnard PG, Bi X-W, Zhou M-F, Peng J-T, Su W-C, Zhao J-H (2009) Mantle-derived gaseous components in ore-forming fluids of the Xiangshan uranium deposit, Jiangxi province, China: Evidence from He, Ar and C isotopes. Chemical Geology 266(1-2):86-95
Hu RZ, Burnard PG, Bi XW, Zhou MF, Pen JT, Su WC, Wu KX (2004) Helium and argon isotope geochemistry of alkaline intrusion-associated gold and copper deposits along the Red River-Jinshajiang fault belt, SW China. Chemical Geology 203(3-4):305-317
Hu RZ, Burnard PG, Turner G, Bi XW (1998) Helium and Argon isotope systematics in fluid inclusions of Machangqing copper deposit in west Yunnan province, China. Chemical Geology 146(1-2):55-63
Hünemohr H (1989) Edelgase in U- and Th-reichen mineralen und die Bestimmung der 21Ne-dicktarget-ausbeute der 18O(alpha, n)21Ne Kernreaktion in Bereich 4.0-8.8 MeV. In, vol Ph.D. Johannes-Gutenberg University, Mainz
Irwin JJ, Reynolds JH (1995) Multiple stages of fluid trapping in the Stripa granite indicated by laser microprobe analysis of Cl, Br, I, K, U, and nucleogenic plus radiogenic Ar, Kr, and Xe in fluid inclusions. Geochimica et Cosmochimica Acta 59(2):355-369
Irwin JJ, Roedder E (1995) Diverse origins of fluid inclusions at Bingham (Utah, USA), Butte (Montana, USA), St. Austell (Cornwall, UK) and Ascension Island (mid-

Atlantic, UK), indicated by laser microprobe analysis of Cl, K, Br, I, Ba + Te, U, Ar, Kr, and Xe. Geochimica et Cosmochimica Acta, 59(2):295-312
Jambon A, Deruelle B, Dreibus G, Pineau F, (1995) Chlorine and bromine abundance in MORB: The contrasting behaviour of the Mid-Atlantic Ridge and East Pacific Rise and implications for chlorine geodynamic cycle: Chemical Geology 126: 101-117
Jean-Baptiste P, Fouquet Y (1996) Abundance and isotopic composition of helium in hydrothermal sulfides from the East Pacific Rise at 13 °N. Geochimica et Cosmochimica Acta 60(1):87-93
Johnson L, Burgess R, Turner G, Milledge JH, Harris JW (2000) Noble gas and halogen geochemistry of mantle fluids: comparison of African and Canadian diamonds. Geochimica et Cosmochimica Acta 64: 717-732
Kelley S (2002) Excess argon in K-Ar and Ar-Ar geochronology. Chemical Geology 188(1-2):1-22
Kelley S, Turner G, Butterfield AW, Shepherd TJ (1986) The source and significance of argon isotopes in fluid inclusions from areas of mineralization. Earth Plan. Sci. Lett. 79:303-318
Kendrick MA (2007) Comment on 'Paleozoic ages and excess Ar-40 in garnets from the Bixiling eclogite in Dabieshan, China: New insights from Ar-40/Ar-39 dating by stepwise crushing by Hua-Ning Qiu and JR Wijbrans'. Geochimica Et Cosmochimica Acta 71(24):6040-6045
Kendrick MA (2012) High precision Cl, Br and I determination in mineral standards using the noble gas method. Chemical Geology 292-293:116-126
Kendrick MA, Baker T, Fu B, Phillips D, Williams PJ (2008a) Noble gas and halogen constraints on regionally extensive mid-crustal Na-Ca metasomatism, the Proterozoic Eastern Mount Isa Block, Australia. Precambrian Research 163(1-2):131-150
Kendrick MA, Burgess R, Harrison D, Bjørlykke A (2005) Noble gas and halogen evidence on the origin of Scandinavian sandstone-hosted Pb-Zn deposits. Geochimica et Cosmochimica Acta 69:109-129
Kendrick MA, Burgess R, Leach D, Pattrick RAD (2002a) Hydrothermal fluid origins in Mississippi valley-type ore deposits: combined noble gas (He, Ar, Kr) and halogen (Cl, Br, I) analysis of fluid inclusions from the Illinois-Kentucky Fluorspar district, Viburnum Trend, and Tri-State districts, mid-continent United States. Econ. Geol. 97(3):452-479
Kendrick MA, Burgess R, Pattrick RAD, Turner G (2001a) Fluid inclusion noble gas and halogen evidence on the origin of Cu-Porphyry mineralising fluids. Geochimica et Cosmochimica Acta 65(16):2651-2668
Kendrick MA, Burgess R, Pattrick RAD, Turner G (2001b) Halogen and Ar-Ar age determinations of inclusions within quartz veins from porphyry copper deposits using complementary noble gas extraction techniques. Chemical Geology 177(3-4):351-370
Kendrick MA, Burgess R, Pattrick RAD, Turner G (2002b) Hydrothermal fluid origins in a fluorite-rich Mississippi valley-type deposit: combined noble gas (He, Ar, Kr) and halogen (Cl, Br, I) analysis of fluid inclusions from the South Pennine Orefield, United Kingdom. Econ. Geol. 97(3):435-451
Kendrick MA, Duncan R, Phillips D (2006c) Noble gas and halogen constraints on mineralizing fluids of metamorphic versus surficial origin: Mt Isa, Australia. Chemical Geology 235(3-4):325-351
Kendrick MA, Honda M, Gillen D, Baker T, Phillips D (2008b) New constraints on regional brecciation in the Wernecke Mountains, Canada, from He, Ne, Ar, Kr, Xe, Cl, Br and I in fluid inclusions. Chemical Geology 255(1-2):33-46

Kendrick MA, Honda M, Oliver NHS, Phillips D (2011b) The noble gas systematics of late-orogenic H2O-CO2 fluids, Mt Isa, Australia. Geochimica et Cosmochimica Acta 75(6):1428-1450
Kendrick MA, Honda M, Walshe J, Petersen K (2011c) Fluid sources and the role of abiogenic-CH4 in Archean gold mineralization: constraints from noble gases and halogens. Precambrian Research 189:313-327
Kendrick MA, Kamenetsky VS, Phillips D, Honda M (2012) Halogen (Cl, Br, I) systemtics of mid-ocean ridge basalts: a Macquarie Island case study. Geochimica et Cosmochimica Acta 81:82-93
Kendrick MA, Mark G, Phillips D (2007) Mid-crustal fluid mixing in a Proterozoic Fe oxide-Cu-Au deposit, Ernest Henry, Australia: Evidence from Ar, Kr, Xe, Cl, Br, and I. Earth and Planetary Science Letters 256(3-4):328-343
Kendrick MA, Miller JM, Phillips D (2006b) Part II: Evaluation of 40Ar-39Ar quartz ages: Implications for fluid inclusion retentivity and determination of initial 40Ar/36Ar values in Proterozoic samples. Geochimica et Cosmochimica Acta 70:2562-2576
Kendrick MA, Phillips D (2009) New constraints on the release of noble gases during in vacuo crushing and application to scapolite Br-Cl-I and 40Ar/39Ar age determinations. Geochimica et Cosmochimica Acta 73(19):5673-5692
Kendrick MA, Phillips D, Miller JM (2006a) Part I. Decrepitation and degassing behaviour of quartz up to 1560 C: Analysis of noble gases and halogens in complex fluid inclusions assemblages. Geochimica et Cosmochimica Acta 70:2540-2561
Kendrick MA, Phillips D, Wallace M, Miller JM (2011d) Halogens and noble gases in sedimentary formation waters and Zn-Pb deposits: A case study from the Lennard Shelf, Australia. Applied Geochemistry 26:2089-2100
Kendrick MA, Scambelluri M, Honda M, Phillips D (2011a) High abundances of noble gas and chlorine delivered to the mantle by serpentinite subduction. Nature Geoscience 4:807-812
Kennedy BM (1988) Noble gases in vent water from the Juan de Fuca Ridge. Geochimica et Cosmochimica Acta 52(7):1929-1935
Kennedy BM, Hiyagon H, Reynolds JH (1990) Neon: a striking crustal uniformity. Earth and Planetary Science Letters 98:277-286
Kennedy BM, Torgersen T, van Soest MC (2002) Multiple atmospheric noble gas components in hydrocarbon reservoirs: A study of the Northwest Shelf, Delaware Basin, SE New Mexico. Geochimica Et Cosmochimica Acta 66(16):2807-2822
Kesler SE (2007) Geochemistry of fluid inclusion brines from Earth's oldest Mississippi Valley-type (MVT) deposits, Transvaal Supergroup, South Africa. Chemical Geology 237:274-288
Kesler SE, Appold MS, Martini AM, Walter LM, Huston TJ, Kyle JR (1995) Na-Cl-Br systematics of mineralising brines in Mississippi Valley-type deposits. Geology 23:641-644
Kharaka YK, Hanor JS (2003) Deep Fluids in the Continents: I. Sedimentary Basins. In: Treatise on Geochemistry, vol. Pergamon, Oxford, pp 1-48
Kharaka YK, Specht DJ (1988) The solubility of noble gases in crude oil at 25-100°C. Applied Geochemistry 3(2):137-144
Kipfer R, Aeschbach-Hertig W, Peeters F, Stute M (2002) Noble Gases in Lakes and Ground Waters. In: Porcelli D, Ballentine CJ, Wieler R (eds) Noble Gases in Geochemistry and Cosmochemistry, vol 47. The Mineralogical Society of America, pp 615-700
Kluge T, Marx T, Scholz D, Niggemann S, Mangini A, Aeschbach-Hertig W (2008) A new tool for palaeoclimate reconstruction: Noble gas temperatures from fluid inclusions in speleothems. Earth and Planetary Science Letters 269(3-4):408-415

Lang JR, Baker T (2001) Intrusion-related gold systems: the present level of understanding. Mineralium Deposita 36(6):477-489
Langmuir CH, Vocke Jr RD, Hanson GN, Hart SR (1978) A general mixing equation with applications to Icelandic basalts. Earth and Planetary Science Letters 37(3):380-392
Large RR, Bull SW, Maslennikov VV (2011) A Carbonaceous Sedimentary Source-Rock Model for Carlin-Type and Orogenic Gold Deposits. Econ. Geol. 106(3):331-358
Leach DL, Dwight B, Lewchuk MT, Symons DTA, de Marsily G, Brannon J (2001) Mississippi Valley-type lead-zinc deposits through geological time: implications from recent age-dating research. Mineralium Deposita 36(8):711-740
Leach DL, Rowan EL (1986) Genetic link between Ouachita Foldbelt Tectonism and the Mississippi Valley-type Lead-Zinc Deposits of the Ozarks. Geology 14(11):931-935
Lee JY, Marti K, Severinghaus JP, Kawamura K, Yoo HS, Lee JB, Kim JS (2006) A redetermination of the isotopic abundances of atmospheric Ar. Geochimica et Cosmochimica Acta 70(17):4507-4512
Li XF, Wang CZ, Hua RM, Wei XL (2010) Fluid origin and structural enhancement during mineralization of the Jinshan orogenic gold deposit, South China. Mineralium Deposita 45(6):583-597
Lippmann-Pipke J, Sherwood Lollar B, Niedermann S, Stroncik NA, Naumann R, van Heerden E, Onstott TC (2011) Neon identifies two billion year old fluid component in Kaapvaal Craton. Chemical Geology 283(3-4):287-296
Lippmann J, Stute M, Torgersen T, Moser DP, Hall JA, Lin L, Borcsik M, Bellamy RES, Onstott TC (2003) Dating ultra-deep mine waters with noble gases and 36Cl, Witwatersrand Basin, South Africa. Geochimica et Cosmochimica Acta 67(23):4597-4619
Lueders V, Niedermann S (2010) Helium Isotope Composition of Fluid Inclusions Hosted in Massive Sulfides from Modern Submarine Hydrothermal Systems. Econ. Geol. 105(2):443-449
Lupton JE, Baker ET, Massoth GJ (1989) Variable 3He/heat ratios in submarine hydrothermal systems: evidence from two plumes over the Juan de Fuca ridge. Nature 337(6203):161-164
Lupton JE, Baker ET, Massoth GJ (1999) Helium, heat, and the generation of hydrothermal event plumes at mid-ocean ridges. Earth and Planetary Science Letters 171(3):343-350
MacCready T, Goleby BR, Goncharov A, Drummond BJ, Lister GS (1998) A framework of overprinting orogens based on interpretation of the Mt Isa deep siesmic transect. Econ. Geol. 93:1422-1434
Mamyrin BA, Anufriyev GS, Kamenskiy IL, Tolstikhin (1970) Determination of the composition of atmospheric helium. Geochemistry International 7:498-505
Mao JW, Li YQ, Goldfarb R, He Y, Zaw K (2003) Fluid inclusion and noble gas studies of the Dongping gold deposit, Hebei Province, China: A mantle connection for mineralization? Econ. Geol. Bull. Soc. Econ. Geol. 98(3):517-534
Mark G (2001) Nd isotope and petrogenetic constraints for the origin of the Mount Angelay igneous complex: implications for the origin of intrusions in the Cloncurry district, NE Australia. Precambrian Research 105:17-35
Mark G, Foster DRW, Pollard PJ, Williams PJ, Tolman J, Darvall M, Blake KL (2004) Stable isotope evidence for magmatic fluid input during large-scale Na-Ca alteration in the Cloncurry Fe oxide Cu-Au district, NW Queensland, Australia. Terra Nova 16:54-61

Mark G, Oliver NHS, Carew MJ (2006) Insights into the genesis and diversity of epigenetic Cu-Au mineralisation in the Cloncurry district, Mt Isa Inlier, northwest Queensland. Australian Journal of Earth Science 53:109-124
Markl G, Bucher K (1998) Composition of fluids in the lower crust inferred from metamorphic salt in lower crustal rocks. Nature 391(6669):781-783
Martin JB, Gieskes JM, Torres M, Kastner M (1993) Bromine and iodine in Peru margin sediments and pore fluids: Implications for fluid origins. Geochimica et Cosmochimica Acta 57(18):4377-4389
Matsuda J, Nagao K (1986) Noble-Gas Abundances in a Deep-Sea Sediment Core from Eastern Equatorial Pacific. Geochem. J. 20(2):71-80
Mavrogenes JA, Bodnar RJ (1994) Hydrogen movement into and out of fluid inclusions in quartz: Experimental evidence and geologic implications. Geochimica et Cosmochimica Acta 58(1):141-148
McCaffrey MA, Lazar B, Holland HD (1986) The evaporation path of seawater and the composition of Br- and K+ with halite. Journal of Sedimentary Petrology 57:928-937
McDougall I, Harrison TM (1999) Geochronology and Thermochronology by the 40Ar/39Ar Method, vol. Oxford University Press, New York
McLaren S, Sandiford M, Hand M (1999) High radiogenic heat-producing granites and metamorphism - An example from the western Mount Isa inlier, Australia. Geology 27(8):679-682
Mernagh T, Bastrakov EN, Zaw K, Wygralak AS, Wyborn LAI (2007) Comparison of fluid inclusion data and mineralisation processes for Australian orogenic gold and intrusion related gold systems. Acta Petrol. Sin. 23:21-32
Moreira M, Blusztajn J, Curtice J, Hart S, Dick H, Kurz MD (2003) He and Ne isotopes in oceanic crust: implications for noble gas recycling in the mantle. Earth and Planetary Science Letters 216(4):635-643
Morelli R, Creaser RA, Seltmann R, Stuart FM, Selby D, Graupner T (2007) Age and source constraints for the giant Muruntau gold deposit, Uzbekistan, from coupled Re-Os-He isotopes in arsenopyrite. Geology 35(9):795-798
Muramatsu Y, Doi T, Tomaru H, Fehn U, Takeuchi R, Matsumoto R (2007) Halogen concentrations in pore waters and sediments of the Nankai Trough, Japan: Implications for the origin of gas hydrates. Applied Geochemistry 22(3):534-556
Muramatsu Y, Fehn U, Yoshida S (2001) Recycling of iodine in fore-arc areas: evidence from the iodine brines in Chiba, Japan. Earth and Planetary Science Letters 192(4):583-593
Muramatsu Y, Wedepohl KH (1998) The distribution of iodine in the earth's crust. Chemical Geology 147(3-4):201-216
Nahnybida T, Gleeson SA, Rusk BG, Wassenaar LI (2009) Cl/Br ratios and stable chlorine isotope analysis of magmatic-hydrothermal fluid inclusions from Butte, Montana and Bingham Canyon, Utah. Mineralium Deposita 44(8):837-848
Neumayr P, Walshe J, Hagemann S, Petersen K, Roache A, Frikken P, Horn L, Halley S (2008) Oxidized and reduced mineral assemblages in greenstone belt rocks of the St. Ives gold camp, Western Australia: vectors to high-grade ore bodies in Archaean gold deposits? Mineralium Deposita 43(3):363-371
Nissenbaum A (1977) Minor and Trace Elements in Dead Sea Water. Chemical Geology 19:99-111
Niedermann S., (2002) Cosmic-Ray-Produced Noble Gases in Terrestrial Rocks: Dating Tools for Surface Processes. In Porcelli, C.J., Ballentine, C.J., and Wieler, R., eds., Noble Gases in Geochemistry and Cosmochemistry, Volume 47: Reviews in

Mineralogy and Geochemistry: Washington DC, Mineralogical Society of America, p. 731-777.
Nier AO (1950) A redetermination of the relative abundances of the isotopes of carbon, nitrogen, oxygen, argon and potassium. Physical Review 77:789-793
O'Nions RK, Oxburgh ER (1988) Helium, volatile fluxes and the development of continental crust. Earth and Planetary Science Letters 90:331-347
Oliver NHS (1995) Hydrothermal History of the Mary Kathleen Fold Belt, Mt Isa Block, Queensland. Australian Journal of Earth Science 42:267-279
Oliver NHS, Butera KM, Rubenach MJ, Marshall LJ, Cleverley JS, Mark G, Tullemans F, Esser D (2008) The protracted hydrothermal evolution of the Mount Isa Eastern Succession: A review and tectonic implications. Precambrian Research 163(1-2):108-130
Oliver NHS, Cartwright I, Wall VJ, Golding SD (1993) The stable isotope signature of kilometre-scale fracture-dominated metamorphic fluid pathways, Mary Kathleen, Australia. Journal of Metamorphic Geology 11:705-720
Oliver NHS, Cleverley JS, Mark G, Pollard PJ, Fu B, Marshall LJ, Rubenach MJ, Williams PJ, Baker T (2004) Modeling the role of sodic alteration in the genesis of iron-oxide-copper-gold deposits, eastern Mt Isa block, Australia. Econ. Geol. 99:1145-1176
Osawa T (2004) A new correction technique for mass interferneces by 40Ar++ and CO2++ during isotope analysis of a small amount of Ne. Journal of Mass Spectrom. Soc. Jpn. 52(4):230-232
Oxburgh ER, O'Nions RK, Hill RI (1986) Helium isotopes in sedimentary basins. Nature 324(6098):632-635
Ozima M, Podosek FA (2002) Noble Gas Geochemistry, vol. Cambridge University Press,
Page RW, Sun S-S (1998) Aspects of geochronology and crustal evolution in the Eastern Fold Belt, Mount Isa Inlier. Australian Journal of Earth Sciences 45:343-362
Painter MGM, Golding SD, Hannan KW, Neudert MK (1999) Sedimentologic, petrographic, and sulfur isotope constraints on fine-grained pyrite formation at Mount Isa Mine and environs, Northwest Queensland, Australia. Econ. Geol. 94(6):883-912
Perkins C, Heinrich, C.A., and Wyborn, L.A.I. (1999) 40Ar/39Ar Geochronology of Copper Mineralisation and Regional Alteration, Mount Isa, Australia. Econ. Geol. 94:23-36
Perkins WG (1984) Mount Isa Silica Dolomite and Copper Orebodies: The Result of a Syntectonic Hydrothermal Alteration System. Econ. Geol. 79(4):601-637
Pettke T, Diamond LW (1997) Oligocene gold quartz veins at Brusson, NW Alps: Sr isotopes trace the source of ore-bearing fluid to over a 10-km depth. Econ. Geol. Bull. Soc. Econ. Geol. 92(4):389-406
Pettke T, Frei R (1996) Isotope systematics in vein gold from Brusson, Val d'Ayas (NW Italy) .1. Pb/Pb evidence for a Piemonte metaophiolite Au source. Chemical Geology 127(1-3):111-124
Pettke T, Frei R, Kramers JD, Villa IM (1997) Isotope systematics in vein gold from Brusson, Val d'Ayas (NW Italy) .2. (U+Th)/He and K/Ar in native Au and its fluid inclusions. Chemical Geology 135(3-4):173-187
Phillips D, Fu B, Wilson CJL, Kendrick MA, Fairmaid AM, Miller JM (2012) Timing of Gold Mineralisation in the Western Lachlan Orogen, SE Australia: A Critical Overview. Australian Journal of Earth Sciences in press
Phillips D, Miller JM (2006) 40Ar/39Ar dating of mica-bearing pyrite from thermally overprinted Archaean gold deposits. Geology 34:397-400
Phillips FM, Castro MC (2003) Groundwater Dating and Residence-time Measurements. In: Treatise on Geochemistry, vol 5. Elsevier, pp 451-497

Phillips GN, Powell R (1993) Link Between Gold Provinces. Econ. Geol. Bull. Soc. Econ. Geol. 88(5):1084-1098
Pili É, Kennedy BM, Conrad ME, Gratier JP (2011) Isotopic evidence for the infiltration of mantle and metamorphic CO2-H2O fluids from below in faulted rocks from the San Andreas Fault system. Chemical Geology 281(3-4):242-252
Pinti DL, Béland-Otis C, Tremblay A, Castro MC, Hall CM, Marcil J-S, Lavoie J-Y, Lapointe R (2011) Fossil brines preserved in the St-Lawrence Lowlands, Québec, Canada as revealed by their chemistry and noble gas isotopes. Geochimica et Cosmochimica Acta 75(15):4228-4243
Pinti DL, Marty B, Andrews JN (1997) Atmosphere-derived noble gas evidence for the preservation of ancient waters in sedimentary basins. Geology 25(2):111-114
Pirajno F (2000) Ore Deposits and Mantle Plumes, vol. Kluwer Academic Publishers, Dordrecht, The Netherlands
Pitre F, Pinti DL (2010) Noble gas enrichments in porewater of estuarine sediments and their effect on the estimation of net denitrification rates. Geochimica et Cosmochimica Acta 74(2):531-539
Plumlee GS, Goldhaber MB, Rowan EL (1995) Potential Role of Magmatic Gases in the Genesis of Illinois-Kentucky Fluorspar Deposits - Implications from Chemical Reaction Path Modelling. Econ. Geol. Bull. Soc. Econ. Geol. 90(5):999-1011
Podosek FA, Bernatowicz TJ, Kramer FE (1981) Adsorption of xenon and krypton on shales. Geochimica et Cosmochimica Acta 45:2401-2415
Podosek FA, Honda M, Ozima M (1980) Sedimentary Noble Gases. Geochimica et Cosmochimica Acta 44:1875-1884
Polito PA, Bone Y, Clarke JDA, Mernagh TP (2001) Compositional zoning of fluid inclusions in the Archaean Junction gold deposit, Western Australia: a process of fluid wall-rock interaction? Australian Journal of Earth Sciences 48(6):833-855
Pollard PJ (2000) Evidence of a magmatic fluid and metal source for Fe-oxide Cu-Au Mineralisation. In: Porter TM (ed) Hydrothermal Iron Oxide Copper Gold & Related Deposits: A Global Perspective, vol. PGC Publishing, Adelaide, pp 27-41
Pollard PJ (2001) Sodic-(calcic) alteration in Fe-oxide-Cu-Au districts: and origin via unmixing of magmatic H2O-CO2-NaCl +/- CaCl2-KCl fluids. Mineralium Deposita 36:93-100
Polya DA, Foxford KA, Stuart F, Boyce A, Fallick AE (2000) Evolution and paragenetic context of low [delta]D hydrothermal fluids from the Panasqueira W-Sn deposit, Portugal: new evidence from microthermometric, stable isotope, noble gas and halogen analyses of primary fluid inclusions. Geochimica et Cosmochimica Acta 64(19):3357-3371
Powell R, Will TM, Phillips GN (1991) Metamorphism in Archean Greenstone Belts - Calculated Fluid Compositions and Implications for Gold Mineralization. Journal of Metamorphic Geology 9(2):141-150
Pujol M, Marty B, Burnard P, Philippot P (2009) Xenon in Archean barite: Weak decay of (130)Ba, mass-dependent isotopic fractionation and implication for barite formation. Geochimica Et Cosmochimica Acta 73(22):6834-6846
Raquin A, Moreira MA, Guillon F (2008) He, Ne and Ar systematics in single vesicles: Mantle isotopic ratios and origin of the air component in basaltic glasses. Earth and Planetary Science Letters 274(1-2):142-150
Reddy SM, Kelley SP, Magennis L (1997) A microstructural and argon laserprobe study of shear zone development at the western margin of the Nanga Parbat-Haramosh Massif, western Himalaya. Contributions to Mineralogy and Petrology 128(1):16-29
Robb LJ (2005) Introduction to Ore-Forming Processes, vol. Blackwell Publishing, p 373

Rock NMS, Groves DI (1988) Do lamprophyres carry gold as well as diamonds? Nature 332(6161):253-255
Roedder E (1971a) Fluid-inclusion Evidence on the Environment of Formation of Mineral Deposits of the Southern Appalachian Valley. Econ Geol 66:777-791
Roedder E (1971b) Fluid inclusion studies on the porphyry-type ore deposits at Bingham, Utah, Butte, Montana, and Climax, Colorado. Econ. Geol. 66(1):98-118
Roedder E (1984) Fluid Inclusions, vol 12. Mineralogical society of America, Bookcrafters, Inc., Chelsea, Michigan, p 646
Rudnick RL, Gao S (2003) Composition of the Continental Crust. In: Treatise of Geochemistry, vol 3. Elsevier Ltd., pp 1-64
Rusk BG, Reed MH, Dilles JH, Klemm LM, Heinrich CA (2004) Compositions of magmatic hydrothermal fluids determined by LA-ICP-MS of fluid inclusions from the porphyry copper-molybdenum deposit at Butte, MT. Chemical Geology 210(1-4):173-199
Russell MJ, Smith FW (1979) Plate Separation, Alkali Magmatism and Fluorite Mineralisation in Northern and Central England. Transactions of the Institution of Mining and Metallurgy Section B-Applied Earth Science 88(FEB):B30-B30
Sanchez V, Stuart FM, Martin-Crespo T, Vindel E, Corbella M, Cardellach E (2010) Helium isotopic ratios in fluid inclusions from fluorite-rich Mississippi Valley-Type district of Asturias, northern Spain. Geochem. J. 44(6):E1-E4
Sandiford M, McLaren S, Neumann N (2002) Long-term thermal consequences of the redistribution of heat-producing elements associated with large-scale granitic complexes. Journal of Metamorphic Geology 20(1):87-98
Scambelluri M, Bottazzi P, Trommsdorff V, Vannucci R, Hermann J, Gòmez-Pugnaire MT, Lòpez-Sànchez Vizcaino V (2001) Incompatible element-rich fluids released by antigorite breakdown in deeply subducted mantle. Earth and Planetary Science Letters 192(3):457-470
Scambelluri M, Piccardo GB, Philippot P, Robbiano A, Negretti L (1997) High salinity fluid inclusions fromed from recycled seawater in deeply subducted alpine serpentinite. Earth and Planetary Science Letters 148:485-499
Scheidegger Y, Baur H, Brennwald MS, Fleitmann D, Wieler R, Kipfer R (2010) Accurate analysis of noble gas concentrations in small water samples and its application to fluid inclusions in stalagmites. Chemical Geology 272(1-4):31-39
Scheidegger Y, Brennwald MS, Fleitmann D, Jeannin PY, Wieler R, Kipfer R (2011) Determination of Holocene cave temperatures from Kr and Xe concentrations in stalagmite fluid inclusions. Chemical Geology 288(1-2):61-66
Schilling JC, Unni CK, and Bender ML (1978) Origin of Chlorine and Bromine in the oceans: Nature 273: 631-636.
Schwarz WH, Trieloff M, Altherr R (2005) Subduction of solar-type noble gases from extraterrestrial dust: constraints from high-pressure low-temperature metamorphic deep-sea sediments. Contributions to Mineralogy and Petrology 149(6):675-684
Shelton KL, Taylor RP, So CS (1987) Stable Isotope Studies of the Dae Hwa Tungsten-Molybdenum Mine, Republic or Korea - Evidence of Progressive Meteoric Water Interaction in a Tungsten-Bearing Hydrothermal System. Econ. Geol. 82(2):471-481
Sherlock S, Kelley S (2002) Excess argon evolution in HP-LT rocks: a UVLAMP study of phengite and K-free minerals, NW Turkey. Chemical Geology 182(2-4):619-636
Siemann MG (2003) Extensive and rapid changes in seawater chemistry during the Phanerozoic: evidence from Br contents in basal halite. Terra Nova 15(4):243-248
Siemann MG, Schramm M (2000) Thermodynamic modelling of the Br partition between aqueous solutions and halite. Geochimica Et Cosmochimica Acta 64(10):1681-1693
Sillitoe RH (2010) Porphyry Copper Systems. Econ. Geol. 105(1):3-41

Simmons SF, Brown KL (2006) Gold in Magmatic Hydrothermal Solutions and the Rapid Formation of a Giant Ore Deposit. Science 314(5797):288-291
Simmons SF, Sawkins FJ, Schlutter DJ (1987) Mantle derived helium in two Peruvian hydrothermal ore deposits. Nature 329:429-432
Smith SP, Kennedy BM (1983) The solubility of noble gases in water and in NaCl brine. Geochimica et Cosmochimica Acta 47:503-515
So CS, Shelton KL, Seidemann DE, Skinner BJ (1983) The Dae Hwa Tungsten-Molybdenum Mine, Republic of Korea - A Geochemical Study. Econ. Geol. 78(5):920-930
Spikings RA, Foster DA, Kohn BP, Lister GS (2002) Post-orogenic (<1500 Ma) thermal history of the Palaeo-Mesoproterozoic, Mt. Isa province, NE Australia. Tectonophysics 349:327- 365
Staudacher T, Allègre CJ (1988) Recycling of oceanic crust and sediments: the noble gas subduction barrier. Earth and Planetary Science Letters 89(2):173-183
Stuart FM, Burnard PG, Taylor RP, Turner G (1995) Resolving mantle and crustal contributions to ancient hydrothermal fluids: He---Ar isotopes in fluid inclusions from Dae Hwa W---Mo mineralisation, South Korea. Geochimica et Cosmochimica Acta 59(22):4663-4673
Stuart FM, Turner G (1992) The abundance and isotopic composition of the noble gases in ancient fluids. Chemical Geology 101:97-109
Stuart FM, Turner G (1998) Mantle-derived Ar-40 in mid-ocean ridge hydrothermal fluids: implications for the source of volatiles and mantle degassing rates. Chemical Geology 147(1-2):77-88
Stuart FM, Turner G, Duckworth RC, Fallick AE (1994) Helium-isotopes as tracers of trapped hydrothermal fluids in ocean-floor sulphides. Geology 22(9):823-826
Sumino H, Burgess R, Mizukami T, Wallis SR, Holland G, Ballentine CJ (2010) Seawater-derived noble gases and halogens preserved in exhumed mantle wedge peridotite. Earth and Planetary Science Letters 294(1-2):163-172
Sun XM, Zhang Y, Xiong DX, Sun WD, Shi GY, Zhai W, Wang SW (2009) Crust and mantle contributions to gold-forming process at the Daping deposit, Ailaoshan gold belt, Yunnan, China. Ore Geology Reviews 36(1-3):235-249
Svensen H, Banks DA, Austreim H (2001) Halogen contents of eclogite facies fluid inclusions and minerals: Caledonides, western Norway. Journal of Metamorphic Geology 19:165-178
Sverjensky DA (1986) Genesis of Missisippi Valley-type Lead-Zinc Deposits. Annual Review of Earth and Planetary Sciences 14:177-199
Swager CP (1985) Syndeformational Carbonate-replacement Model for the Copper Mineralization at Mount Isa, Northwest Queensland: A Microstructural Study. Econ. Geol. 80:107-125
Taylor HP (1997) Oxygen and hydrogen isotope relationships in hydrothermal mineral deposits. In: Barnes HL (ed) Geochemistry of hydrothermal ore deposits, vol. John Wiley and Sons, Inc., New York, pp 229-302
Thomas HV, Large RE, Bull SW, Maslennikov V, Berry RF, Fraser R, Froud S, Moye R (2011) Pyrite and Pyrrhotite Textures and Composition in Sediments, Laminated Quartz Veins, and Reefs at Bendigo Gold Mine, Australia: Insights for Ore Genesis. Econ. Geol. 106(1):1-31
Tolstikhin I, Kamensky I, Tarakanov S, Kramers J, Pekala M, Skiba V, Gannibal M, Novikov D (2010) Noble gas isotope sites and mobility in mafic rocks and olivine. Geochimica et Cosmochimica Acta 74(4):1436-1447
Tomaru H, Fehn U, Lu ZL, Matsumoto R (2007a) Halogen systematics in the Mallik 5L-38 gas hydrate production research well, Northwest Territories, Canada: Implications for

the origin of gas hydrates under terrestrial permafrost conditions. Applied Geochemistry 22(3):656-675
Tomaru H, Fehn U, Lu ZL, Takeuchi R, Inagaki F, Imachi H, Kotani R, Matsumoto R, Aoike K (2009) Dating of Dissolved Iodine in Pore Waters from the Gas Hydrate Occurrence Offshore Shimokita Peninsula, Japan: 129I Results from the D/V Chikyu Shakedown Cruise. Resource Geology 59(4):359-373
Tomaru H, Lu Z, Snyder GT, Fehn U, Hiruta A, Matsumoto R (2007b) Origin and age of pore waters in an actively venting gas hydrate field near Sado Island, Japan Sea: Interpretation of halogen and 129I distributions. Chemical Geology 236(3-4):350-366
Torgersen T (2010) Continental degassing flux of (4)He and its variability. Geochem. Geophys. Geosyst. 11
Torgersen T, Kennedy BM, van Soest MC (2004) Diffusive separation of noble gases and noble gas abundance patterns in sedimentary rocks. Earth and Planetary Science Letters 226(3-4):477-489
Torgersen T, O'Donnell J (1991) The Degassing Flux from the Solid Earth - Release by Fracturing. Geophysical Research Letters 18(5):951-954
Turner G (1988) Hydrothermal fluids and argon isotopes in quartz veins and cherts. Geochimica et Cosmochimica Acta 52:1443-1448
Turner G, Bannon MP (1992) Argon Isotope Geochemistry of Inclusion Fluids from Granite-Associated Mineral Veins in Southwest and Northwest England. Geochimica et Cosmochimica Acta 56(1):227-243
Turner G, Burnard P, Ford JL, Gilmour JD, Lyon IC, Stuart FM (1993) Tracing fluid sources and interactions. Philisophical transactions of the Royal Society London A 344:127-140
Turner G, Stuart F (1992) Helium Heat Ratios and Deposition Temperatures of Sulfides from the Ocean-Floor. Nature 357(6379):581-583
Viets JG, Hofstra AH, Emsbo P (1996) Solute composition of fluid inclusions in sphalerite from North American and European Mississippi Valley-Type ore deposits: ore fluids derived from evaporated seawater. Society of Economic Geologists Special Publication 4:465-482
Viets JG, Leach DL (1990) Genetic Implications of Regional and Temporal Trends in Ore Fluid Geochemistry of Mississippi Valley -Type Deposits in the Ozark Region. Econ. Geol. 85:842-861
Valkiers S, Vendelbo D, Berglund M, de Podesta M (2010) Preparation of argon Primary Measurement Standards for the calibration of ion current ratios measured in argon. International Journal of Mass Spectrometry 291(1–2):41-47
Wallace MW, Middleton HA, Johns B, Marshallsea S (2002) Hydrocarbons and Mississippi Valley-type Sulfides in the Devonian Reef Complexes of the eastern Lennard Shelf, Canning Basin, Western Australia. In: Keep M, Moss SJ (eds) The Sedimentary Basins of Western Australia 3: Proceedings of the Petroleum Exploration Society of Australia Symposium, Perth, WA., vol., Perth, WA, pp 795-816
Warren C, Sherlock S, Kelley S (2011) Interpreting high-pressure phengite 40Ar/39Ar laserprobe ages: an example from Saih Hatat, NE Oman. Contributions to Mineralogy and Petrology 161(6):991-1009
Webber AP, Roberts S, Burgess R, Boyce AJ (2011) Fluid mixing and thermal regimes beneath the PACMANUS hydrothermal field, Papua New Guinea: Helium and oxygen isotope data. Earth and Planetary Science Letters 304(1-2):93-102
Wei HX, Sun XM, Zhai W, Shi GY, Liang YH, Mo RW, Han MX, Yi JZ (2010) He-Ar-S isotopic compositions of ore-forming fluids in the Bangbu large-scale gold deposit in southern Tibet, China. Acta Petrol. Sin. 26(6):1685-1691

Wilde AR (2011) Mount Isa copper orebodies: improving predictive discovery. Australian Journal of Earth Sciences 58(8):937-951
Wilkinson JJ, Stoffell B, Wilkinson CC, Jeffries TE, Appold MS (2009) Anomalously Metal-Rich Fluids Form Hydrothermal Ore Deposits. Science 323(5915):764-767
Winckler G, Kipfer R, Aescbach-Hertig W, Botz R, Schmidt M, Schuler S, Bayer R (2000) Sub sea floor boiling of Red Sea Brines: New indication from noble gas data. Geochimica et Cosmochimica Acta 64(9):1567-1575
Yardley BWD (2005) 100th Anniversary Special Paper: Metal concentrations in crustal fluids and their relationship to ore formation. Econ. Geol. 100(4):613-632
Yardley BWD, Banks D, Bottrell SH, Diamond LW (1993) Post-metamorphic gold-quartz veins from N.W. Italy: the composition and origin of the ore fluid. Mineral. Mag. 57:407-422
Yokochi R, Marty B, Pik R, Burnard P (2005) High He-3/He-4 ratios in peridotite xenoliths from SW Japan revisited: Evidence for cosmogenic He-3 released by vacuum crushing. Geochem. Geophys. Geosyst. 6:12
Zaikowski A, Kosanke BJ, Hubbard N (1987) Noble gas composition of deep brines from the Palo Duro Basin, Texas. Geochimica et Cosmochimica Acta 51:73-84
Zeng Z, Qin Y, Zhai S (2001) He, Ne and Ar isotope compositions of fluid inclusions in hydrothermal sulfides from the TAG hydrothermal field Mid-Atlantic Ridge. Science in China Series D: Earth Sciences 44(3):221-228
Zherebtsova IK, Volkova NN (1966) Experimental study of behaviour of trace elements in the process of natural solar evaporation of Black Sea water and Lake Sasky-Sivash brine. Geochemistry international 3:656-670
Zhou S, Ye X (2002) Noble gas isotopic compositions of deep carbonate rocks from the Tarim Basin. Chinese Science Bulletin 47(9):774-778
Ziegler JF (1980) Hanfbook of stopping cross-sections for energentic ions in all elements, vol. Pergamon Press, New York
Zuber A, Weise SM, Osenbruck K, Matenko T (1997) Origin and age of saline waters in Busko Spa (Southern Poland) determined by isotope, noble gas and hydrochemical methods: evidence of interglacial and pre-quaternary warm climate recharges. Applied Geochemistry 12(5):643-660

Table 11.1. Noble gas proxy isotopes produced by irradiation

Parent element	Nuclear reaction	Proxy isotope
Cl	$^{37}Cl(n, \gamma)^{38}Cl(\beta)^{38}Ar$	$^{38}Ar_{Cl}$
Br	$^{79}Br(n, \gamma)^{80}Br(\beta)^{80}Kr$	$^{80}Kr_{Br}$
I	$^{127}I(n, \gamma)^{128}I(\beta)^{128}Xe$	$^{128}Xe_{I}$
K	$^{39}K(n,p)^{39}Ar$	$^{39}Ar_{K}$
Ca	$^{40}Ca(n,\alpha)^{37}Ar$	$^{37}Ar_{Ca}$
U	Fission	$^{134}Xe_{U}$

Extended ^{40}Ar-^{39}Ar methodology enables simultaneous measurement of the halogens, K and U with naturally occurring noble gas isotopes (^{36}Ar, ^{40}Ar, ^{84}Kr, ^{129}Xe, ^{130}Xe) in irradiated samples (Kendrick, 2012).

Table 11.2. Diagnostic noble gas isotope ratios

	$^{3}He/^{4}He$ (R/Ra)	$^{20}Ne/^{22}Ne$	$^{21}Ne/^{22}Ne$	$^{40}Ar/^{36}Ar$
Atmosphere	1	9.8	0.029	299
Crust	<0.1	<9.8	>0.029	298-100,000
Mantle (MORB)	8	12.5	0.058	30,000-40,000

The $^{3}He/^{4}He$ ratio (R/Ra) is given relative to the atmospheric ratio (Ra) of 1.4×10^{-6} (Mamyrin et al., 1970). Recent determinations of $^{40}Ar/^{36}Ar$ in modern air are 299 (Lee et al., 2006; Valkiers et al. 2010), compared to the lower value of 296 that is still widely used in the literature (Nier, 1950). Atmospheric and representative mantle values from various sources (Graham, 2002; Ozima and Podosek, 2002; Holland and Ballentine, 2006).

Table 11.3. Non-radiogenic noble gases in selected fluid and rock reservoirs

	^{36}Ar mol g^{-1} ($\times 10^{-12}$)	$^{20}Ne/^{36}Ar$	$^{84}Kr/^{36}Ar$	$^{130}Xe/^{36}Ar$	notes
Air		0.524	0.0207	0.000113	1.
Air Saturated Water					
Meteroic water (0 °C)	75	0.122	0.0428	0.000474	2.
Seawater (25 °C)	34	0.175	0.0359	0.000348	3.
Bittern Brine (29 °C)	7	0.249	0.0341	0.000285	4.
Lithologies					
Dry marine sediments (n = 16)	0.2-12	0.003-0.77	0.04-0.29	0.0007-0.004	5.
Carbonate rock (n =3)	0.1-200	0.05-19	0.02-0.05	nd.	6.
Shale (n = 12)	0.04-6	0.05-6	0.02-0.4	0.0007-0.15	7.
Meta-sediments (n = 5)	0.01-0.4	0.2-1.1	nd.	nd.	8.
Altered-basalt	0.06-0.3	0.01-0.07	0.03-0.07	0.001-0.004	9.
Antigorite-serpentinites (n = 5)	0.09-5	0.06-0.1	0.03-0.06	0.0004-0.002	10.
Crystalline basement	0.01-0.7	0.2-6.5	0.01-0.11	0.0001-0.009	11.

Notes: 1-3) data from Ozima and Podosek (2002). 4) Based on 29 °C NaCl brines (Smith and Kennedy, 1983). 5) Unconsolidated sediments or mud (Matsuda and Nagao, 1986; Amari and Ozima, 1988; Staudacher and Allègre, 1988; Schwarz et al., 2005). 6) (Zhou and Ye, 2002) 7) (Podosek et al., 1980;1981) 8) metamorphosed pelagic sediments (Schwarz et al., 2005). 9) (Staudacher and Allègre, 1988). 10)(Kendrick et al., 2011a). 11) Includes metamorphic rocks, granites and gneisses, range of relative abundance ratios estimated from Fig 2 of Drescher et al. (1998).

Table 11.4. Halogens in selected fluid and rock reservoirs

	Halogen concentrations	Br/Cl ($\times 10^{-3}$)	I/Cl ($\times 10^{-6}$)	notes
		molar ratios		
Seawater	3.5 wt % salt	1.54 ± 0.02	0.84 ± 0.04	1.
Bittern brine	~30 wt % salt	1.5-12	0.8-7	2.
Halite	100 wt % NaCl	0.05	0.002	3.
Rock salt (halite)	100 wt % NaCl	0.04-0.15	0.2	4.
Sylvite	100 wt % KCl	0.3	0.07	5.
Carnallite	100 wt. % $KMgCl_3.6(H_2O)$	0.45	1-2	6.
Organic matter	100's of ppm Br + I	(Br/I ~ 1-10)		7.
Mica/amphibole	0 to ~1wt.% Cl or F	0.05-0.2	1-12	8.
Metm. devol. fluids	<5 to 20 wt % salt	variable	variable	9.
Metm. desicc. fluids	<100 wt % salt	<40	variable	10.
Magmatic fluids	2-60 wt % salt	0.6-1.8	10-70	11.
MORB	10-1000 ppm Cl	1.6 ± 0.2	40 ± 30	12.

Notes: 1) Seawater Br/Cl (McCaffrey et al., 1986); 19,350 ppm Cl, 67.3 ppm Br (Drever, 1997), 58 ppb I (Fuge and Johnson, 1986). 2) Bittern brines produced by evaporation of seawater (Zherebtsova and Volkova, 1966; Nissenbaum, 1977; McCaffrey et al., 1986). 3) Based on precipitation from seawater and partition coefficients of $D_{Br/Cl} \sim 0.03$ and $D_{I/Cl} \sim 0.003$ (where $D_{Br/Cl} = Br/Cl_{halite}/Br/Cl_{seawater}$; Holser, 1979; Hermann, 1980; Siemann and Schramm, 2000). 4) Rock salt I/Cl inferred from fluid data of (Bohlke and Irwin, 1992a). Br/Cl based on measure values (McCaffrey et al., 1986) and measured Br abundances of 40-200 ppm (Fontes and Matray, 1993; Siemann, 2003). 5) Based on precipitation from seawater and partition coefficients of $D_{Br/Cl} \sim 0.2$ and $D_{I/Cl} \sim 0.09$ (Holser, 1979). 6) Based on precipitation from seawater and partition coefficients of $D_{Br/Cl} \sim 0.3$ and $D_{I/Cl} \sim 2$-3 (Holser, 1979). 7) Concentrations in organic-rich sediments and Br/I estimated from sedimentary marine pore fluids (Fuge and Johnson, 1986; Martin et al., 1993; Muramatsu et al., 2007; Kendrick et al., 2011d). 8) Very limited data (n = 2; Kendrick, 2012). 9) The salinity range estimated for fluids produced by breakdown of hydrous minerals does not include halogen rich lithologies such as serpentinites or meta-evaporites (Kendrick et al., 2006c). 10) Fluid produced by metamorphic desication e.g. partitioning of $H_2O > Cl > Br$ into mica or amphibole (Markl and Bucher, 1998; Svensen et al., 2001; Kendrick et al., 2006c). 11) Variable salinities are expected in magmatic fluids (Cline and Bodnar, 1991), reported Br/Cl and I/Cl (Irwin and Roedder, 1995; Kendrick et al., 2001; Nahnybida et al., 2009). 12) Composition of Maquarie Island basalt glasses (Kendrick et al., 2012), see also Schilling et al. (1978) and Jambon et al. (1995).

Table 11.5. Crustal fluids with radiogenic noble gas isotope signatures

		Trapping age	$^{3}He/^{4}He$	$^{21}Ne/^{22}Ne$	$^{20}Ne/^{22}Ne$	$^{40}Ar/^{36}Ar$	$^{136}Xe/^{132}Xe$	notes
Fluid inclusions								
Mt Isa	H_2O-CO_2	1.55-1.5 Ga	?	0.36	9.2	40,000	0.71	1.
St Ives	CH_4-rich	2.65 Ga	<0.01	0.56	8.3	50,000	0.4	2.
Wernecke	H_2O	1.6 Ga	<0.02	0.35	6.6	40,000		3.
Ailaoshan	H_2O-CO_2	50 Ma	1.3	0.47	11.5	>9000	0.45	4.
Witwatersrand	?	2 Ga ?	0.01	0.59	8.2	>100,000	0.35	5.
Geo-fluids								6.
McElmo Dome well gases	CO_2	0	0.17	0.11	8.9	25,000		7.
Witwatersrand fracture-hosted	H_2O with CH_4	0	<0.04	0.16	8.9	9000	0.55	8.
Air			1	0.029	9.8	299	0.33	9.

Notes: 1) Radiogenic signatures in samples dominated by CO_2-only fluid inclusions and H_2O-CO_2 fluid inclusions (Kendrick et al., 2011a). 2) Samples containing CH_4 fluid inclusions (Kendrick et al., 2011b). 3) (Kendrick et al., 2008). 4) (Sun et al., 2009). 5) (Lippmann-Pipke et al., 2011). 6) Fluid inclusions are expected to have the most radiogenic noble gas isotope signatures because geo-fluids sampled from depths of 1-3 km are more likely to mix with surface derived groundwater or other atmospheric components than fluid inclusions trapped at depths of 6-10 km. 7) (Gilfillan et al., 2008). 8) (Lippmann et al., 2003; Lippmann-Pipke et al., 2011). 9) Table 11.2 and Ozima and Podosek (2002).

Figure captions

Fig 11.1. *Fluid inclusions observed in transmitted light during microthermometry. a) low temperature monophase water inclusions in birefringent calcite. b) two-phase liquid-vapour fluid inclusions. c) high salinity fluid inclusions with multiple daughter minerals. d) Liquid CO_2 fluid inclusions. e) mixed liquid CO_2 and H_2O fluid inclusion containing daughter minerals. f) Large decrepitated fluid inclusions, medium sized CH_4-N_2 fluid inclusions (see j), and a trail of small secondary inclusions. g) A single daughter bearing fluid inclusion during microthermometry, note homogenisation by halite dissolution and then leakage. h) multi-solid fluid inclusion. i) mixed CO_2-H_2O fluid inclusion above and below CO_2 homogenisation temperature. j) Liquid CH_4 fluid inclusion showing critical homogeniston at -102 °C, thus indicating the presence of ~30 vol. % N_2. Abbreviations: v = vapour, l = liquid, H = halite.*

Fig 11.2: *Contours of $^3He/^4He$ production ratios for fluid inclusions with variable Li/U and different host rock U concentrations (which controls the neutron flux). The neutron flux in the rock is calculated following Ballentine and Burnard (2002) for a typical rhyolite composition assuming that U +Th are hosted in silicate phases. Elevated $^3He/^4He$ production ratios are possible in Li-rich fluid inclusions, but ^3He production rates are low (see text).*

Fig 11.3*. Noble gas release by: a) in vacuo crushing in a modified Nupro® valve, note the resulting skewed grain size distribution. b) Degassing during stepped heating irradiated quartz. The low temperature peak is attributed to noble gas release during decrepitation of >3-4 µm sized fluid inclusions. The high temperature release is attributed to decrepitation of very small fluid inclusions (<1-2 µm), or gases trapped within fluid inclusions that have already leaked and then re-annealed (Fig 11.1g; Kendrick et al., 2006b). The relative size of these peaks varies between samples (Kendrick et al., 2006a; Fairmaid et al., 2011).*

Fig 11.4*. The $^3He/^4He$ versus $^4He/^{40}Ar^*$ systematics of selected magmatic and formation water derived ore fluids (Stuart and Turner, 1992; Stuart et al., 1995; Burnard and Polya, 2004; Hu et al., 1998; 2004; Kendrick et al., 2002b;2005). The stars represent the mean MORB mantle and crustal production ratios, the grey box represents the range of compositions expected in crust with variable K:U:Li compositions. Low temperature fluids are typically enriched in ^4He relative to $^{40}Ar^*$ (Ballentine and Burnard, 2002). Analyses obtained by in vacuo crushing.*

Fig 11.5*. Noble gas systematics of MVT fluid inclusions. a) The $^{130}Xe/^{36}Ar$ versus $^{84}Kr/^{36}Ar$ values are expressed as fractionation values such that Air has F = 1 [e.g. $F(Ng/^{36}Ar)_{air} = (Ng/^{36}Ar)_{sample}/(Ng/^{36}Ar)_{air}$; Ng = ^{130}Xe or ^{84}Kr]. Air and air-saturated water (ASW) are shown as stars, note that the best fit regression through the South Pennine data does not intersect air. b) $^{40}Ar/^{36}Ar$ is not correlated with $^{129}Xe/^{36}Ar$ indicating the data are not simply explained by the presence of modern air contamination. c) Noble gas abundance ratios are fractionated by increasing salinity (triangle shows bittern brine) or dissolution of (noble gas rich) hydrocarbons [stars = oil equilibrated with ASW; circles = gas equilibrated with ASW; square = gas equilibrated with oil; fractionation factors calculated for different volume ratios (Bosch and Mazor, 1988; Ballentine et al., 2002)]. d) Noble gas abundance ratios are also fractionated during interaction with sedimentary rocks. Data obtained by laser ablation*

(Böhlke and Irwin, 1992a) and sequential crushing of multiple samples (see Fig 11.6; Kendrick et al., 2002ab; 2005; 2011d). Sedimentary rock data in (d) are from Matsuda and Nagoa (1986) and Podosek et al. (1980).

Fig 11.6. *Halogen systematics of MVT ore fluids, showing individual laser analyses for Hansonburg and sample averages from other locations (Bohlke and Irwin, 1992; Kendrick et al., 2002ab; 2005; 2011d). Reference fields include seawater, the seawater evaporation trajectory (S.E.T.; Zherebtsova and Volkova, 1966), evaporites (Table 11.4; Holser, 1979; Fontes and Matray, 1993), sedimentary marine pore fluids with seawater-corrected Br*/I of 0.5-1.5 (dark grey envelope) and organic matter with Br*/I<10 (light grey envelope). The pore fluid trend is defined with data from Fehn et al. (2000; 2003; 2006; 2007); Muramatsu et al. (2001; 2007) and Tomaru et al. (2007ab; 2009); see Kendrick et al. (2011d).*

Fig 11.7*. Noble gas relative abundance patterns for fluid inclusions in VMS deposits from mid-ocean ridge spreading centres and back arc rifts (Turner and Stuart, 1992; Stuart and Turner, 1998; Zeng et al., 2001; Lueders and Niedermann, 2010). Abundance ratios are normalised to air:* $F(Ng/^{36}Ar)_{air} = (Ng/^{36}Ar)_{sample}/(Ng/^{36}Ar)_{air}$*; such that Air = 1; Ng =* ^{4}He*,* ^{20}Ne*,* ^{84}Kr *or* ^{130}Xe*.*

Fig 11.8*. The He-Ar systematics of fluid inclusions with a magmatic origin in various hydrothermal ore deposits. a) The Ailaoshan data obtained by 1-3 crushes of 15 sulphide samples exemplify the parabolic shape expected for binary mixing in He-Ar four isotope diagrams (Burnard et al., 1999). However, in this case, a third end-member is revealed by the* $^{4}He/^{40}Ar$ *versus* $^{3}He/^{40}Ar$ *plot (b). c) Porphyry-style ore fluids from Arizonan Porphyry copper deposits (9 samples; Kendrick et al., 2001) and porphyry-related copper and gold deposits of the Red River–Jinshajiang fault belt in SW China (24 samples; Hu et al., 1998; 2004). d) Fluid inclusion data for granite-associated Panasqueria tin-tungsten deposit, Portugal (12 samples; Burnard and Polya, 2004).*

Fig 11.9*. Apparent* ^{36}Ar *concentrations determined from fluid inclusion salinity and the maximum* $Cl/^{36}Ar$ *measured during sequential crushing. Note, analyses shown for Laisvall fluid inclusions have* $^{84}Kr/^{36}Ar$ *of 0.04-0.07 and* $Cl/^{36}Ar$ *is not correlated with* $^{40}Ar/^{36}Ar$ *in the Erro Tobbio fluid inclusions, conclusively demonstrating these analyses have not been influenced by modern air contaminants (see text). The range of ASW encompasses 0 °C meteoric water and 25 °C seawater. Data from various sources (Kelley et al., 1986; Turner and Bannon, 1992; Irwin and Roedder, 1995; Kendrick et al., 2001a; 2002ab; 2005;2011ac; Fairmaid et al., 2011; Fu et al., 2012). Abbreviations: N.Am. = North American mid-continent; Pen. = Pennine; Len.S. = Lennard Shelf; Alm = Almirez (serpentines final breakdown); Vic = Victorian Gold deposits; St.I. = St. Ives.*

Fig 11.10*. Noble gas fractionation during hydrothermal boiling of porphyry copper deposit ore fluids (19 samples; Kendrick et al., 2001a). Hydrothermal boiling refers to separation of liquid and vapour* H_2O *phases. a)* $Cl/^{36}Ar$ *versus* $^{40}Ar/^{36}Ar$*, the residual liquid phase has higher* $Cl/^{36}Ar$ *and lower* $^{40}Ar^{*}/Cl$ *ratios than the parent fluid. b)* $F(^{84}Kr/^{36}Ar)_{air}$ *versus* $F(^{130}Xe/^{36}Ar)_{air}$*, the residual liquid phase acquires higher* $^{130}Xe/^{36}Ar$ *and* $^{84}Kr/^{36}Ar$ *ratios than the parent fluid. Noble gas abundance ratios are written as F-values [*$F(Ng/^{36}Ar)_{air}$ *=*

[$(Ng/^{36}Ar)_{sample}/(Ng/^{36}Ar)_{air}$]; Air = 1; Ng = ^{130}Xe or ^{84}Kr]. Data obtained by sequential crushing.

***Fig 11.11**. The halogen systematics of fluid inclusions in magmatic-hydrothermal ore deposits (showing sample means). a) Fluid inclusions from Ascension granite xenoliths, porphyry-style deposits and St. Austell Sn-W mineralisation, Cornwall (Irwin and Roedder, 1995; Kendrick et al., 2001a), are relatively close to MORB composition (Kendrick et al., 2012). Interpreted magmatic fluids involved in iron-oxide copper gold mineralisation (Wernecke, Canada and Ernest Henry, Australia), and igneous mica and amphibole (Kendrick et al., 2007; 2008b; Kendrick, 2012) are also shown. Possible causes of compositional variation are shown inset. b) Fluid inclusions from Panasqueria deposit are strongly enriched in Br and I derived from organic sources (Polya et al., 2000). Note Br*/I indicates the seawater-corrected Br/I ratio (see Fig 11.6).*

***Fig 11.12** Serpentinite breakdown fluids from Erro Tobbio, Italy. a) Fluid inclusion $Cl/^{36}Ar$ versus $^{40}Ar/^{36}Ar$ and b) $^{130}Xe/^{36}Ar$ versus $^{84}Kr/^{36}Ar$ compositions measured by in vacuo crushing olivine and Ti-clinohumite (F = fractionation value normalised to air; Air = 1). The fluids released by crushing do not define a mixing line with air (a) and the fluid inclusions faithfully record the Ar-Kr-Xe isotope signature of the antigorite-schist (modified after Kendrick et al. 2011a). c) Transmitted light photomicrograph showing a ~1cm wide olivine-Ti-clinohumite-dioside vein in antigorite schist; and d) a primary fluid inclusion with visible halite daughter crystal and vapour bubble (photographs courtesy of M. Scambelluri).*

***Fig 11.13**. Noble gas relative abundance ratios for gold-related fluid inclusions from Tienshan gold deposits (Graupner et al., 2006; 2010). Note quartz fluid inclusions are strongly depleted in He relative Ar in sulphide or scheelite fluid inclusions, but all minerals are strongly enriched in light noble gases relative to ASW. Yellow boxes show the range of noble gas abundance ratios in altered oceanic basalts and serpentinites (Staudacher and Allegre, 1988; Kendrick et al., 2011a).*

***Fig 11.14**. Fluid inclusion Br/Cl and I/Cl for Victorian gold deposits, Australia. a) Sample mean and standard deviation, distinguished on the basis of tectonic zone (modified after Fu et al. (2012)). The Melbourne Zone is shale rich compared to the Bendigo and Stawell Zones. b) Sequential analyses for 13 samples obtained by stepped heating and in vacuo crushing. The best fit slope gives a Br/I ratio of 5.6, that is within the range of organic matter. The intercept is interpreted as altered-volcanic rocks (modified after Fairmaid et al. 2011). The MORB field is after Kendrick et al. (2012) and the composition of altered-volcanics (alt. voc.) is based on adding Cl-rich mica and amphibole to MORB (cf. Fig. 11.11).*

***Fig 11.15.** Fluid inclusion $^{40}Ar/^{36}Ar$ versus $Cl/^{36}Ar$ for quartz and carbonate samples from the St Ives goldfield, Western Australia. The data are corrected for post-entrapment production of $^{40}Ar^*$, based on a mineralisation age of 2.65 Ga. Slopes with constant $^{40}Ar^*/Cl$ are shown for reference. CH_4 fluid inclusions associated with reduced alteration*

assemblages have higher $^{40}Ar/^{36}Ar$ than H_2O-CO_2 fluid inclusion associated with oxidised alteration assemblages (modified after Kendrick et al., 2011c). Data obtained by sequential crushing and stepped heating of six samples.

***Fig 11.16**. Halogens in omphacite and garnet hosted primary fluid inclusions showing fractionation during eclogite facies metamorphism (Svensen et al., 2001). The compositions of igneous mica, amphibole (Kendrick, 2012) and MORB (Kendrick et al., 2012) are also shown.*

***Fig 11.17**. K-Ar isochron diagram showing data for stepped heating quartz samples from the Proterozoic Mt Isa Inlier and Archean Yilgran Terranes of Australia (see Kendrick et al., 2006c; 2007; 2011c). For clarity, only the samples with very high $^{40}Ar/^{36}Ar$ are shown and uncertainty is not indicated. The highest $K/^{36}Ar$ ratios were obtained for low gas volume steps between 700 and 1100 °C (cf. Fig 11.3b). Sample Q5 from the 2.65 Ga St Ives goldfield had a total correction for in situ production of radiogenic $^{40}Ar^*$ of only 1.8% (Kendrick et al., 2011c). The fluid inclusions have apparent ages of up to 11 Ga that reflect the presence of excess $^{40}Ar^*$.*

***Fig 11.18**. Fluid inclusion abundance ratios for radiogenic noble gas isotopes. a) Samples from the Mt Isa Inlier, sequential crushing shows Ne/Xe enrichment in two samples that are dominated by CO_2 –only fluid inclusions (Kendrick et al., 2011b). b) Fluid inclusions from the St Ives goldfield of Western Australia (hosted by 10 quartz and sulphide samples), record $^4He/^{40}Ar^*$ ratios similar to expected production ratios (Kendrick et al., 2011c).*

***Fig 11.19.** Noble gas mixing model for fluid inclusions related to ore deposition and regional alteration in the Mt Isa Inlier (Kendrick et al., 2011b). The r-values in each plot describe the mixing trends curvature, where r is related to the relative abundance of the denominator isotopes (e.g. equation 11.1; section 5.4.1; Langmuir et al., 1978). The indicated range of 'estimated basement compositions' is based on typical noble gas abundances in sedimentary and basement rocks (Table 11.2), realistic K, Th and U concentrations and 600 Myr of radiogenic ingrowth (see Kendrick et al. (2011b) for a full discussion of the model and uncertainties). Data obtained by sequential crushing of 13 samples.*

***Fig 11.20**. Fluid inclusion halogen and $^{40}Ar/^{36}Ar$ data obtained by stepped heating Ernest Henry quartz. Individual steps are shown as small symbols, large symbols with drop lines represent weighted means for each sample (modified after Kendrick et al. 2007).*

***Fig 11.21.** Noble gas and halogen data for fluid inclusions related to Mt Isa copper mineralisation. a) sequential Br/Cl and I/Cl analyses of silica-dolomite alteration showing the seawater evaporation trajectory (Zherebtsova and Volkova, 1966), the composition of igneous mica and amphibole (Kendrick, 2012) and organic Br*/I ratios of 0.5-8. b) The sample maximum $^{40}Ar/^{36}Ar$ ratio and calculated ^{36}Ar concentration. Bittern brines with 0.07×10^{-10} mol ^{36}Ar g^{-1} and the estimated compositional range of basement-derived metamorphic fluids (Fig 11.19; Kendrick et al., 2006c) are shown for reference.*

Fig 11.22. *Neon isotope data for fluids in three Precambrian terranes (Kendrick et al., 2011bc; Lippmann-Pipke et al., 2011). The average $^{21}Ne^*/^{22}Ne^*$ of ~0.5 determined for the majority of fluids in sedimentary basins is shown for reference (Kennedy et al., 1990; Ballentine and Burnard, 2002). Fluid inclusions show much greater variation in neon isotope composition than basinal fluids, with $^{21}Ne^*/^{22}Ne^*$ varying from 0.1 up to 3.3 ± 0.2 (Lippmann-Pipke et al., 2011). The red star indicates the estimated composition of Mt Isa's basement the symbols follow Fig 11.19.*

Fig 1.

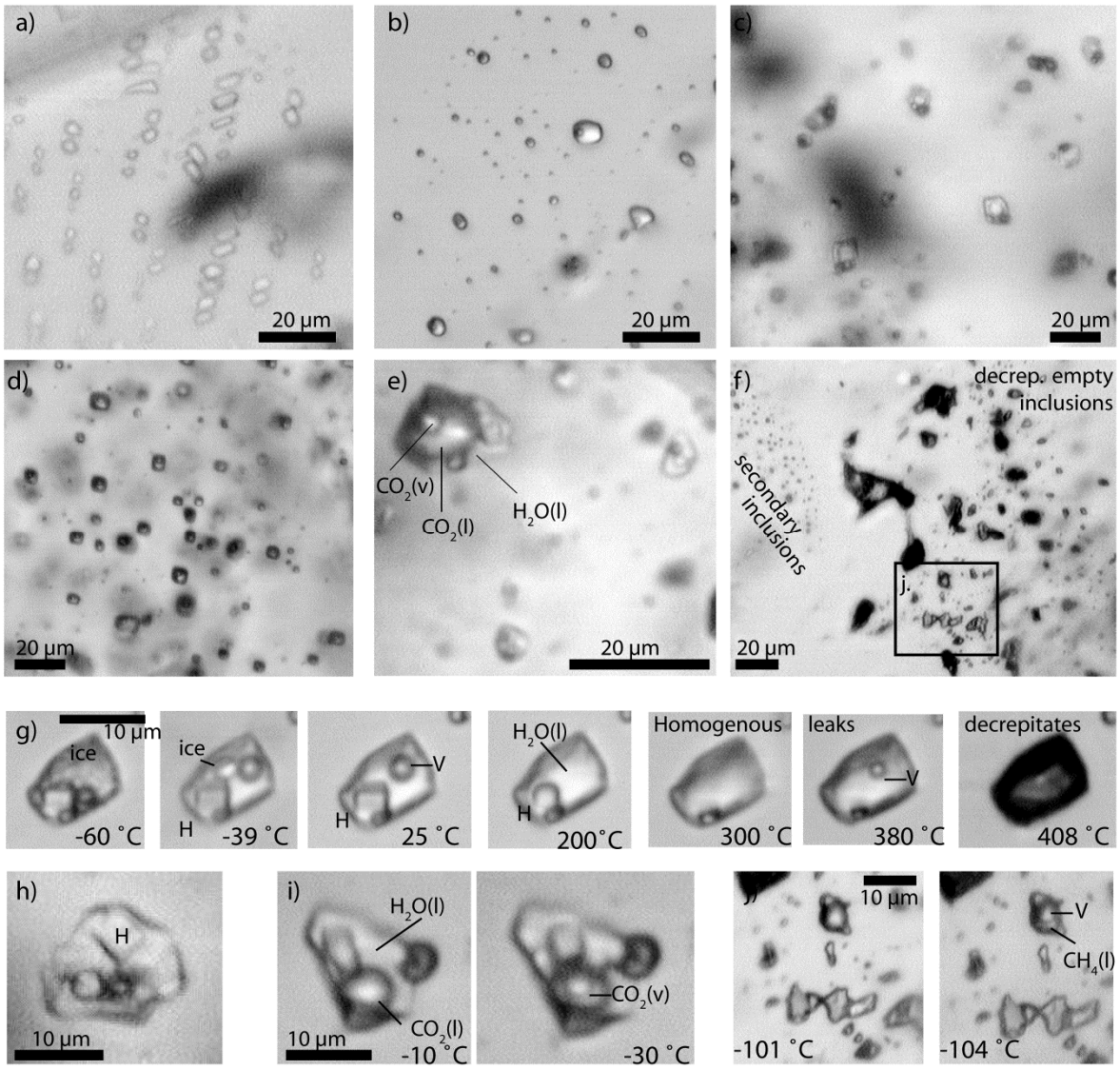
a)
20 µm
b)
20 µm
c)
20 µm
d)
20 µm
e)
CO2(v)
CO2(l)
H2O(l)
20 µm
f)
decrep. empty inclusions
secondary inclusions
j.
20 µm
g)
10 µm
ice
-60 ˚C
ice
H
-39 ˚C
V
H
25 ˚C
H2O(l)
H
200˚C
Homogenous
300 ˚C
leaks
V
380 ˚C
decrepitates
408 ˚C
h)
H
10 µm
i)
H2O(l)
CO2(l)
10 µm
-10 ˚C
CO2(v)
-30 ˚C
j)
10 µm
-101 ˚C
V
CH4(l)
-104 ˚C

Fig 2

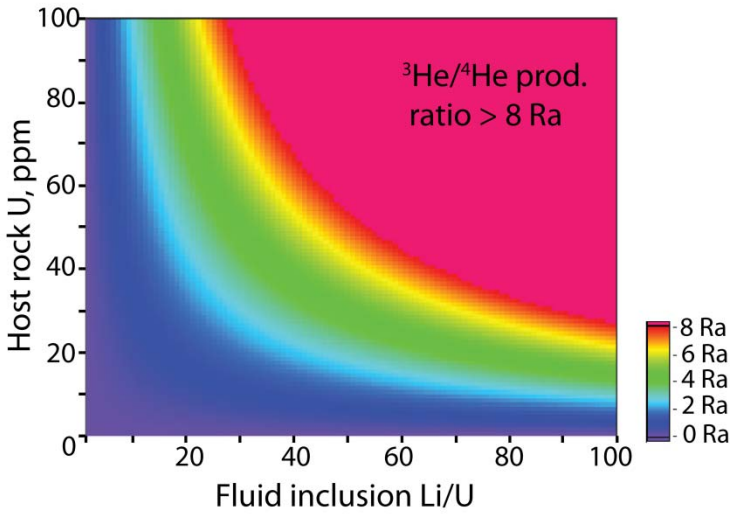
^{3}He/^{4}He prod.
ratio > 8 Ra
Host rock U, ppm
Fluid inclusion Li/U
0
20
40
60
80
100
8 Ra
6 Ra
4 Ra
2 Ra
0 Ra

Fig 3

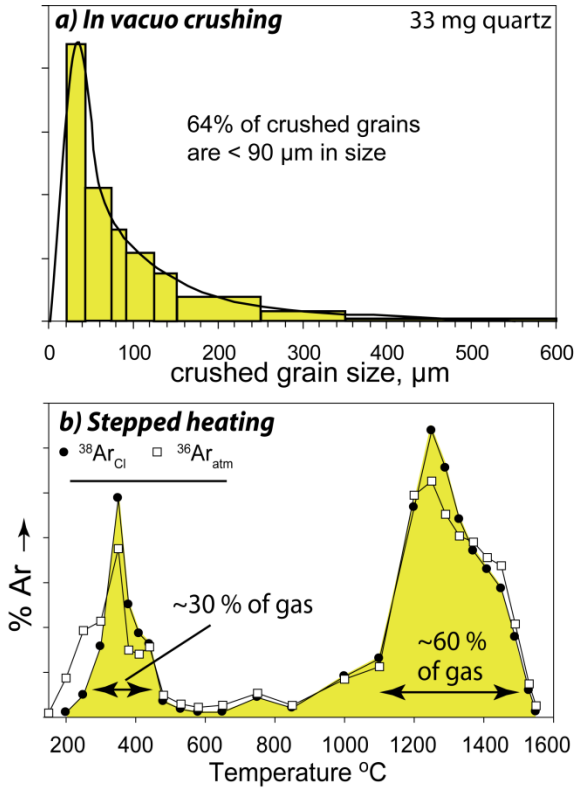
a) In vacuo crushing
33 mg quartz
64% of crushed grains
are < 90 µm in size
0
100
200
300
400
500
600
crushed grain size, µm
b) Stepped heating
$^{38}Ar_{Cl}$
$^{36}Ar_{atm}$
% Ar →
~30 % of gas
~60 %
of gas
200
400
600
800
1000
1200
1400
1600
Temperature °C

Fig 4

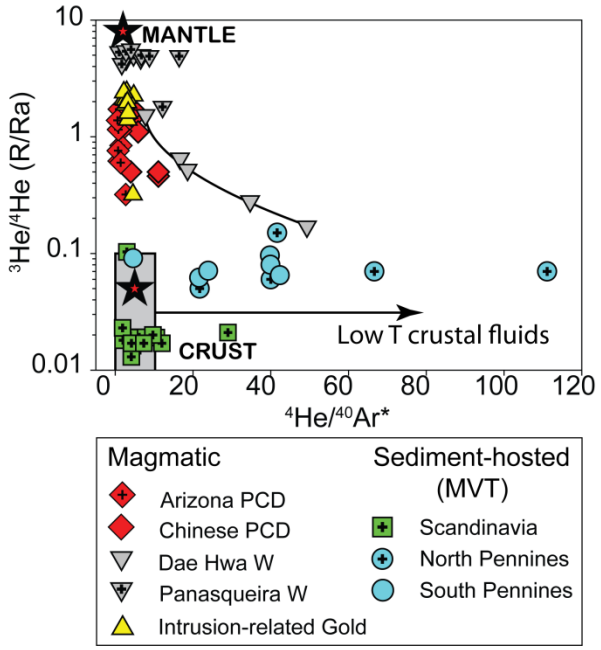
10
1
0.1
0.01
$^3He/^4He$ (R/Ra)
MANTLE
CRUST
Low T crustal fluids
0
20
40
60
80
100
120
$^4He/^{40}Ar^*$
Magmatic
Arizona PCD
Chinese PCD
Dae Hwa W
Panasqueira W
Intrusion-related Gold
Sediment-hosted (MVT)
Scandinavia
North Pennines
South Pennines

Fig 5.

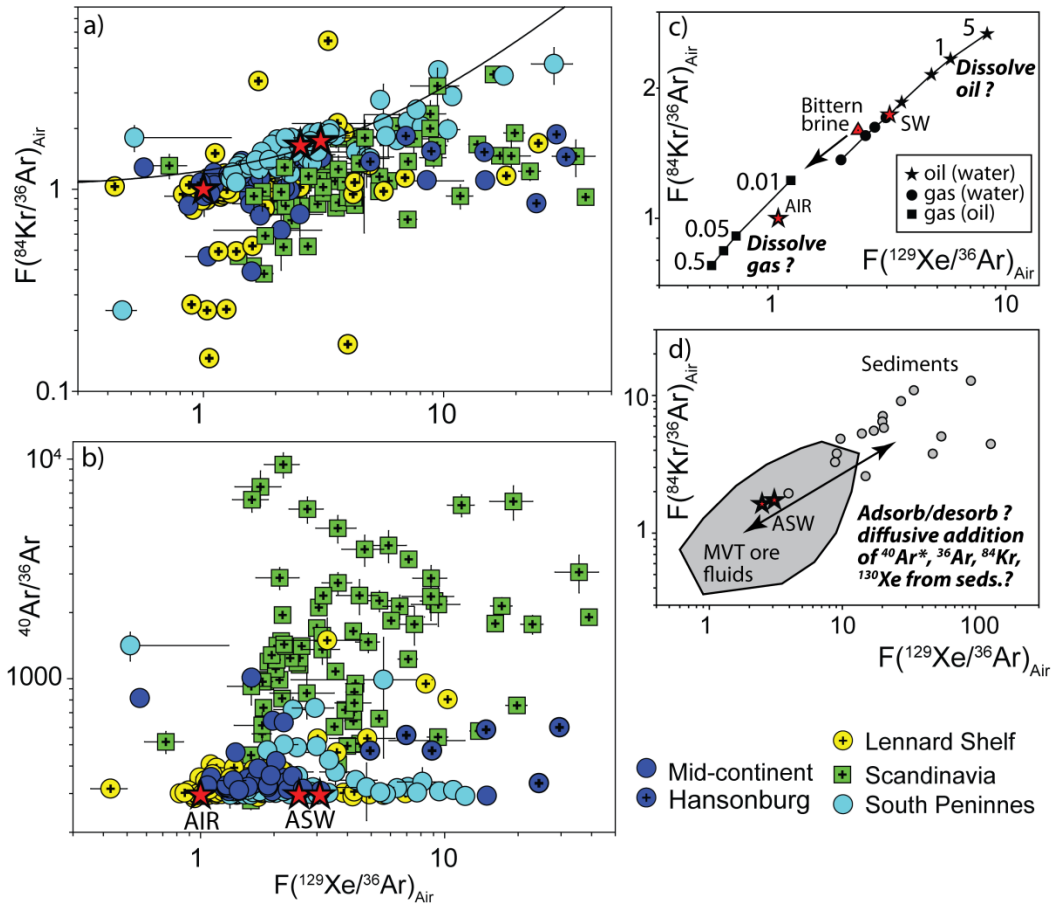
a)
$F(^{84}Kr/^{36}Ar)_{Air}$
0.1
1
1
10
b)
$^{40}Ar/^{36}Ar$
10^4
1000
AIR
ASW
1
10
$F(^{129}Xe/^{36}Ar)_{Air}$
c)
$F(^{84}Kr/^{36}Ar)_{Air}$
2
1
5
1
Dissolve oil ?
Bittern brine
SW
0.01
AIR
0.05
0.5
Dissolve gas ?
oil (water)
gas (water)
gas (oil)
1
10
$F(^{129}Xe/^{36}Ar)_{Air}$
d)
$F(^{84}Kr/^{36}Ar)_{Air}$
10
1
Sediments
ASW
MVT ore fluids
Adsorb/desorb ? diffusive addition of $^{40}Ar^*$, ^{36}Ar, ^{84}Kr, ^{130}Xe from seds.?
1
10
100
$F(^{129}Xe/^{36}Ar)_{Air}$
Mid-continent
Hansonburg
Lennard Shelf
Scandinavia
South Peninnes

Fig 6

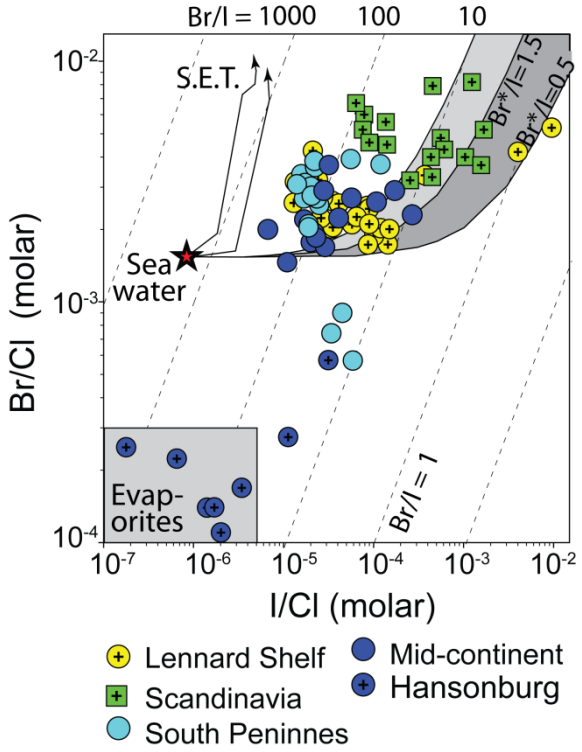
Br/I = 1000
100
10
S.E.T.
Sea water
Br*/I=1.5
Br*/I=0.5
Br/I = 1
Evap-orites
Br/Cl (molar)
I/Cl (molar)
Lennard Shelf
Scandinavia
South Peninnes
Mid-continent
Hansonburg

Fig 7

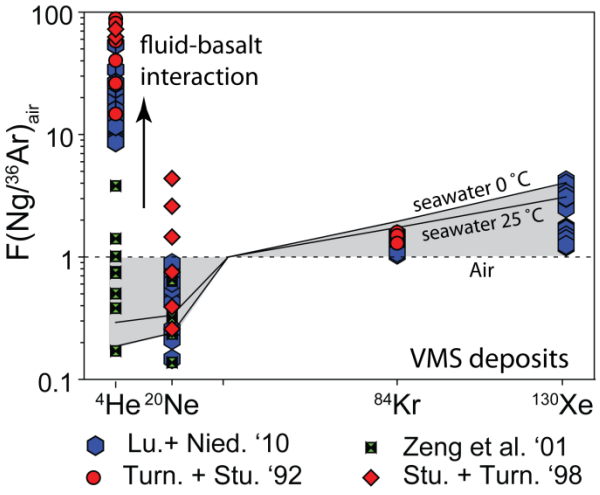
100
10
1
0.1
F(Ng/36Ar)air
fluid-basalt
interaction
seawater 0 °C
seawater 25 °C
Air
VMS deposits
4He 20Ne
84Kr
130Xe
Lu.+ Nied. '10
Turn. + Stu. '92
Zeng et al. '01
Stu. + Turn. '98

Fig 8

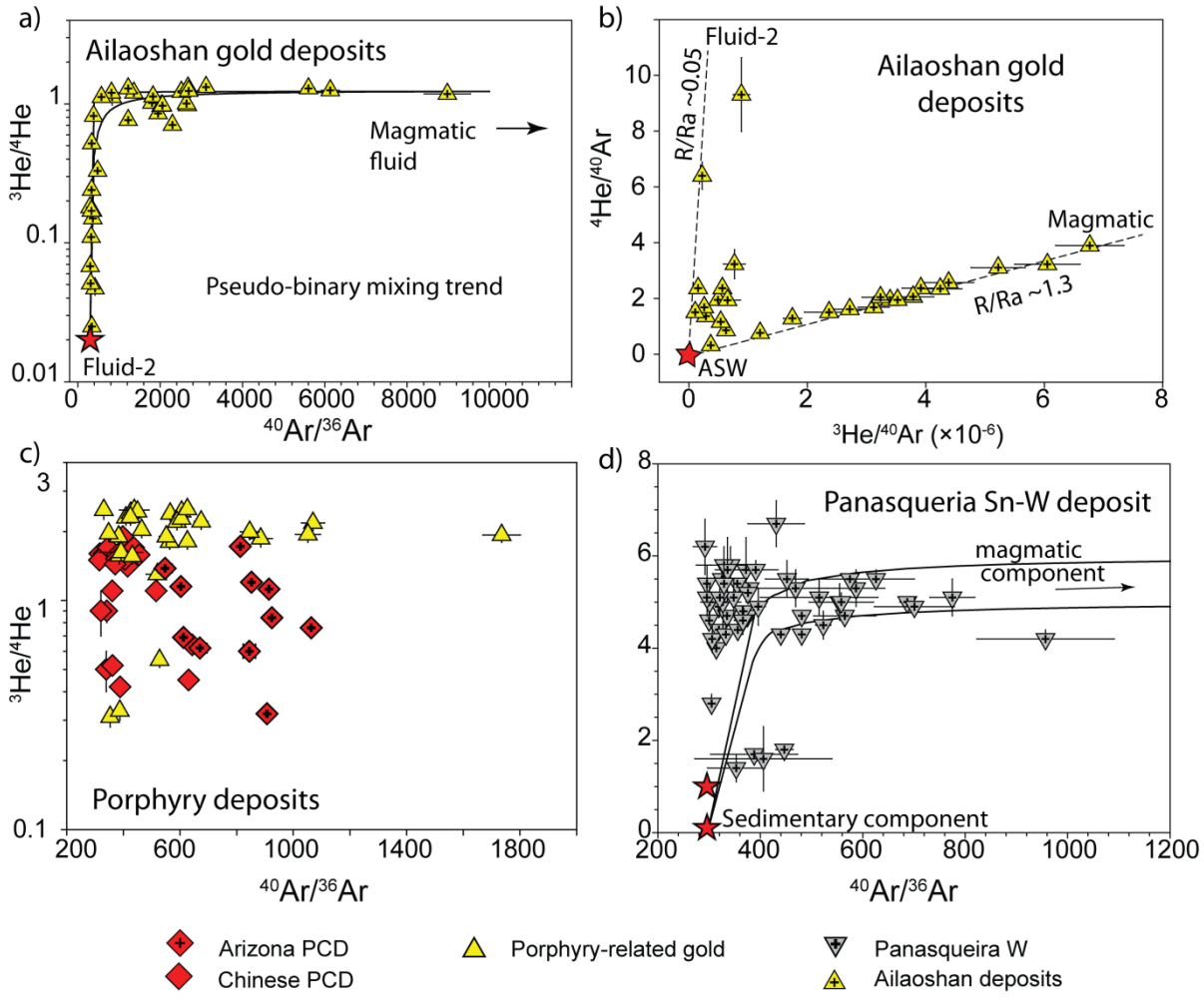
a)
Ailaoshan gold deposits
Magmatic fluid
Pseudo-binary mixing trend
Fluid-2
$^{3}He/^{4}He$
$^{40}Ar/^{36}Ar$
b)
Fluid-2
R/Ra ~0.05
Ailaoshan gold deposits
Magmatic
R/Ra ~1.3
ASW
$^{4}He/^{40}Ar$
$^{3}He/^{40}Ar$ (×10^{-6})
c)
Porphyry deposits
$^{3}He/^{4}He$
$^{40}Ar/^{36}Ar$
d)
Panasqueria Sn-W deposit
magmatic component
Sedimentary component
$^{40}Ar/^{36}Ar$
Arizona PCD
Chinese PCD
Porphyry-related gold
Panasqueira W
Ailaoshan deposits

Fig 9.

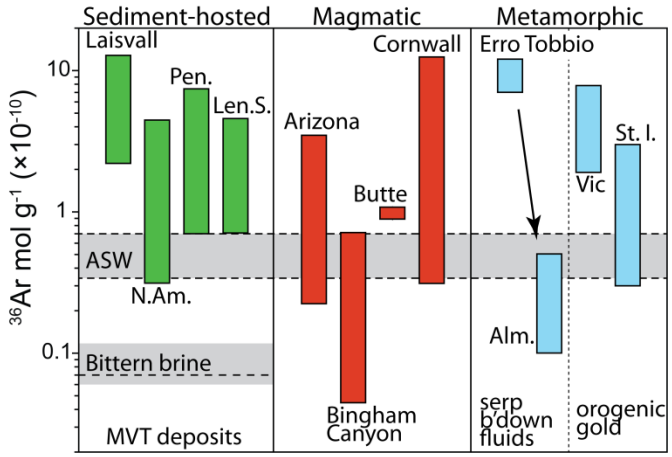
Sediment-hosted
Magmatic
Metamorphic
Laisvall
Pen.
Len.S.
N.Am.
ASW
Bittern brine
MVT deposits
Arizona
Butte
Cornwall
Bingham Canyon
Erro Tobbio
Alm.
serp b'down fluids
Vic
St. I.
orogenic gold
10
1
0.1
^{36}Ar mol g^{-1} (×10^{-10})

Fig 10.

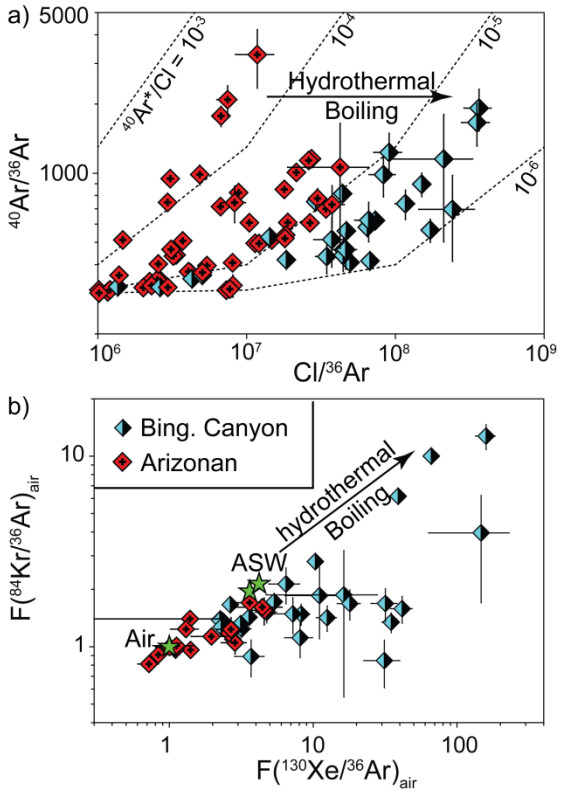
a)
5000
1000
$^{40}Ar/^{36}Ar$
$^{40}Ar^*/Cl = 10^{-3}$
10^{-4}
10^{-5}
10^{-6}
Hydrothermal
Boiling
10^6
10^7
10^8
10^9
$Cl/^{36}Ar$
b)
Bing. Canyon
Arizonan
10
1
$F(^{84}Kr/^{36}Ar)_{air}$
hydrothermal
Boiling
ASW
Air
1
10
100
$F(^{130}Xe/^{36}Ar)_{air}$

Fig 11

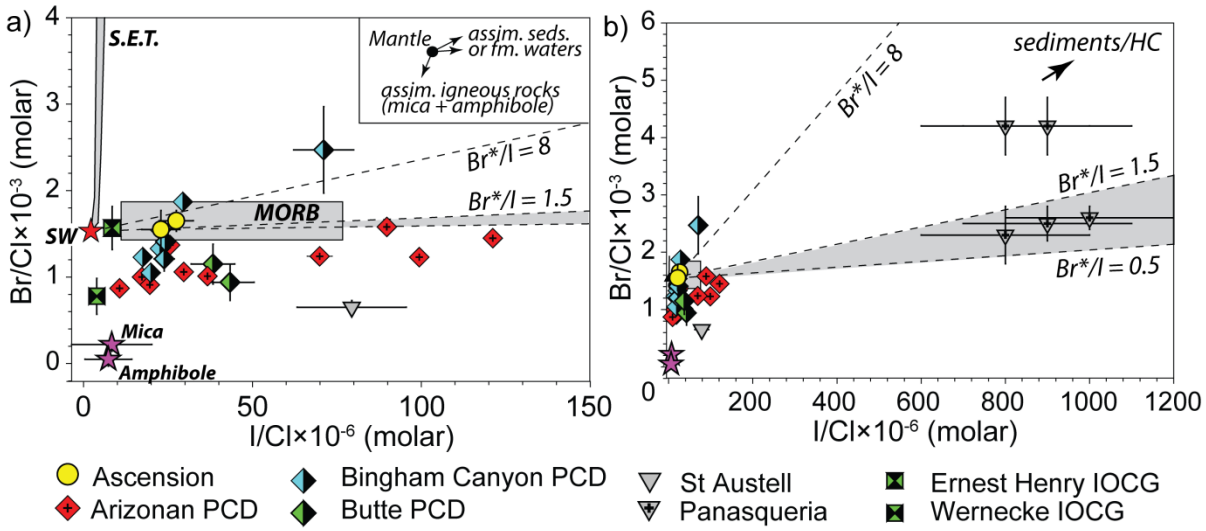
a)
S.E.T.
Mantle
assim. seds. or fm. waters
assim. igneous rocks (mica + amphibole)
Br*/I = 8
Br*/I = 1.5
MORB
SW
Mica
Amphibole
Br/Cl×10-3 (molar)
I/Cl×10-6 (molar)
b)
sediments/HC
Br*/I = 8
Br*/I = 1.5
Br*/I = 0.5
Br/Cl×10-3 (molar)
I/Cl×10-6 (molar)
Ascension
Arizonan PCD
Bingham Canyon PCD
Butte PCD
St Austell
Panasqueria
Ernest Henry IOCG
Wernecke IOCG

Fig 12.

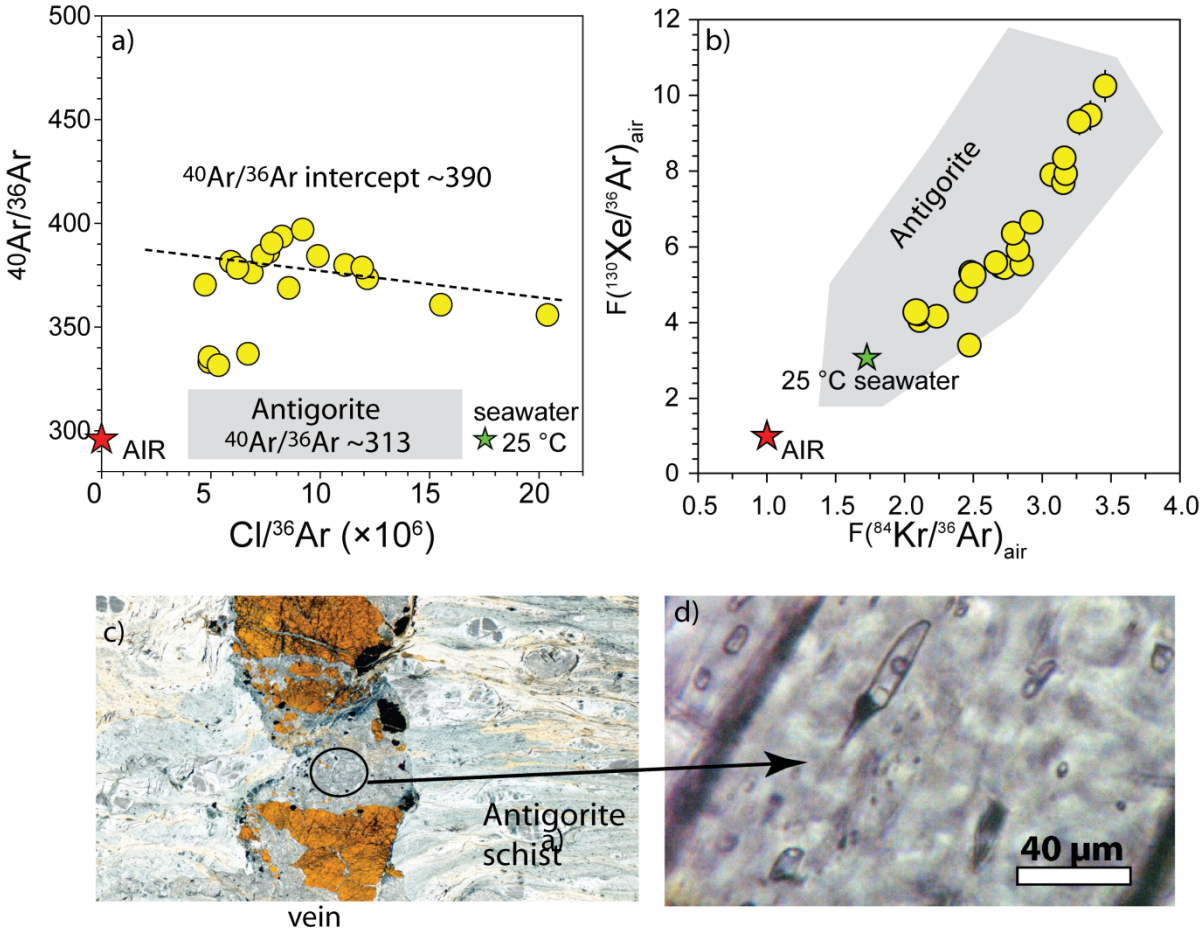
a)
$^{40}Ar/^{36}Ar$ intercept ~390
Antigorite
$^{40}Ar/^{36}Ar$ ~313
AIR
seawater
25 °C
$^{40}Ar/^{36}Ar$
$Cl/^{36}Ar$ (×10^6)
b)
Antigorite
25 °C seawater
AIR
$F(^{130}Xe/^{36}Ar)_{air}$
$F(^{84}Kr/^{36}Ar)_{air}$
c)
Antigorite schist
vein
d)
40 µm

Fig 13.

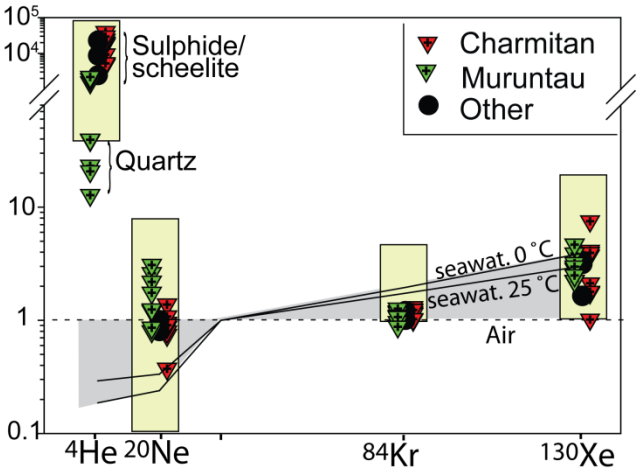
10^5
10^4
10
1
0.1
Sulphide/
scheelite
Quartz
Charmitan
Muruntau
Other
seawat. 0 °C
seawat. 25 °C
Air
^{4}He
^{20}Ne
^{84}Kr
^{130}Xe

Fig 14.

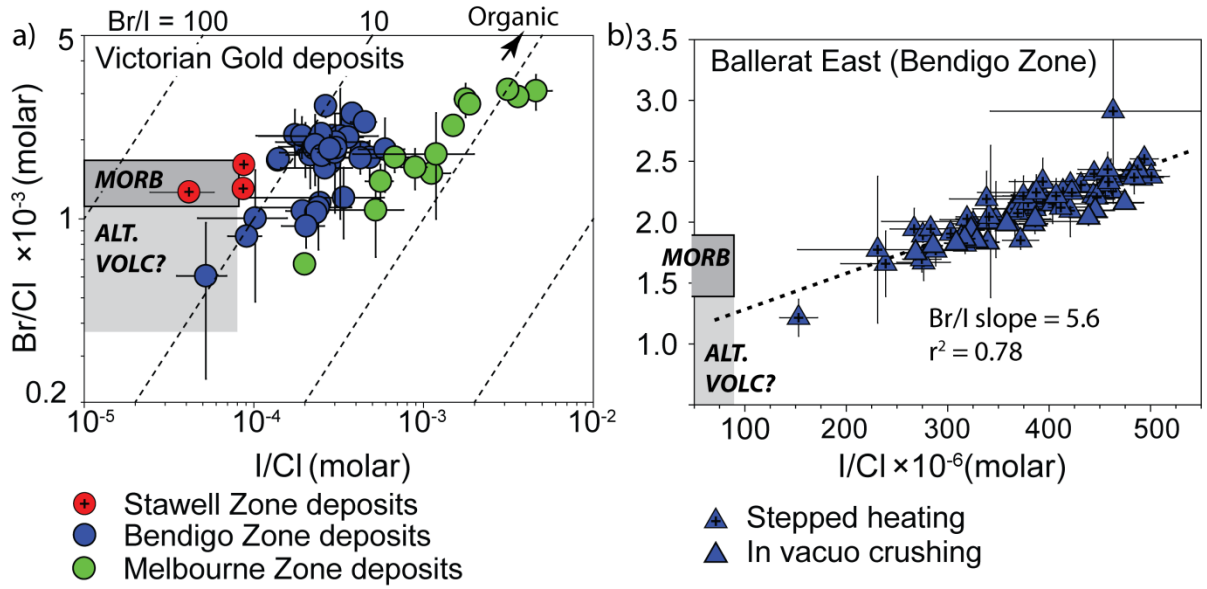
a)
Br/I = 100
10
Organic
Victorian Gold deposits
MORB
ALT.
VOLC?
Br/Cl ×10-3 (molar)
I/Cl (molar)
Stawell Zone deposits
Bendigo Zone deposits
Melbourne Zone deposits
b)
Ballerat East (Bendigo Zone)
MORB
ALT.
VOLC?
Br/I slope = 5.6
r2 = 0.78
I/Cl ×10-6(molar)
Stepped heating
In vacuo crushing

Fig 15.

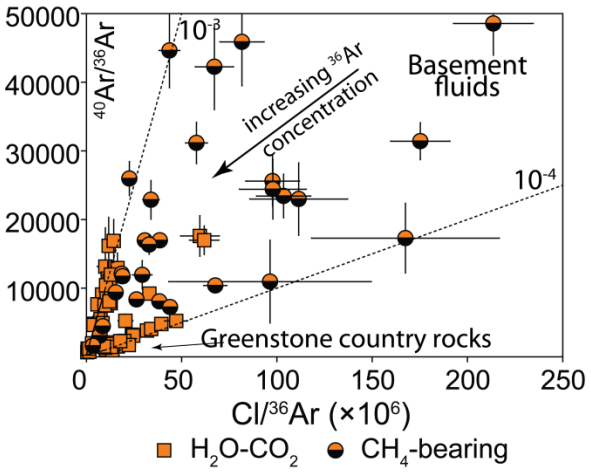
50000
40000
30000
20000
10000
$^{40}Ar/^{36}Ar$
10^{-3}
increasing ^{36}Ar concentration
Basement fluids
10^{-4}
Greenstone country rocks
0
50
100
150
200
250
$Cl/^{36}Ar$ (×10^6)
H_2O-CO_2
CH_4-bearing

Fig 16.

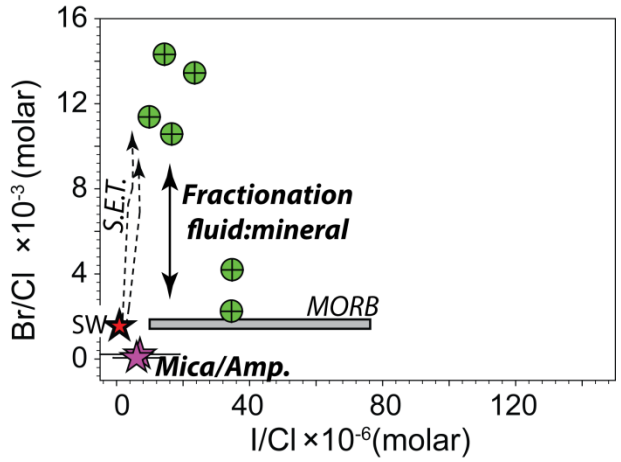
16
12
8
4
0
Br/Cl ×10-3 (molar)
S.E.T.
Fractionation
fluid:mineral
MORB
SW
Mica/Amp.
0
40
80
120
I/Cl ×10-6(molar)

Fig 17.

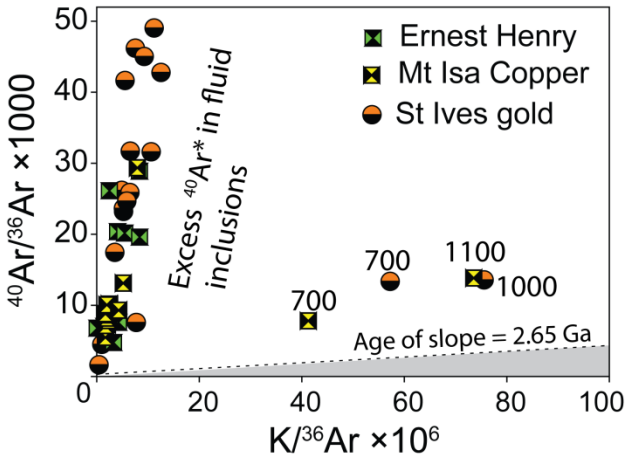
Ernest Henry
Mt Isa Copper
St Ives gold
Excess $^{40}Ar^*$ in fluid inclusions
700
1100
1000
700
Age of slope = 2.65 Ga
$^{40}Ar/^{36}Ar \times 1000$
$K/^{36}Ar \times 10^6$
0
10
20
30
40
50
20
40
60
80
100

Fig 18.

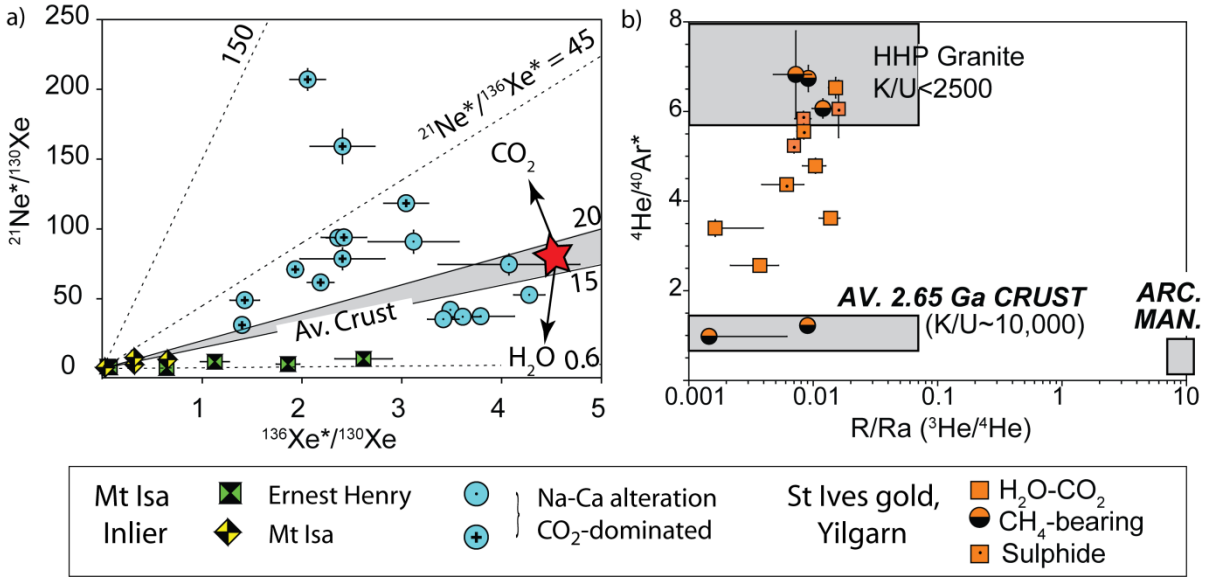
a)
b)
150
$^{21}Ne^*/^{136}Xe^* = 45$
CO_2
20
15
Av. Crust
H_2O 0.6
$^{21}Ne^*/^{130}Xe$
$^{136}Xe^*/^{130}Xe$
HHP Granite
K/U<2500
AV. 2.65 Ga CRUST
(K/U~10,000)
ARC.
MAN.
$^4He/^{40}Ar^*$
R/Ra ($^3He/^4He$)
Mt Isa Inlier
Ernest Henry
Mt Isa
Na-Ca alteration
CO_2-dominated
St Ives gold, Yilgarn
H_2O-CO_2
CH_4-bearing
Sulphide

Fig 19.

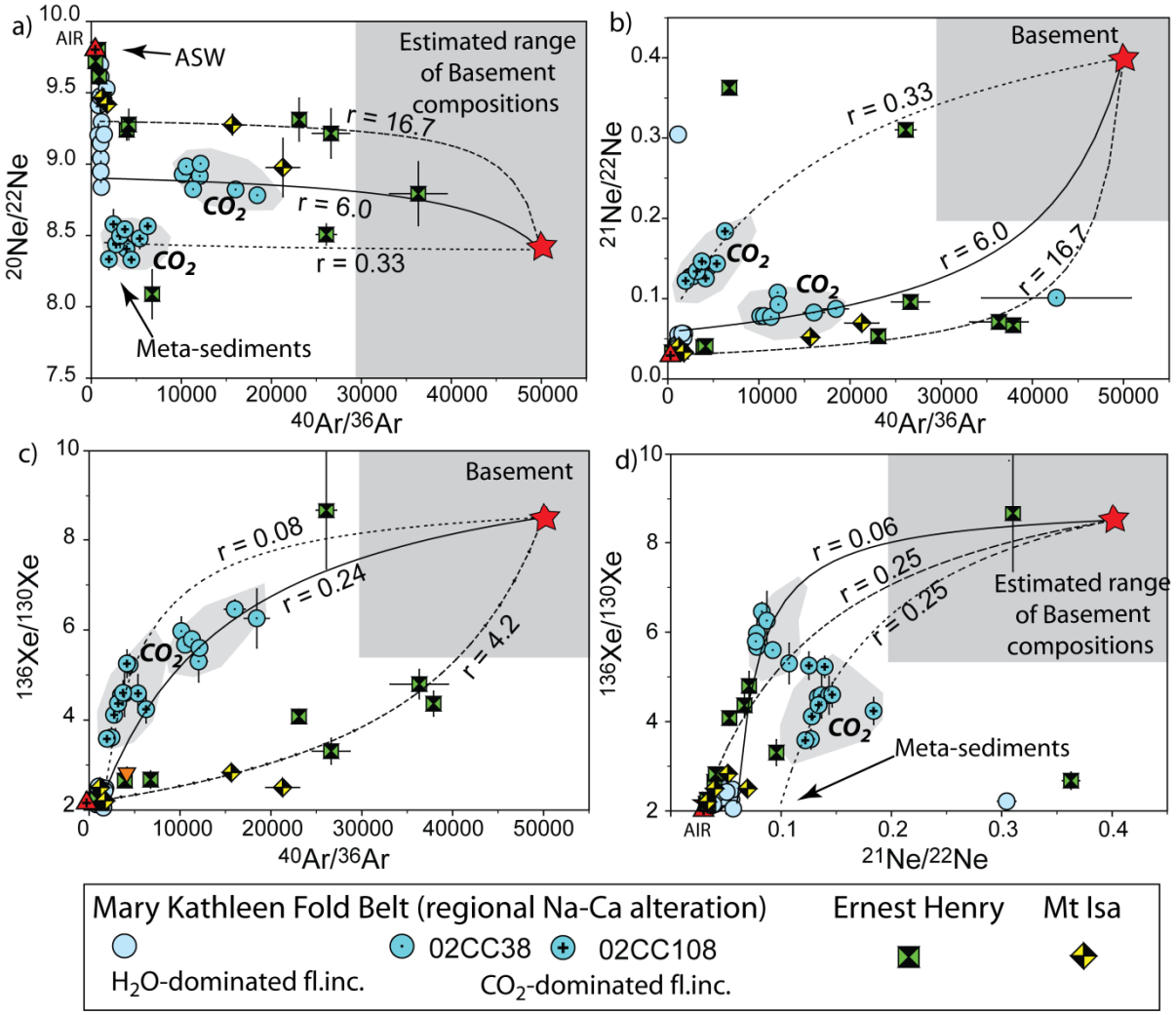
a)
AIR
ASW
Estimated range of Basement compositions
r = 16.7
r = 6.0
r = 0.33
CO2
CO2
Meta-sediments
20Ne/22Ne
40Ar/36Ar
b)
Basement
r = 0.33
r = 6.0
r = 16.7
CO2
CO2
21Ne/22Ne
40Ar/36Ar
c)
Basement
r = 0.08
r = 0.24
r = 4.2
CO2
136Xe/130Xe
40Ar/36Ar
d)
r = 0.06
r = 0.25
r = 0.25
Estimated range of Basement compositions
CO2
Meta-sediments
AIR
136Xe/130Xe
21Ne/22Ne
Mary Kathleen Fold Belt (regional Na-Ca alteration)
02CC38
02CC108
H2O-dominated fl.inc.
CO2-dominated fl.inc.
Ernest Henry
Mt Isa

Fig 20

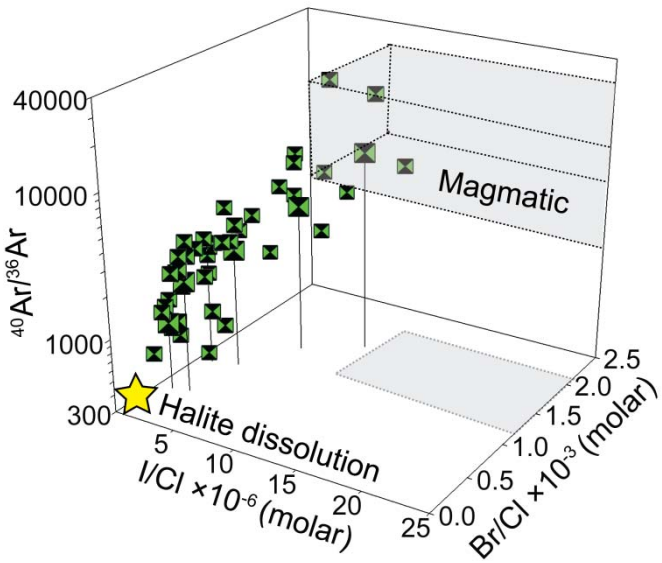
40000
10000
1000
300
$^{40}Ar/^{36}Ar$
Magmatic
Halite dissolution
5
10
15
20
25
I/Cl ×10^{-6} (molar)
0.0
0.5
1.0
1.5
2.0
2.5
Br/Cl ×10^{-3} (molar)

Fig 21.

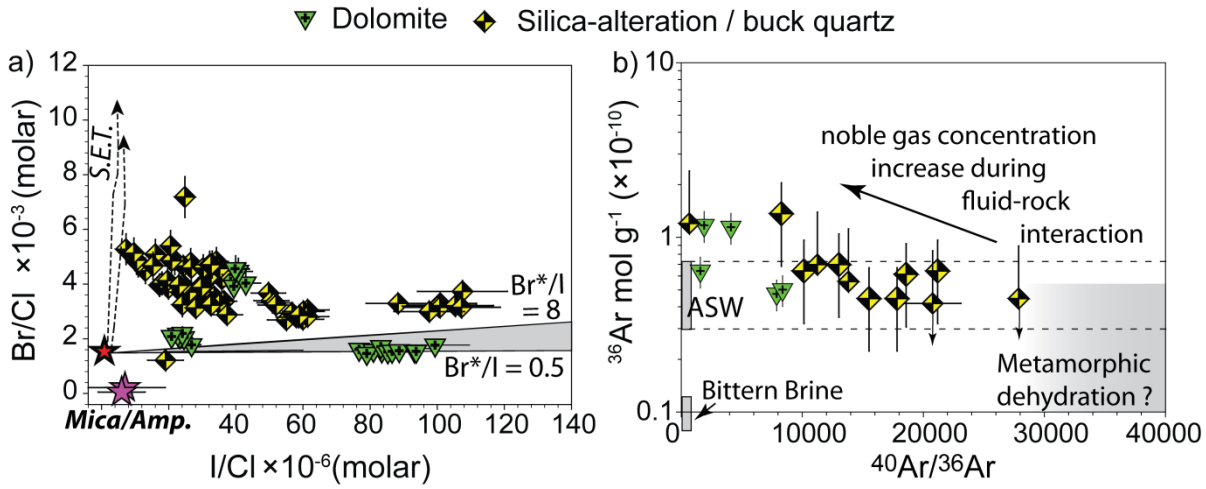
Dolomite
Silica-alteration / buck quartz
a)
Br/Cl ×10-3 (molar)
S.E.T.
Br*/I = 8
Br*/I = 0.5
Mica/Amp.
I/Cl ×10-6(molar)
b)
36Ar mol g-1 (×10-10)
noble gas concentration increase during fluid-rock interaction
ASW
Bittern Brine
Metamorphic dehydration ?
40Ar/36Ar

Fig 22

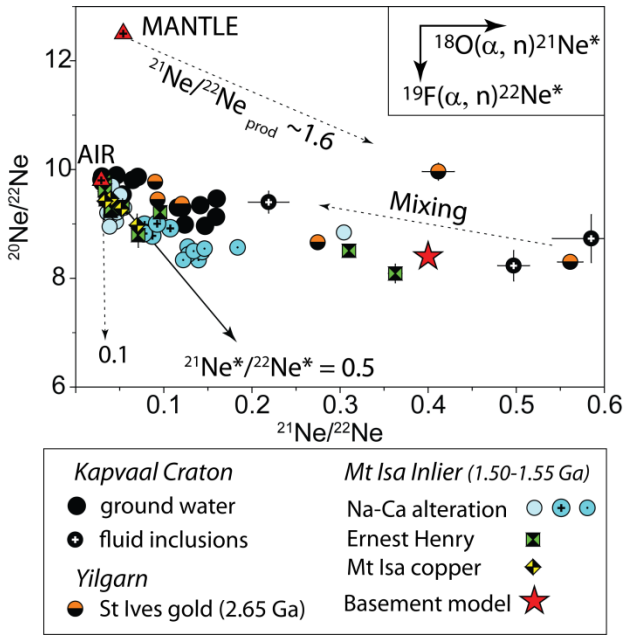
MANTLE
$^{21}Ne/^{22}Ne_{prod}$ ~1.6
$^{18}O(\alpha, n)^{21}Ne^*$
$^{19}F(\alpha, n)^{22}Ne^*$
AIR
Mixing
0.1
$^{21}Ne^*/^{22}Ne^* = 0.5$
$^{20}Ne/^{22}Ne$
$^{21}Ne/^{22}Ne$
12
10
8
6
0.1
0.2
0.3
0.4
0.5
0.6
Kapvaal Craton
ground water
fluid inclusions
Yilgarn
St Ives gold (2.65 Ga)
Mt Isa Inlier (1.50-1.55 Ga)
Na-Ca alteration
Ernest Henry
Mt Isa copper
Basement model